Thermodynamic Studies on the Multistate Thermal Transitions of Globular Proteins

by

Shun-ichi Kidokoro

Department of Physics, Faculty of Science,

the University of Tokyo

January 1988

Submitted to the University of Tokyo in partial fulfillment of the requirements for the Degree of Doctor of Science

Abstract

Some recent developments of the thermodynamic studies on the multistate thermal transitions of globular proteins are presented. The statistical mechanical basis and new methods of the scanning calorimetry data analysis for the multistate system are described in Chapter 1 and Chapter 2. In the analyses, a thermodynamic state is defined as an ensemble of the microstates of the system, assuming the heat capacity function and two integral constants. Upon these assumptions, the multistate system can be analyzed by deconvolution method even when the system includes self-dissociation/association process, using the relation between the partition function (or molar fraction function) and the enthalpy function. The obtained thermodynamic parameters are refined by non-linear least-squares fitting method. By the methods, the thermal transitions of porcine pepsinogen at various pH values, from pH 6.8 to 9.0 are analyzed to be four-state transitions in Chapter 3. The pH dependence of the thermodynamic functions of the protein is discussed.

Contents

Introduction

A great amount of scanning calorimetry data on macromolecules such as proteins, tRNAs, and DNAs have been reported with high precision (Privalov 1979, for a review). These investigations give the heat capacity functions of the system, and we can easily obtain the enthalpy functions by integrating them. Direct observation of the thermodynamic functions is the most distinctive feature of calorimetry.

By comparing the calorimetric enthalpy with the van't Hoff enthalpy, it has been confirmed that the thermal transitions of many small globular proteins can be described with a two-state model. With accumulating these thermodynamic data of proteins, some general physical properties which are common among many globular proteins are revealed, such as the coincidence of specific enthalpy values at 110 ℃ (Privalov 1979), the relationship between the difference heat capacity of the transition and the hydration effect of the buried surface in the tertiary structure (Ooi & Oobatake 1988), and the calorimetric observation of low temperature denaturation which is predicted from the thermodynamic functions of high temperature denaturation (Privalov 1986). Using the thermodynamic parameters determined by the scanning calorimetry, the energy probability distribution functions are determined, and the energy fluctuations of the proteins are discussed strictly by statistical mechanics (Cooper 1984).

On the other hand, after Freire and Biltonen presented a statistical deconvolution method for the multistate system

(Freire & Biltonen 1978a), the complex thermal denaturations of tRNAs and some proteins were analyzed by this method (Privalov 1982, for a review). However the necessity of the assumptions for the deconvolution has not yet been clearly discussed. Furthermore, the method is even wrongly regarded as being free from a priori assumptions of the state of the system.

In Chapter 1, a statistical mechanical basis and new methods for the determination of thermodynamic functions from scanning calorimetry data are presented (Kidokoro & Wada 1987). These methods are extended for the system that includes self-dissociation/association process in Chapter 2 (Kidokoro et al. 1988). By these methods, the thermal transitions of porcine pepsinogen at various pH values are analyzed to be four-state transitions, and the pH dependence of the thermodynamic functions of the states is discussed in Chapter 3.

By the present paper, the precise analyses of scanning calorimetry data for the determination of the thermodynamic functions are established, and the scanning calorimetry is proved to be an excellent measurement of the thermodynamic properties for multistate thermal transitions of globular proteins.

Chapter 1. Statistical thermodynamic analysis of calorimetry data

Abstract

A theoretical basis and new methods for the determination of thermodynamic functions from scanning calorimetry data are presented. A thermodynamic state is defined here as an ensemble of microstates in the system, and it can be defined only through assumptions of its heat capacity function and the two integral constants. With these assumptions, scanning calorimetry data can be analyzed using the single or double (or multi-) deconvolution presented here. New equations to calculate the van't Hoff enthalpy function and the calorimetric enthalpy function are presented. It is proved that the agreement of these two functions is a necessary and sufficient factor for the condition that the system can be described with the assumed two-state model.

1.1 Introduction

Recently, many have reported the equilibrium multi-state transition of biological macromolecules by changing such external conditions of these macromolecules in solution as temperature, pH or concentration of the denaturant (Kim & Baldwin 1982, for a review, Saito & Wada 1983ab). Thermal transitions have been studied by thermodynamic measurement with scanning microcalorimetry as well as with spectroscopic method. By comparing the calorimetric enthalpy with the van't Hoff enthalpy, it has been confirmed that the thermal transitions of many small globular proteins can be described with a two-state approximation (Privalov 1979, for a review). After Freire and Biltonen presented a statistical deconvolution method for multistate system (Freire & Biltonen 1978a), the complex thermal denaturations of tRNAs and some proteins have been analyzed by this method (Privalov 1982, for a review). However, the necessity of the assumptions for the deconvolution has not yet been clearly shown. Furthermore, the method is wrongly regarded as being free from a priori assumptions on the state of the system.

In this chapter, I show the necessity of the assumptions for the form of thermodynamic functions of states, clarifying what the popular word "state" means in the method. I develop the deconvolution method, showing that the essential point of the deconvolution is to obtain the partition function which would be given if some states of the system whose form of thermodynamic functions are assumed were hypothetically excluded.

I clarify the relation between the deconvolution method and the traditional procedure in which the calorimetric enthalpy is compared with the van't Hoff enthalpy at the midpoint temperature of the transition. Although many small globular proteins have been confirmed by the traditional method to be described by the two-state model, the agreement between these two kinds of enthalpy values at the midpoint temperature is a necessary but not a sufficient factor to satisfy the condition that the system can be described by the two-state model. I present new equations for obtaining the van't Hoff enthalpy function and the calorimetric enthalpy function on temperature from experimental calorimetry data that satisfy the traditional definitions of the van't Hoff enthalpy value and the calorimetric enthalpy value at the midpoint temperature, respectively. I prove that the agreement of the van't Hoff enthalpy function with the calorimetric enthalpy function is not only a necessary but also a sufficient factor for the condition that the system can be described by the two-state model.

1.2. Meaning of "state" in calorimetry data analysis

Proteins in solution have a great degree of conformational freedom. Backbone chain and side chains fluctuate by changing the dihedral angles, ϕ, ψ, ω and χ of each residues. Even if these internal rotations were fixed, water molecules around the protein particles would possess a great variety of configurations and conformations. And even if all the coordinates of constituent atoms of proteins, water molecules, and ions or other solutes were fixed, there would be a great number of quantum mechanical states of electrons. There are thus a tremendous number of microstates in the system which we must take into account.

A thermodynamic state is defined as an ensemble of some of these microstates. The canonical partition function of the whole system, Z(T), is defined by Eq.(1.1a), and when all the microstates are classified, for example, into n thermodynamic states, the function is given by Eq.(1.1b),

$$Z(T) = \sum_{\mu}^{N} \omega_{\mu} \exp(-\epsilon_{\mu}/RT) \qquad (1.1a)$$

$$Z(T) = \sum_{i}^{n} \sum_{\mu \in i} \omega_{\mu} \exp(-\epsilon_{\mu}/RT) \qquad (1.1b)$$

where N is the total number of microstates of the system; ω_{μ} and ϵ_{μ} are the degeneracy and energy of the μ-th microstate, respectively; $\sum_{\mu \in i}$ means the summation of all the microstates

which participate in i-th thermodynamic state (ensemble); and R is a gas constant. In this chapter, the Latin suffixes, i,j,k,... are used for the thermodynamic states and the Greek suffixes, $\mu, \nu, \eta, \ldots$ are used for the microstates.

Gibbs free energy function of i-th thermodynamic state, $G_i(T)$, and enthalpy function of the state, $H_i(T)$, are defined by Eqs.(1.2a) and (1.2b), respectively, where the molar fraction of μ-th microstate in i-th thermodynamic state, $f^i_\mu(T)$, is defined by Eq.(1.2c).

$$\exp(-G_i(T)/RT) = \sum_{\mu \in i} \omega_\mu \exp(-\epsilon_\mu/RT) \qquad (1.2a)$$

$$H_i(T) = \sum_{\mu \in i} \epsilon_\mu f^i_\mu(T) \qquad (1.2b)$$

$$f^i_\mu(T) = \omega_\mu \exp(-\epsilon_\mu/RT) \; / \sum_{\nu \in i} \omega_\nu \exp(-\epsilon_\nu/RT) \qquad (1.2c)$$

$H_i(T)$ is the mean energy among all the microstates of i-th thermodynamic state, and it is easy to confirm that $G_i(T)$ and $H_i(T)$ satisfy the well-known thermodynamic equation:

$$\frac{d}{dT}\,(G_i(T)/T) = -\,H_i(T)/T^2 \qquad (1.3)$$

The partition function of the system is described by

$$Z(T) = \sum_i^n \exp(-G_i(T)/RT) \qquad (1.4)$$

Thus, a given system can be described by the thermodynamic functions $G_i(T)$ (i=1,...,n) of n thermodynamic states instead of N microstates. Considering that all thermodynamic properties are derived from this partition function, it is interesting that any number of thermodynamic states and any ways of dividing the microstates into thermodynamic states are allowed to analyze the thermodynamic data such as calorimetry. To ask, then, how many thermodynamic states the system consists of or how the functions of these thermodynamic states differ, is meaningless without some assumptions on the properties of the thermodynamic states.

As Eq.(1.2a) shows, a certain ensemble of microstates determines a Gibbs free energy function; reversing this, the Gibbs free energy function determines the ensemble of microstates. Experimentally we can define an ensemble, that is, a thermodynamic state only through determination of the Gibbs free energy function.

When we analyze the data of scanning calorimetry, the determination of the Gibbs free energy function can be made through the determination of the heat capacity function and two constants as shown in the next section.

1.3. Necessary assumptions for the deconvolution of scanning calorimetry data

When the heat capacity function of the whole system is obtained experimentally, the heat capacity function of a thermodynamic state must be assumed first. For example, Fig.1.1 illustrates a typical calorimetry data of thermal denaturation of protein together with the assumed heat capacity functions of native and heat-denatured states. The native and heat-denatured states of many globular proteins can be considered as thermodynamic states, that is, they can be respected as ensembles of many microstates, respectively. Fortunately, their heat capacity functions can be well approximated by linear functions on temperature (Privalov 1979, for a review).

Once the form of the heat capacity function of a certain thermodynamic state is assumed, the enthalpy function and Gibbs free energy function of the state are determined by Eqs.(1.3) and (1.5) with two integral constants:

$$C_i(T) = \frac{d}{dT} H_i(T) \qquad (1.5)$$

where $C_i(T)$ is the assumed heat capacity function of i-th thermodynamic state.

Traditionally, this assumption was considered simply as a baseline extrapolation problem, but I must emphasize that baseline itself has definitive information on thermodynamic functions of the state; in other words, the assumptions of the form of baseline determine the form of the thermodynamic

functions. It is distinctive from other non-thermodynamic measurements such as spectroscopic method.

The two integral constants can be determined when the values of $H_i(T)$ and $G_i(T)$ at a certain temperature are determined. I will not comment further on the absolute values, however, because our interest is in determining the difference of thermodynamic functions between thermodynamic states.

The heat capacity function, C(T), and the enthalpy function, H(T), of the whole system are described by Eqs.(1.6a) and (1.6b), respectively, where the molar fraction of μ-th microstate, $f_\mu(T)$, is defined by Eq.(1.6c).

$$H(T) = \sum_\mu \varepsilon_\mu f_\mu(T) \tag{1.6a}$$

$$C(T) = \frac{d}{dT} H(T) \tag{1.6b}$$

$$f_\mu(T) = \omega_\mu \exp(-\varepsilon_\mu/RT) \; / \; \sum_\nu \omega_\nu \exp(-\varepsilon_\nu/RT) \tag{1.6c}$$

H(T) represents the mean energy among all microstates of the system, and it is described by the partition function, Z(T), as

$$H(T) = RT^2 \frac{d}{dT} \log Z(T) \tag{1.7}$$

Throughout this paper, "log" means natural logarithm always.

These functions can be described as one of the special classifications of microstates into certain thermodynamic states, in which the whole system is regarded as one thermodynamic state.

Obviously, in general, C(T) and H(T) become complicated functions, in contrast to the previous simple temperature functions $C_i(T)$ and $H_i(T)$.

A difference heat capacity function and a difference enthalpy function of the whole system referred to the i-th state, $\Delta C_i(T)$ and $\Delta H_i(T)$, are defined by

$$\Delta C_i(T) = C(T) - C_i(T) \tag{1.8a}$$

$$\Delta H_i(T) = H(T) - H_i(T) \tag{1.8b}$$

Experimentally, $\Delta C_i(T)$ can be calculated from C(T) and $C_i(T)$ by Eq.(1.8a), and $\Delta H_i(T)$ can be obtained by Eq.(1.9), where h_i must be assumed as $\Delta H_i(T_i)$:

$$\Delta H_i(T) = \int_{T_i}^{T} \Delta C_i(T)\, dT + h_i \tag{1.9}$$

Although T_i may be set at any temperature in principle, it should be chosen so as to satisfy the condition that the contribution of the microstates which do not belong to i-th thermodynamic state is as small as possible, where h_i could be assumed to be zero. A detailed discussion of h_i is presented in the next section.

From $\Delta H_i(T)$, the partition function referred to i-th thermodynamic state, $Z_i(T)$, which is defined by Eq.(1.10) can be calculated experimentally by Eq.(1.11) where z_i must be assumed

to be $Z_i(T_i)$. These equations are easily obtained from Eqs.(1.3) and (1.7):

$$Z_i(T) = Z(T)\ \exp(G_i(T)/RT) \tag{1.10}$$

$$Z_i(T) = z_i\ \exp\left[\ \int_{T_i}^{T} (\Delta H_i(T)/RT^2)dT\ \right] \tag{1.11}$$

Here, the molar fraction of i-th thermodynamic state, $f_i(T)$, which is defined by Eq.(1.12) is related to $Z_i(T)$ as Eq.(1.13) shows:

$$f_i(T) = \sum_{\mu \in i} f_\mu(T) \tag{1.12}$$

$$f_i(T) = 1\ /\ Z_i(T) \tag{1.13}$$

Thus, if the molar fraction of i-th state is regarded as almost 1 at $T = T_i$, z_i can be assumed to be 1. In many case of the deconvolution, however, this assumption causes some difficulties, as discussed in detail later.

To summarize, by the assumption of the heat capacity function of a thermodynamic state, $C_i(T)$, and two constants, h_i and z_i, we have experimentally obtained the partition function referred to the thermodynamic state.

1.4 Theory of deconvolution

The partition function, $Z_i(T)$, calculated experimentally in the previous section, is described by Eq.(1.14) using microstates:

$$Z_i(T) = 1 + \sum_{\nu \in i} \omega_\nu \exp[-(\varepsilon_\nu - G_i(T))/RT] \qquad (1.14)$$

where $\sum_{\nu \in i}$ means the summation of the microstates which do not participate in i-th thermodynamic state.

In the right-hand side of this equation, the contribution of all the microstates of i-th thermodynamic state is contained in the first term, 1. Then, by excluding this contribution, we have

$$Z_i^{(i)}(T) = Z_i(T) - 1 \qquad (1.15)$$

where $Z_i^{(i)}(T)$ is the partition function of a hypothetical system which does not contain the microstates of i-th thermodynamic state but consists of all the remaining microstates. I call the thermodynamic functions of this kind of hypothetical system hypothetical thermodynamic functions.

The hypothetical enthalpy function, $\Delta H_i^{(i)}(T)$, and the hypothetical heat capacity function, $\Delta C_i^{(i)}(T)$, are defined by Eqs.(1.16a) and (1.16d) where the hypothetical molar fraction is defined by Eq.(1.16c):

$$\Delta H_i^{(i)}(T) = H^{(i)}(T) - H_i(T) \qquad (1.16a)$$

$$H^{(i)}(T) = \sum_{\mu \in i} \epsilon_\mu f_\mu^{(i)}(T) \qquad (1.16b)$$

$$f_\mu^{(i)}(T) = \omega_\mu \exp(-\epsilon_\mu/RT) \; / \; \sum_{\nu \in i} \omega_\nu \exp(-\epsilon_\nu/RT) \qquad (1.16c)$$

$$\Delta C_i^{(i)}(T) = C^{(i)}(T) - C_i(T) \qquad (1.16d)$$

$$C^{(i)}(T) = \frac{d}{dT} H^{(i)}(T) \qquad (1.16e)$$

Equations (1.17a) and (1.17b) would then hold:

$$\Delta H_i^{(i)}(T) = RT^2 \frac{d}{dT} \log Z_i^{(i)}(T) \qquad (1.17a)$$

$$\Delta C_i^{(i)}(T) = \frac{d}{dT} \Delta H_i^{(i)}(T) \qquad (1.17b)$$

Using Eqs.(1.11),(1.13),(1.15),(1.16) and (1.17), $\Delta H_i^{(i)}(T)$ and $\Delta C_i^{(i)}(T)$ can be described without partition function as

$$\Delta H_i^{(i)}(T) = \frac{\Delta H_i(T)}{1 - f_i(T)} \qquad (1.18a)$$

$$\Delta C_i^{(i)}(T) = \frac{\Delta C_i(T)}{1 - f_i(T)} - \frac{\Delta H_i(T)^2 f_i(T)}{RT^2 \, (\, 1 - f_i(T) \,)^2} \qquad (1.18b)$$

Now, by Eq.(1.19) we can calculate the hypothetical heat capacity function, $C^{(i)}(T)$, which would be observed if the system did not include i-th thermodynamic state as

$$C^{(i)}(T) = \Delta C_i^{(i)}(T) + C_i(T) \qquad (1.19)$$

The function of Eq.(1.18a) has the same form as the key function of the deconvolution method of Freire and Biltonen (1978a). I have shown that it is the hypothetical enthalpy function and can be derived generally from the hypothetical partition function.

The heat capacity function $C^{(i)}(T)$ of the new hypothetical system is now obtained. It should be deconvoluted in the same way as the heat capacity function of the given system $C(T)$; that is, the heat capacity function of a new thermodynamic state, $C_j(T)$, must be assumed in order to proceed to the next deconvolution. Then, $\Delta C_j^{(i)}(T)$ can be calculated as

$$\Delta C_j^{(i)}(T) = C^{(i)}(T) - C_j(T) \qquad (1.20)$$

and $\Delta H_j^{(i)}(T)$, $Z_j^{(i)}(T)$ and $f_j^{(i)}(T)$ are calculated in the same manner as Eqs.(1.9),(1.11) and (1.13) with two new constants $h_j^{(i)}$ and $z_j^{(i)}$. The new hypothetical partition function, $Z_j^{(i,j)}(T)$, the new hypothetical enthalpy function, $\Delta H_j^{(i,j)}(T)$, and the new hypothetical heat capacity functions, $\Delta C_j^{(i,j)}(T)$ and $C^{(i,j)}(T)$, of the new system from which both i-th and j-th state are excluded, are obtained.

The procedure should be continued until the new hypothetical heat capacity function can be regarded as the heat capacity function of one thermodynamic state. For example, if we assume that the new hypothetical heat capacity function, $C^{(i,j)}(T)$, is

that of the k-th thermodynamic state, $C_k(T)$, the following equations are assumed to hold:

$$\Delta C_k^{(i,j)}(T) = C^{(i,j)}(T) - C_k(T) = 0 \qquad (1.21a)$$

$$\Delta H_k^{(i,j)}(T) = 0 \qquad (1.21b)$$

$$Z_k^{(i,j)}(T) = 1 \qquad (1.21c)$$

$$f_k^{(i,j)}(T) = 1 \qquad (1.21d)$$

The difference enthalpy function between j-th and k-th state $\Delta H_{jk}(T)$, which is defined by Eq.(1.22a), and that between i-th and j-th state $\Delta H_{ij}(T)$ can be calculated as Eqs.(1.22b) and (1.22c), respectively.

$$\Delta H_{jk}(T) = H_k(T) - H_j(T) \qquad (1.22a)$$

$$\Delta H_{jk}(T) = \Delta H_j^{(i,j)}(T) - \Delta H_k^{(i,j)}(T) \qquad (1.22b)$$

$$\Delta H_{ij}(T) = \Delta H_i^{(i)}(T) - \Delta H_j^{(i)}(T) \qquad (1.22c)$$

Similarly, the difference Gibbs free energy function between j-th and k-th state $\Delta G_{jk}(T)$, which is defined by Eq.(1.22d), and that between i-th and j-th state $\Delta G_{ij}(T)$ are calculated as Eqs.(1.22e) and (1.22f), respectively.

$$\Delta G_{jk}(T) = G_k(T) - G_j(T) \qquad (1.22d)$$

$$\Delta G_{jk}(T) = RT \log[\, Z_k^{(i,j)}(T) \,/\, Z_j^{(i,j)}(T) \,] \qquad (1.22e)$$

$$\Delta G_{ij}(T) = RT \log[\, Z_j^{(i)}(T) \,/\, Z_i^{(i)}(T) \,] \qquad (1.22f)$$

The molar fractions of j-th and k-th states in the original system can be calculated by

$$f_j(T) = [\, 1 - f_i(T) \,]\, f_j^{(i)}(T) \qquad (1.23a)$$

$$f_k(T) = [\, 1 - f_i(T) - f_j(T) \,]\, f_k^{(i,j)}(T) \qquad (1.23b)$$

When more thermodynamic functions appear during this deconvolution process, the form of Eqs.(1.22) and (1.23) may be easily changed to deal with them.

As shown in Fig.1.1, it frequently happens that the heat capacity function of two or more thermodynamic states can be assumed from the beginning. When these states are not "exclusive to each other", the results of the deconvolution which is obtained if we start from a different thermodynamic state, will generally be different, even if there are no errors in an experiment and analysis.

We define any two thermodynamic states as "exclusive to each other" when the molar fraction of all the microstates in common between the two states is zero, that is to say, Eq.(1.24) holds:

$$\sum_{\mu \in i \cap j} f_{\mu}(T) = 0 \qquad (1.24)$$

where $\sum_{\mu \in i \cap j}$ means the summation of microstates belonging to both i-th and j-th state.

When it does not hold, a certain part of j-th state which also belongs to i-th state, for example, is excluded by the subtraction of the contribution of i-th state from the partition function. Then, the results of the deconvolution depend on the order of thermodynamic state used in the method.

When Eq.(1.24) holds, on the contrary, in theory the results do not depend on the order of the deconvolution, and can be obtained as shown in the following without the recursive procedure above.

For example, as illustrated in Fig.1.1, we can calculate $\Delta H_i(T)$ and $\Delta H_j(T)$ independently, assuming $C_i(T)$, $C_j(T)$, h_i and h_j [see Eq.(1.9)]. From these functions, $Z_i(T)$ and $Z_j(T)$ can be calculated by Eq.(1.11) using z_i and z_j. Then we can calculate directly the partition function $Z_i^{(i,j)}(T)$ by Eq.(1.25a) because the contribution of j-th thermodynamic state to $Z_i(T)$ is given by Eq.(1.25b):

$$Z_i^{(i,j)}(T) = Z_i(T) - 1 - Z_i(T) \;/\; Z_j(T) \qquad (1.25a)$$

$$\exp(-\Delta G_{ij}(T)/RT) = Z_i(T) \;/\; Z_j(T) \qquad (1.25b)$$

Using this relation, $\Delta H_i^{(i,j)}(T)$ and $\Delta C_i^{(i,j)}$ can be calculated directly by Eqs.(1.26a) and (1.26b), respectively,

$$\Delta H_i^{(i,j)}(T) = \frac{\Delta H_i(T) - \Delta H_{ij}(T) f_j(T)}{1 - f_i(T) - f_j(T)} \qquad (1.26a)$$

$$\Delta C_i^{(i,j)}(T) = \frac{\Delta C_i(T) - \Delta C_{ij}(T) f_j(T)}{1 - f_i(T) - f_j(T)}$$

$$- \frac{\Delta H_i(T)^2 f_i(T) + \Delta H_j(T)^2 f_j(T) - \Delta H_{ij}(T)^2 f_i(T) f_j(T)}{RT^2 (1 - f_i(T) - f_j(T))^2} \qquad (1.26b)$$

where $\Delta H_{ij}(T)$ and $\Delta C_{ij}(T)$ can be calculated by Eqs.(1.27a) and (1.27b), respectively:

$$\Delta H_{ij}(T) = \Delta H_i(T) - \Delta H_j(T) \qquad (1.27a)$$

$$\Delta C_{ij}(T) = C_j(T) - C_i(T) \qquad (1.27b)$$

In this paper, I call the deconvolution by Eq.(1.18) a single deconvolution and that by Eq.(1.26) a double deconvolution.

Generally, a multi-deconvolution can be defined. When the heat capacity function of m thermodynamic states, from 1-st to m-th state, is assumed from the beginning, the hypothetical thermodynamic functions of the system which does not contain these states, $\Delta H_1^{(1,2,\ldots,m)}(T)$, $C^{(1,2,\ldots,m)}(T)$ are obtained by

$$\Delta H_1^{(1,2,\ldots,m)}(T) = \frac{\Delta H_1(T) - \sum_{i=2}^{m} \Delta H_{1i}(T) f_i(T)}{1 - \sum_{i=1}^{m} f_i(T)} \qquad (1.28a)$$

$$C^{(1,2,\ldots,m)}(T) = \frac{C(T) - \sum_{i=1}^{m} C_i(T) f_i(T)}{1 - \sum_{i=1}^{m} f_i(T)}$$

$$- \frac{\sum_{i=1}^{m} \Delta H_i^2(T) f_i(T) - \sum\sum_{i>j} \Delta H_{ij}^2(T) f_i(T) f_j(T)}{RT^2 \left(1 - \sum_{i=1}^{m} f_i(T) \right)^2} \qquad (1.28b)$$

As shown by Filimonov et al. (1982), the right-hand side of Eq.(1.18a) diverges around $T=T_i$ when $h_i=0$ and $z_i=1$ [see Fig.1.2(a) and (b)]. This divergence is due to the assumed value of z_i and h_i as shown in the following.

When the approximated values, 0 and 1 are taken for h_i and z_i, respectively, $\Delta H_i^*(T)$, $Z_i^*(T)$ and $f_i^*(T)$ are obtained by Eqs.(1.9), (1.11) and (1.13). They are related to the true values, h_i and z_i, and the true functions, $\Delta H_i(T)$ and $f_i(T)$, by

$$\Delta H_i^*(T) = \Delta H_i(T) - h_i \qquad (1.29a)$$

$$f_i^*(T) = z_i f_i(T) \exp\left[\frac{h_i}{R} \left(\frac{1}{T_i} - \frac{1}{T} \right) \right] \qquad (1.29b)$$

Then we have

$$\frac{\Delta H_i^*(T)}{1-f_i^*(T)} = \frac{\Delta H_i(T)}{1-f_i(T)} \times [1-f_i(T)] \times \frac{1-h_i/\Delta H_i(T)}{1-f_i^*(T)} \qquad (1.30a)$$

As the first term of the right-hand side is the true function that we want, this function is well-approximated by the function of the left-hand side if the second and the third terms on the right are almost 1 within all the temperature range. We can expand the second and third terms into a series of $\Delta T/T_i$ where $\Delta T = T-T_i$, and we get Eq.(1.30b) if the higher terms of $\Delta T/T_i$ are neglected. As seen in this figure, it diverges around $T = T_i$.

$$(1-f_i(T)) \frac{1-h_i/\Delta H_i(T)}{1-f_i^*(T)} \fallingdotseq \frac{2RT_i}{h_i}(1-1/z_i) \left(\frac{\Delta T}{T_i}\right)^{-1} \qquad (1.30b)$$

$$(\Delta T \ll T_i)$$

Therefore, the function of the left-hand side of Eq.(1.30a) is far different from the true function around $T = T_i$.

It frequently happens that this divergence affects the data even at the transition temperature region; the function then goes up before it comes down to the true enthalpy value of the intermediate state as seen in Fig.1.2(b). When we calculate $\Delta H_i^{(i,j)}(T)$ by the double deconvolution presented in this section, however, the function does not go up in the transition region because the final state has been already excluded; then we

get a more precise enthalpy function of the intermediate state as seen in Figs.1.2(a) and (b).

1.5 Two-state analysis

As seen in Fig.1.1, we assume $C_i(T)$ and $C_j(T)$ as the heat capacity function of two thermodynamic states. The problem is whether this system can be described with these two thermodynamic states or not.

If we use the double deconvolution, the problem becomes very simple, that is, whether the sum of $f_i(T)$ and $f_j(T)$, which are obtained by the deconvolution, is 1 within the experimental errors in all the temperature range. In this section, I show that this problem can be solved even without using $f_i(T)$ and $f_j(T)$ explicitly. The method shown here is found to be related to the traditional two-state method.

If we assume that this system consists of only these two states and that they are exclusive with each other, we can calculate the midpoint temperature and two kinds of difference enthalpy functions as shown in the following.

$\Delta H_i(T)$ and $\Delta H_j(T)$ can be calculated with the assumption of h_i and h_j (usually these values are assumed to be zero) by Eq.(1.9). The calorimetric enthalpy function, $\Delta H^{cal}(T)$, is defined as

$$\Delta H^{cal}(T) = \Delta H_i(T) - \Delta H_j(T) \qquad (1.31)$$

This is the same function as $\Delta H_{ij}(T)$ [see Eq.(1.27a)], and thus it represents the difference heat capacity function between these two states exactly even if the system consists of many thermodynamic states. It is clear that the definition of

Eq.(1.31) satisfies the traditional definition of calorimetric enthalpy at the midpoint temperature (see Privalov 1979 and Fig.1.1); there is no reason why we have to use only the value at that temperature. It is also clear that the calculation of the area with this equation is not an approximation of other calculation methods such as that of the area between the heat capacity curve and the assumed sigmoidal heat capacity base line (Fukada et al. 1983). This sigmoidal curve is generally defined as

$$\langle C \rangle(T) = \sum_i C_i(T) f_i(T) \tag{1.32}$$

However, we do not initially know how to calculate this function, while the calculation by Eq.(1.31) is shown to be exact.

If we take the two-state approximation, $\Delta H_i(T)$ and $\Delta H_j(T)$ will be described as

$$\Delta H_i(T) = \Delta H_{ij}(T) f_j(T) \tag{1.33a}$$

$$\Delta H_j(T) = - \Delta H_{ij}(T) f_i(T) \tag{1.33b}$$

From these equations, it is easily confirmed that Eq.(1.34a) is a necessary and sufficient condition of Eq.(1.34b) if $\Delta H_{ij}(T)$ is not zero.

$$f_i(T) = f_j(T) \tag{1.34a}$$

$$\Delta H_i(T) = - \Delta H_j(T) \qquad (1.34b)$$

The temperature at which Eq.(1.34a) holds is called the midpoint temperature of the transition. Traditionally the midpoint temperature is defined at that temperature where the areas of both high- and low-temperature sides are the same, that is, the area between the two heat capacity curves of the system and i-th states is the same as the area between the two curves of the system and j-th states. This is confirmed by the equivalence of the two conditions, Eqs.(1.34a) and (1.34b). The temperature which satisfies these equations is designated Tm in two-state analysis.

Using Eqs.(1.33a) and (1.33b), the equilibrium constant K(T) can be obtained from $\Delta H_i(T)$ and $\Delta H_j(T)$ as

$$K(T) = \frac{f_j(T)}{f_i(T)}$$

$$= - \frac{\Delta H_i(T)}{\Delta H_j(T)} \qquad (1.35)$$

Then, we can get the van't Hoff enthalpy function, $\Delta H^{vH}(T)$, which is related to the equilibrium constant K(T) as

$$\Delta H^{vH}(T) = RT^2 \frac{d}{dT} \log K(T) \qquad (1.36)$$

From Eqs.(1.35) and (1.36), the function can be calculated using $\Delta H_i(T)$, $\Delta H_j(T)$, $\Delta C_i(T)$ and $\Delta C_j(T)$ by

$$\Delta H^{vH}(T) = RT^2 \left[\frac{\Delta C_i(T)}{\Delta H_i(T)} - \frac{\Delta C_j(T)}{\Delta H_j(T)}\right] \qquad (1.37)$$

It is easily confirmed that this definition includes the traditional definition of the enthalpy value at T = Tm.

$$\Delta H^{vH}(Tm) = \frac{4RTm^2}{\Delta H^{cal}(Tm)} \left[C(Tm) - \frac{C_i(Tm)+C_j(Tm)}{2}\right] \qquad (1.38)$$

There is no reason why we must use only the enthalpy value at Tm. As seen in Fig.1.2(c), for example, $\Delta H^{cal}(T)$ and $\Delta H^{vH}(T)$ are well reproduced within a wide range of temperature. The disagreement of these functions in the figure shows that this system cannot be described with the two-state model.

In the traditional analysis, $\Delta H^{vH}(Tm)$ can be equal to $\Delta H^{cal}(Tm)$ even if the system does not consist of these two states. For example, it is clear from Eq.(1.38) that $\Delta H^{vH}(Tm)$ is determined only by the values of C(Tm) and $\Delta H^{cal}(Tm)$. Then, $\Delta H^{vH}(Tm)$ and $\Delta H^{cal}(Tm)$ will be not changed, for example, if C(T) is changed in some of the temperature regions lower than Tm keeping the area of $\Delta H_i(Tm)$ not to be changed. This is because the agreement of $\Delta H^{vH}(Tm)$ with $\Delta H^{cal}(Tm)$ is not a sufficient factor of the two-state condition.

If this system consists of only these two thermodynamic states, the two kinds of enthalpy functions must agree with each other. On the other hand, in the following, I show that the system can be described by the two-state model if, within the

entire temperature region of the experiment, $\Delta H^{vH}(T)$ agrees with $\Delta H^{cal}(T)$. If so, Eq.(1.39a) holds from Eqs.(1.35) and (1.36). Considering that Eqs.(1.40a) and (1.40b) are correct even when the system consists of multi-state, Eq.(1.39b) holds.

$$\frac{d}{dT} \log\left(-\frac{\Delta H_i(T)}{\Delta H_j(T)}\right) = \frac{\Delta H_{ij}(T)}{RT^2} \tag{1.39a}$$

$$= \frac{d}{dT}\left(-\frac{\Delta G_{ij}(T)}{RT}\right) \tag{1.39b}$$

$$\Delta H^{cal}(T) = \Delta H_{ij}(T) \tag{1.40a}$$

$$\frac{d}{dT}\left(-\frac{\Delta G_{ij}(T)}{RT}\right) = \frac{\Delta H_{ij}(T)}{RT^2} \tag{1.40b}$$

When both sides of Eq.(1.39b) are integrated, we get Eq.(1.41) with an integral constant c_1.

$$\frac{\Delta H_i(T)}{\Delta H_j(T)} = -c_1 \exp\left(-\frac{\Delta G_{ij}(T)}{RT}\right) \tag{1.41}$$

When we describe Eq.(1.41) with the partition functions, $Z_i(T)$ and $Z_j(T)$, between which Eq.(1.25b) always holds, we get Eq.(1.42), and then we get Eqs.(1.43) with another integral constant c_2.

$$\frac{d}{dT} \log Z_i(T) = \frac{d}{dT} \log\left[\, 1 + c_1 \exp(-\Delta G_{ij}(T)/RT) \,\right] \tag{1.42}$$

$$Z_i(T) = c_2[\ 1 + c_1 \exp(-\Delta G_{ij}(T)/RT)\ ] \qquad (1.43a)$$

$$Z_j(T) = c_2[\ c_1 + \exp(\Delta G_{ij}(T)/RT)\ ] \qquad (1.43b)$$

We assume that in the low-temperature region $\exp[-\Delta G_{ij}(T)/RT]$ should be almost 0 and $Z_i(T)$ should be almost 1, and that in the high-temperature region $\exp[\Delta G_{ij}(T)/RT]$ should be almost 0 and $Z_j(T)$ should be almost 1. Then c_1 and c_2 are determined to be 1. Thus we get Eq.(1.44) and the equation shows that this system can be described by the i-th and j-th states only.

$$Z_i(T) = 1 + \exp[-\Delta G_{ij}(T)/RT] \qquad (1.44)$$

1.6 Discussion

For the deconvolution, the only thing we must do is to assume the heat capacity function of the state; there is no need to consider the properties of microstates such as their energies and their populations, which are dependent on temperature. Fortunately, except in the region of transition, the heat capacity functions of macromolecules are found to be well approximated by linear functions in many cases. Then we easily assume one heat capacity function for a thermodynamic state, which includes a great number of microstates significantly populated in a certain temperature range.

The definition of a thermodynamic state in this chapter is very extensive. It is possible to assume a set of microstates that include some thermal transitions as one thermodynamic state. For example, the analysis of the complex thermal denaturation of a protein which has several independent domains is most effective when the heat capacity function of transition of some parts of the domains is measured separately. In this case, we can easily subtract the contribution of the domains from the heat capacity function of the whole protein using the single- or double-deconvolution procedure, without considering the detail of the thermal transition of the domains.

As seen in the sections on deconvolution and the two-state analysis, assumptions of the heat capacity functions of the two thermodynamic states in the double deconvolution are the same as that in the two-state analysis obtaining Tm, $\Delta H^{cal}(T)$, and $\Delta H^{vH}(T)$. The analysis is simple to check as to whether or not

the system can be described in terms of the two-state model. In order to obtain Tm and $\Delta H^{vH}(T)$, we must assume that the system consists of the two thermodynamic states. If the system does not, a conflict will arise, so that $\Delta H^{vH}(T)$ does not agree with $\Delta H^{cal}(T)$. However, no assumptions for the thermodynamic states other than the assumed two thermodynamic states are necessary in the double deconvolution. If the system consists of the two states, and if these states are exclusive to each other, their total molar fraction becomes 1 at any temperature in the deconvolution. In the previous section, I proved that this condition is equivalent to the condition that $\Delta H^{cal}(T)$ agrees with $\Delta H^{vH}(T)$ at any temperature.

In the double deconvolution, it sometimes happens that the total molar fraction of the assumed two states exceeds one. This difficulty occurs (1) when the two states are not exclusive to each other, (2) when the system includes intermolecular interactions, or (3) when we assume the heat capacity function of the state to be incorrect.

Traditionally, all the assumed thermodynamic states are considered to be exclusive to each other a priori. However, it is not certain that any two assumed thermodynamic states can always be considered exclusive. The exclusive properties of thermodynamic states must be considered seriously, for example, when we deal with the low-temperature denaturation of protein. In theory, the heat-denatured state is expected to become stable again when the temperature is decreased (Privalov et al. 1986). In this case the thermodynamic state, which is dominant in the lower temperature range, and the heat-denatured state are not

expected to be exclusive to each other.

In respect to case (2) above, if self-association or dissociation occurs during the denaturation of proteins, for example, the $\Delta H^{vH}(T)$ will exceed $\Delta H^{cal}(T)$, and the same time, the sum of $f_i(T)$ and $f_j(T)$ will exceed 1. I will discuss the deconvolution method for this kind of system in the next chapter in detail.

With regard to case (3) above, I must point out that some particular data points of the calorimetric measurement are used selectively for the determination of the heat capacity function of thermodynamic states in this method. If we use an incorrect heat capacity function, the results of the recurrent procedure will be different from the true one. Since the observed data are the sum of the true heat capacity function of the system and Gaussian noise, the best way to analyze the data may be a least-squares method. The heat capacity functions should be determined so as to satisfy all the experimental data. A least-squares method applied to the determination of the thermodynamic functions deals with all the data points equally (see Chapter 2 and 3).

The effect of the ambiguous assumptions of two constants, h_i and z_i, is shown in the section on the theory of deconvolution. In the theory of Freire and Biltonen (1978a), h_i and z_i are taken implicitly as 0 and 1, respectively. In almost all cases, there will be no reason to take any other values than these initially. One way to improve these approximations is to modify these values after the calculation of thermodynamic functions and populations

of other states at $T = T_i$, and to redeconvolute the data using the modified values of h_i and z_i, until these values converge. Generally, this procedure should include the modification of the heat capacity functions of the states. But if we try to modify these functions in each step, the recursive procedure will become very complicated, and we had better use a simpler method such as least-squares method.

The parameter-fitting problem becomes nonlinear as shown in the next chapter. An iterating procedure such as the Gauss-Newton method is necessary in order to search for the minimum of the residual sum of squares, and this generally requires a good initial parameter set. If the initial parameters greatly deviate from the true ones, a long time is required to search for the minimum or the iteration may end at the local minimum. Moreover, we first assume the number of the states in the fitting model.

We can use the results of the deconvolution of the previous section for determining the state number of the fitting model and the initial values of the parameters. I will discuss the fitting method using the double deconvolution to analyze the multistate thermal denaturation of a globular protein in Chapter 3.

Table 1.1

Parameters for three-state model

State-i	State-1	State-2	State-3
$\frac{d}{dT}C_i$ [a] ($JK^{-2}mol^{-1}$)	130	130	130
$C_i(320)$ ($kJK^{-1}mol^{-1}$)	22	25	28
$\Delta H_{1i}(320)$ [b] (kJ/mol)	0	200	400
Tm_{1i} [c] (K)	–	320	320

The heat capacity functions $C_1(T)$, $C_3(T)$ and the difference enthalpy function $\Delta H_{13}(T)$ are determined to simulate the thermal denaturation of lysozyme. The heat capacity functions of native and heat-denatured states of this protein were reported to be linear functions on temperature whose temperature dependences $\frac{d}{dT}C_i(T)$ (i=1,3) are the same, 131 $JK^{-2}mol^{-1}$. The heat capacity of the native state at 293 K was reported to be about 18.5 $kJK^{-1}mol^{-1}$ and that of the denatured state was reported to be greater than this by about 6 $kJK^{-1}mol^{-1}$. Then, at 320 K these heat capacity functions are about 22 $kJK^{-1}mol^{-1}$ and 28 $kJK^{-1}mol^{-1}$, respectively. The difference enthalpy value at 320 K was reported to be about 400 $kJK^{-1}mol^{-1}$ (Khechinashvili et al. 1973, Privalov et al. 1974)

In this model, the difference enthalpy function of the intermediate state (state-2), $\Delta H_{12}(T)$ is determined as it satisfies the following equation:

$$\Delta H_{12}(T) = \Delta H_{13}(T) / 2$$

For example, if the protein consists of two independent domains whose enthalpy functions are the same, the intermediate state of the thermal denaturation has the half difference enthalpy function of the completely heat-denatured state.

Temperature range of the data is from 280 K to 360 K. The number of data points is 401, and the temperature interval of the data points is 0.2 K.

a) $C_i(T)$ is the heat capacity function of i-th state. $\frac{d}{dT}C_i(T)$ is constant. Thus, $C_i(T)$ is a linear function on temperature. T is absolute temperature.

b) $\Delta H_{1i}(T)$ is the enthalpy difference of i-th state referred from 1-st state. In this model, $\Delta H_{1i}(T)$ becomes a linear function on temperature because the $C_i(T)$s are linear functions and the $\frac{d}{dT} C_i(T)$ (i=1,2,3) are the same in all the states.

c) Tm_{1i} means the equimolar-fraction temperature of 1-st and i-th state. At this temperature, the Gibbs free energies of these states are equal ($G_i(T) = G_1(T)$ at $T = Tm_{1i}$).

Figure captions

Fig.1.1 Typical data of scanning calorimetry, C(T), (solid line). Two assumed heat capacity functions, $C_i(T)$, $C_j(T)$, (broken lines). $\Delta H_i(T)$ and $-\Delta H_j(T)$ at T = 322 K are represented by the hatched areas.

Fig.1.2 Results of the single and double deconvolution and the two-state analysis of test data whose parameters are listed in Table 1.1. I use the true heat capacity functions of state-1 and state-3 in the table for the analysis.

(a) 1;$\Delta H_1(T)$, 2;$\Delta H_1^{(1)}(T)$, 3;$\Delta H_1^{(1,3)}(T)$ (where $h_1=h_3=0$, $z_1=z_3=1$, $T_1=280$ K, and $T_3=360$ K are used) and 4;$\Delta H_1^{(1,3)}(T)^{true}$ (where true values of h_i and z_i are used) which can not be distinguished from $\Delta H_{12}(T)$ calculated from Table 1.

(b) 1;test data C(T), 2;$C_1^{(1)}(T)$, 3;$C_1^{(1,3)}(T)$ ($h_1=h_3=0$, $z_1=z_3=1$, $T_1=280$ K, and $T_3=360$ K are used) and 4;$C_1^{(1,3)}(T)^{true}$ (where true values of h_i and z_i are used) which is identical to $C_2(T)$ calculated from Table 1.1.

(c) 1;calculated calorimetric enthalpy function, $\Delta H^{cal}(T)$, which can not be distinguish with line 2;$\Delta H_{13}(T)$ evaluated from Table 1.1, 3;calculated van't Hoff enthalpy function, $\Delta H^{vH}(T)$, ($h_1=h_3=0$ is assumed) and 4;true van't Hoff enthalpy function $\Delta H^{vH}(T)^{true}$ where true values of h_1 and h_3 are used.

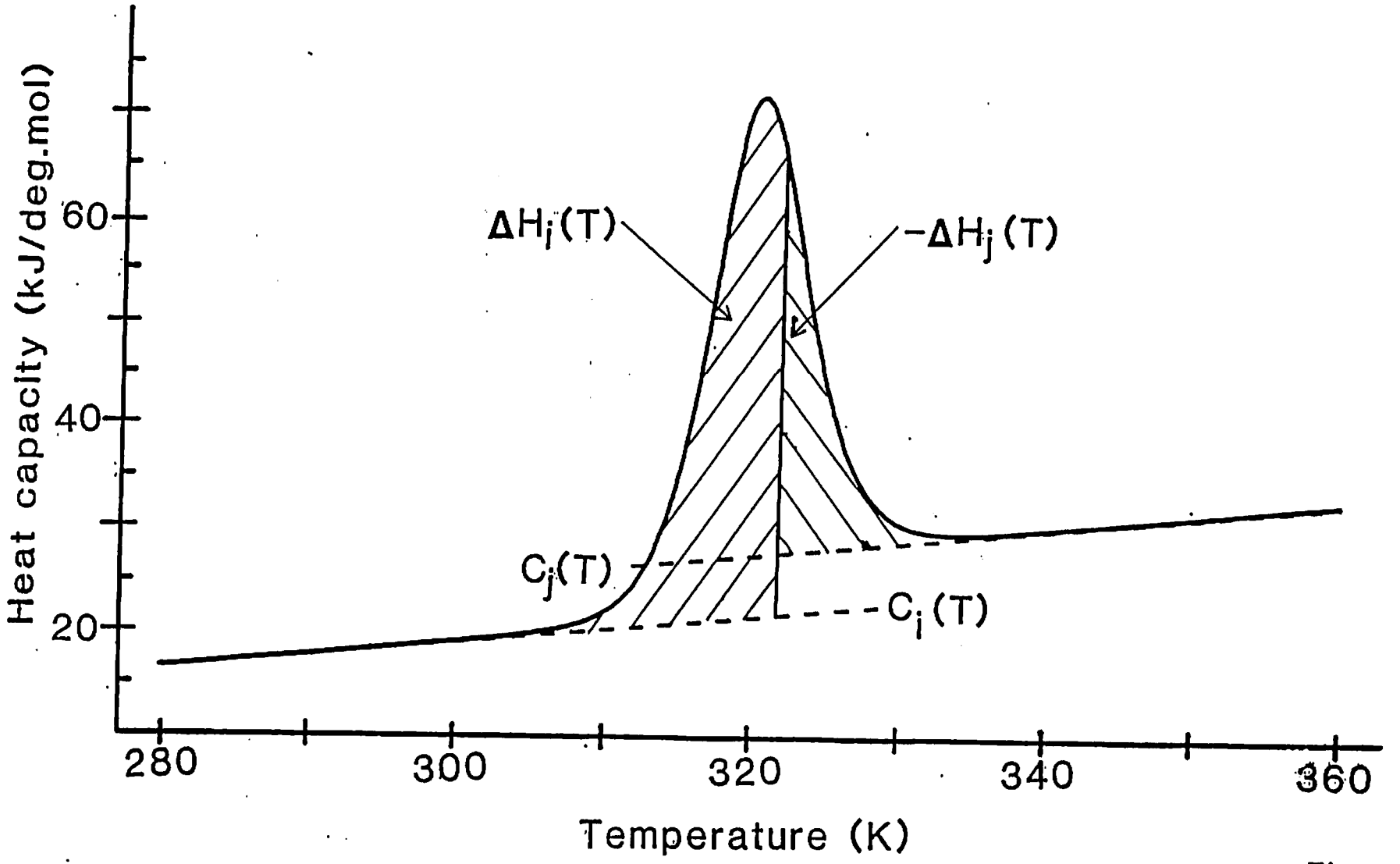
Heat capacity (kJ/deg.mol)
60
40
20
280
300
320
340
360
Temperature (K)
ΔHi(T)
-ΔHj(T)
Cj(T)
Ci(T)

Fig. 1.1

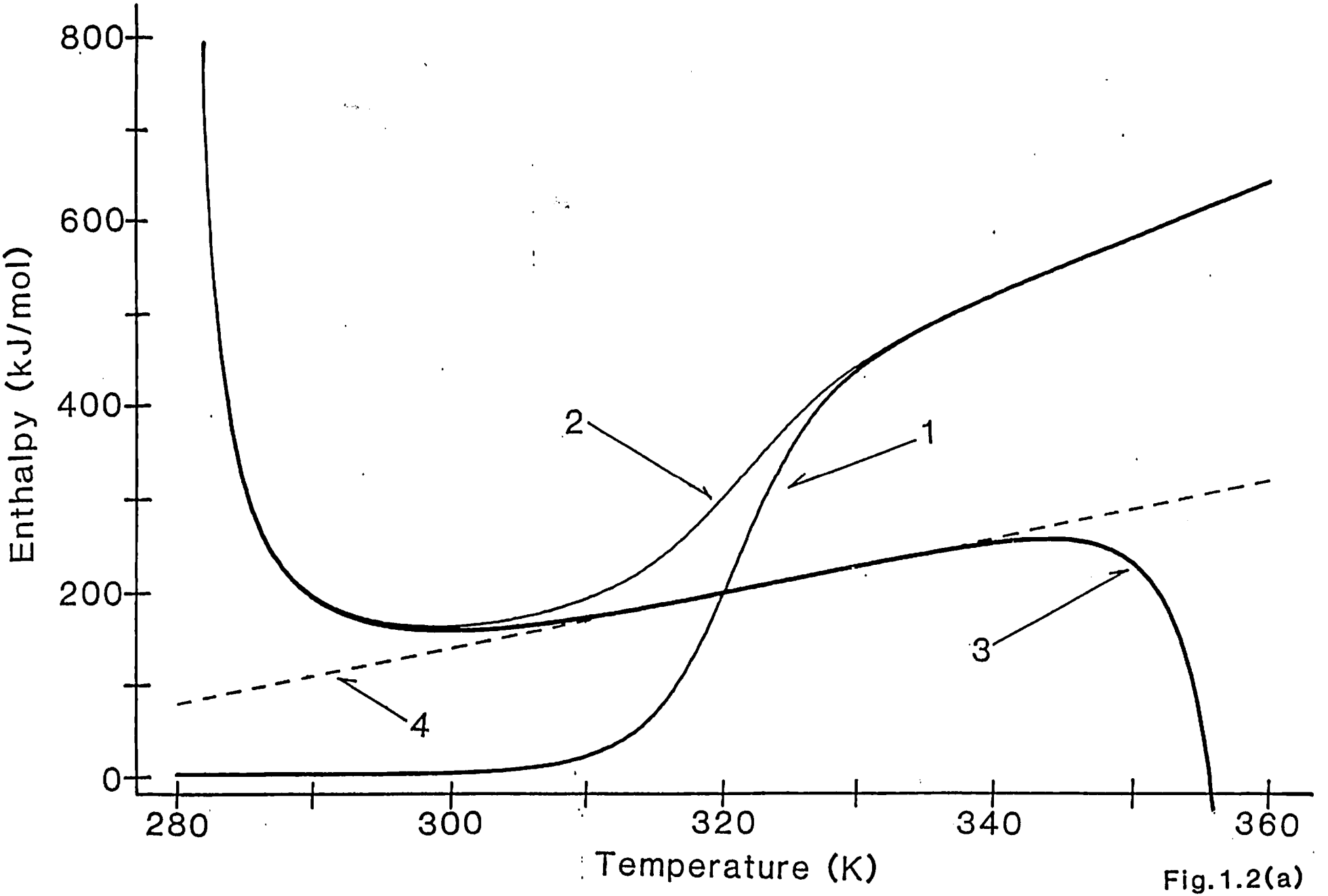
800
600
400
200
0
Enthalpy (kJ/mol)
280
300
320
340
360
Temperature (K)
1
2
3
4

Fig.1.2(a)

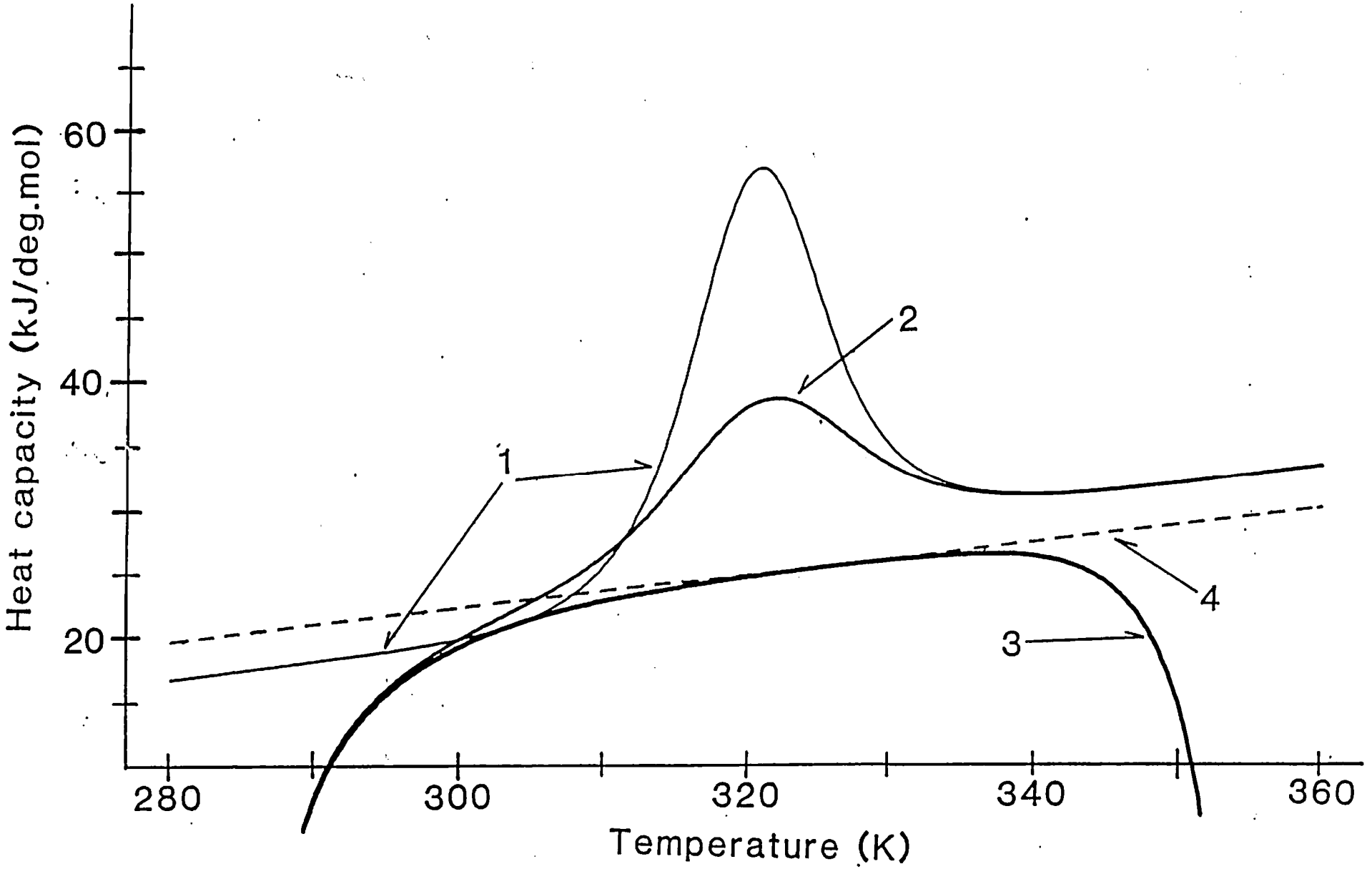
Heat capacity (kJ/deg.mol)
60
40
20
280
300
320
340
360
Temperature (K)
1
2
3
4

Fig. 1.2(b)

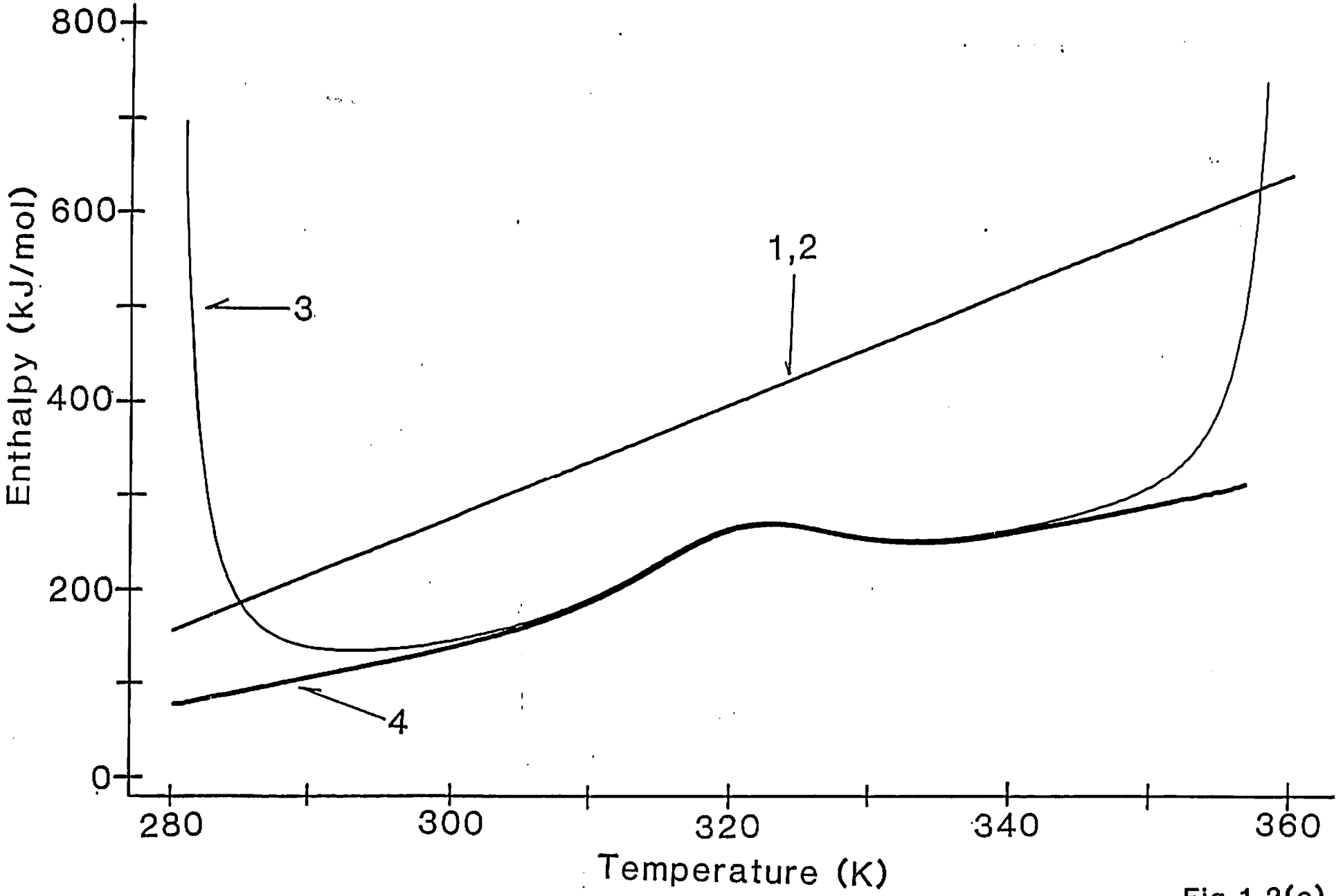
800
600
400
200
0
Enthalpy (kJ/mol)
1,2
3
4
280
300
320
340
360
Temperature (K)

Fig.1.2(c)

Chapter 2. Statistical thermodynamic analysis of calorimetry data for the system that includes self-dissociation/association process

Abstract

The basic relations between the molar fractions and the scanning calorimetry data for the system that includes self-dissociation/association process such as

$$m_0A_0 \rightleftarrows m_1A_1 \rightleftarrows m_2A_2 \rightleftarrows \cdots \rightleftarrows m_nA_n$$

are presented, where m_i is the stoichiometric coefficient of the i-th state A_i. The relations are described for each state-j as

$$\frac{d}{dT}\left[-m_j \log f_j(T) + \sum_i m_i f_i(T) \right] = \Delta H_j(T)/RT^2$$

where $f_j(T)$ is the molar fraction function of state-j, and $\Delta H_j(T)$ is the difference enthalpy function of the system referred to the state-j, which can be obtained by scanning calorimetry; R is the gas constant; and T is the absolute temperature. By these relations, scanning calorimetry data can be deconvoluted in order to determine the thermodynamic functions by means of single and double deconvolution. The concentration dependence of the data is analyzed by a method presented in this chapter. The non-linear least-squares fitting method for the determination of the functions is discussed. For an example of the application of this method to the actual scanning calorimetry

data, thermodynamic data of multistate thermal transition of Vibrio parahaemolyticus hemolysin are analyzed.

2.1 Introduction

Many scanning calorimetry data of macromolecules such as proteins, tRNAs, and DNAs have been reported with high precision. These investigations give the heat capacity functions of the system, and we can easily obtain the enthalpy functions by integrating them. Direct observation of the thermodynamic functions is the most distinctive feature of calorimetry.

By comparing the calorimetric enthalpy function, $\Delta H^{cal}(T)$, with the van't Hoff enthalpy function, $\Delta H^{vH}(T)$, we can find whether the transition of the system is two-state mechanism or not (Chapter 1). When $\Delta H^{vH}(T)$ is smaller than $\Delta H^{cal}(T)$ over all the temperature region, it indicates that the transition is a multi-state one as shown in the previous chapter, while, if $\Delta H^{vH}(T)$ is greater than $\Delta H^{cal}(T)$, it indicates that there exist some inter-molecular interactions.

The deconvolution method of calorimetry data for the isomeric reaction including native N, denatured D, and intermediate states I_i,

$$N \rightleftarrows I_1 \rightleftarrows I_2 \rightleftarrows \ldots \rightleftarrows D$$

was presented by Freire and Biltonen (1978a), and I developed a new deconvolution method in the previous chapter.

Some calorimetric investigations about thermal denaturation of oligomeric proteins such as Streptomyces subtilisin inhibitor (SSI, Takahashi & Sturtevant 1981) and Staphylococcul nuclease (Calderon et al. 1985) have been reported recently. In the

latter case, a value of the ratio $\Delta H^{vH}(T)/\Delta H^{cal}(T)$ is 1.45 at pH 7.0 at the temperature of the maximal excess heat, and the temperature is independent of the protein concentration. They concluded that the protein is partially dimerized and that the extent of dimerization of unfolded protein is the same as that of the native protein. This conclusion means that their model includes at least four species, namely, native monomer, native dimer, denatured dimer, and denatured monomer. Only an isomeric two-state analysis, however, was applied to their detailed experimental data. In the former case, the experimental data were apparently able to be fitted well by their two-state model including the dissociation process of the dimeric protein. The van't Hoff enthalpy which is calculated by their two-state model is, however, 1.65 times as large as the calorimetric enthalpy. It was stated in their paper that this results "can only be accounted for on the basis of some degree of intermolecular (dimer-dimer) cooperation."

For the multi-state system including the reaction of self-dissociation and association, however, no deconvolution method has been presented yet. In this chapter, I present a novel deconvolution method for the system as follows. Basic relations between molar fraction functions and calorimetry data are presented in Section 2.2. Using the relations, deconvolution methods for the system in order to determine the thermodynamic functions from the scanning calorimetry data are described in Sections 2.3 and 2.4. Defining a van't Hoff enthalpy function for the system, a two-state analysis is presented in Section 2.5.

The concentration dependence of the reaction, which is a distinctive feature of the system, is also analyzed by our new method in Section 2.6. A least-squares method for the system is discussed in Section 2.7. A simulated model, with three states, namely, dimeric native state, monomeric denatured state, and tetrameric intermediate state, as are expected in the case of SSI, is analyzed by our procedure in order to show how our deconvolution method works. An application of this method to the actual scanning calorimetry data of Vibrio parahaemolyticus hemolysin is presented.

2.2 Basic relations between molar fraction functions and calorimetry data

We consider a general equilibrium equation

$$m_0A_0 \rightleftarrows m_1A_1 \rightleftarrows m_2A_2 \rightleftarrows \ldots \rightleftarrows m_nA_n \qquad (2.1)$$

where m_i (i=0,1,2,....,n) is the stoichiometric coefficient of the i-th state A_i. In this chapter, I discuss the thermodynamics of equilibrium systems, and I assume that the all species A_i of Eq.(2.1) are in equilibrium. When they are in equilibrium, the thermodynamic properties are obtained only from the Gibbs free energies of the thermodynamic states, and they do not depend on the actual pathway of the reaction.

Two kinds of thermodynamic equations on which my theory is based are

$$\frac{(A_j)^{m_j}}{(A_i)^{m_i}} = \exp[\, -\Delta G_{ij}(T)/RT\,] \qquad (2.2)$$

and

$$\sum_i \frac{1}{m_i}(A_i) = M \qquad (2.3)$$

where (A_i) indicates the molar concentration of the i-th thermodynamic state. Eq.(2.2) represents the law of mass action, and Eq.(2.3) represents the mass conservation law. M is

conserved during the reaction, and named as the reduced molar concentration. The Gibbs free energy difference is defined as

$$\Delta G_{ij}(T) = m_j G_j(T) - m_i G_i(T) \qquad (2.4)$$

where $G_i(T)$ is the molar Gibbs free energy of the i-th state. In this chapter, the thermodynamic functions of the system, such as the heat capacity function, $C(T)$, the enthalpy function, $H(T)$, and the thermodynamic differences between two states; the Gibbs free energy changes, $\Delta G_{ij}(T)$, and the enthalpy differences, $\Delta H_{ij}(T)$, are described by the unit per mole of the reduced molar concentration. On the other hand, the thermodynamic functions of a thermodynamic state such as $G_i(T)$, $H_i(T)$ and $C_i(T)$ are described by the unit per mole of the i-th state A_i.

The molar fraction function of the i-th state is defined by

$$f_i = \frac{1}{Mm_i} \ (A_i) \qquad (i=0,1,2,\ldots,n) \qquad (2.5)$$

Using the functions, Eq.(2.3) becomes

$$\sum_i f_i = 1 \qquad (2.6)$$

and Eq.(2.2) becomes

$$\frac{(m_j f_j)^{m_j}}{(m_i f_i)^{m_i}} = \exp(- \Delta G^a_{ij}(T)/RT) \qquad (2.7)$$

where the apparent Gibbs free energy difference is defined as

$$\Delta G^{a}_{ij}(T) = m_j G^{a}_{j}(T) - m_i G^{a}_{i}(T) \qquad (2.8)$$

and the apparent Gibbs free energy of the i-th thermodynamic state is defined as

$$G^{a}_{i}(T) = G_i(T) + RT \log M \qquad (2.9)$$

It is worthwhile to notice the following relations:

$$\Delta G^{a}_{ij}(T) = \Delta G_{ij}(T) + (m_j - m_i)\, RT \log M \qquad (2.10a)$$

$$\Delta S^{a}_{ij}(T) = \Delta S_{ij}(T) - (m_j - m_i)\, R \log M \qquad (2.10b)$$

$$\Delta H^{a}_{ij}(T) = \Delta H_{ij}(T) \qquad (2.10c)$$

where the enthalpy difference, $\Delta H_{ij}(T)$, is defined as

$$\Delta H_{ij}(T) = m_j H_j(T) - m_i H_i(T) \qquad (2.11)$$

and other thermodynamic difference functions are defined similarly.

The distinctive feature of the systems which include self-dissociation/association process is that the molar fraction function, f_i, is not only a function of temperature but also a

function of the reduced molar concentration as seen in Eqs.(2.7), and (2.10a). In order to avoid the complexity, however, the concentration dependence of the thermodynamic functions is not described explicitly in this chapter.

I present my theory using molar concentration as the unit of concentration. The molar concentration unit seems to be too large as typical protein concentrations for the precise scanning calorimetry experiments are of the order of 10^{-5} mol/l. Theoretically, however, any order of molar concentration such as μmol/l (micro mole per liter) can be used instead of mol/l, and then the Gibbs free energy $G_i(T)$ and entropy $S_i(T)$ are given as values at the concentration of the unit in μmol/l. It is rather the relative ratios of the concentrations among the different samples examined than the absolute ones that make differences of their apparent Gibbs free energies. Therefore we do not indicate the unit of the concentration explicitly, and $G_i(T)$ and $S_i(T)$ are considered to be the values at the currently used concentration unit (10^{-5} mol/l, μmol/l, etc.).

The molar enthalpy function of the whole system, H(T), is defined as

$$H(T) = \sum_i \frac{(A_i)}{M} H_i(T) \qquad (2.12a)$$

Using Eq.(2.5), we obtain

$$H(T) = \sum_i m_i f_i(T) H_i(T) \qquad (2.12b)$$

From Eq.(2.7), the following equation holds:

$$\frac{d}{dT}\left(m_j \log f_j - m_i \log f_i\right) = \frac{d}{dT}\left[-\Delta G^{a}_{ij}(T)/RT\right]$$

$$= \frac{\Delta H_{ij}(T)}{RT^2} \qquad (2.13)$$

Therefore, the following equation holds:

$$f_i m_j \frac{d}{dT} \log f_j - m_i \frac{d}{dT} f_i = (m_j H_j f_i - m_i H_i f_i)/RT^2$$

Summing up with the suffix, i, of both sides of the equation from 0 to n, we obtain

$$m_j \frac{d}{dT} \log f_j - \sum_i m_i \frac{d}{dT} f_i = (m_j H_j - H)/RT^2$$

Therefore we obtain finally,

$$\frac{d}{dT}\left(-m_j \log f_j + \sum_i m_i f_i\right) = \Delta H_j/RT^2 \qquad (2.14)$$

where the difference enthalpy function of the system referred to j-th state, $\Delta H_j(T)$, is defined as

$$\Delta H_j(T) = H(T) - m_j H_j(T) \qquad (2.15)$$

and this function can be calculated directly from scanning calorimetry data as shown in the next section.

Equations (2.6) and (2.14) are the basic equations for the deconvolution of the system described in Eq.(2.1). It is worthwhile to point out that the molar fraction function, f_j, cannot be determined only from $\Delta H_j(T)$ unless all the stoichiometric coefficients are the same. If all the stoichiometric coefficients, m_i (i=0,1,2,...n), are 1, Eq.(2.14) becomes

$$-\frac{d}{dT}\log f_j(T) = \Delta H_j(T)/RT^2 \qquad (2.16)$$

which was the basic equation for the deconvolution of isomeric mechanism discussed in the previous chapter. In this case, the molar fraction function $f_j(T)$ can be calculated from $\Delta H_j(T)$ only.

Equation (2.14) is derived also by the statistical mechanical treatment as shown in the Appendix.

2.3 Single deconvolution

By scanning calorimetry, the heat capacity function of the system, $C(T)$, is measured within some temperature region. When we assume one heat capacity function of a thermodynamic state, $m_i C_i(T)$, we can calculate the difference heat capacity function, $\Delta C_i(T)$, as

$$\Delta C_i(T) = C(T) - m_i C_i(T) \tag{2.17}$$

From the function, the difference enthalpy function referred to the i-th state is calculated as

$$\Delta H_i(T) = \int_{T_i}^{T} \Delta C_i(T)\, dT + \Delta H_i^* \tag{2.18}$$

where a constant ΔH_i^* is assumed to be $\Delta H_i(T_i)$. It should be noticed that what we must assume is the heat capacity function of the state per mole of the reduced concentration, $m_i C_i(T)$, (see Fig.2.1). There is no need to assume the value of m_i in this stage, namely for the calculation of the difference heat capacity function and the difference enthalpy function.

When we obtain the difference enthalpy function, $\Delta H_0(T)$, we can calculate the molar fraction function of 0-th state if we assume that the system can be described by the following two-state model.

$$m_0 A_0 \rightleftarrows m_1 A_1 \tag{2.19}$$

From Eqs.(2.6) and (2.14), the following equations hold:

$$\frac{d}{dT}\left(-m_0 \log f_0 + m_0 f_0 + m_1 f_1 \right) = \Delta H_0/RT^2 \qquad (2.20a)$$

$$f_0 + f_1 = 1 \qquad (2.20b)$$

By Eq.(2.20b), f_1 in Eq.(2.20a) is eliminated as

$$\frac{d}{dT}\left[-m_0 \log f_0 + (m_0 - m_1) f_0 \right] = \Delta H_0/RT^2 \qquad (2.21)$$

Integrating both sides of the equation from T_0 to T, we obtain

$$m_0 \log[f_0(T)/f_0^*] - (m_0 - m_1)[f_0(T) - f_0^*] + F_0(T) = 0 \qquad (2.22)$$

where we must assume a constant f_0^* as $f_0(T_0)$, and $F_0(T)$ is defined as

$$F_0(T) = \int_{T_0}^{T} \Delta H_0(T)/RT^2 \, dT \qquad (2.23)$$

The numerical solutions of Eq.(2.22) at various temperatures give the molar fraction function, $f_0(T)$.

Considering the left hand side of Eq.(2.22) is a function of f_0, $J(f_0)$ is defined as

$$J(f_0) = m_0 \log(f_0/f_0^*) - (m_0-m_1)(f_0 - f_0^*) + F_0$$

It can be easily shown that the following equations hold.

$$J(0) = -\infty$$

$$J(f_0^*) = F_0$$

$$\frac{d}{df} J(f) = m_0(1-f)/f + m_1 > 0 \qquad (0 < f < f_0^* \leq 1)$$

Because F_0 is usually positive, and $J(f)$ is a continuous function, the above conditions indicate that only one solution of Eq.(2.22) exists between 0 and f_0^*. I use Newton's method to solve the equation.

As the system was assumed to be two-state, we can describe $\Delta H_0(T)$ as

$$\Delta H_0(T) = \Delta H_{01}(T) f_1(T) \tag{2.24}$$

Then we can calculate $\Delta H_{01}(T)$ from experimental data as

$$\Delta H_{01}(T) = \frac{\Delta H_0(T)}{f_1(T)} = \frac{\Delta H_0(T)}{1-f_0(T)} \tag{2.25}$$

When we differentiate both sides of Eq.(2.25), we obtain

$$\Delta C_{01}(T) = \frac{\Delta C_0(T)}{1-f_0(T)} - \frac{\Delta H_0(T)^2 f_0(T)}{RT^2(1-f_0(T))^2[(m_1-m_0)f_0(T)+m_0]} \quad (2.26)$$

As the following equation holds, we can calculate $C_1(T)$.

$$m_1C_1(T) = m_0C_0(T) + \Delta C_{01}(T) \quad (2.27)$$

These procedure is called single deconvolution for the system which includes self-dissociation/association process.

It is worth noting that if the system consists of more thermodynamic states than two, and all the stoichiometric coefficients of the states other than state-0 are the same, namely, if the following equation holds in Eq.(2.1);

$$m_1 = m_2 = \ldots = m_n$$

it is easy to show that the single deconvolution is exact even in this system. In this case, however, we must denote the calculated functions $\Delta H_{01}(T)$ and $m_1C_1(T)$ as $\Delta H_0^{(0)}(T)$ and $C^{(0)}(T)$, respectively. They were defined as the hypothetical functions which would be observed if the system did not include 0-th state. The hypothetical functions were introduced in the previous chapter. In this case, they are defined as

$$\Delta H_0^{(0)}(T) = H^{(0)} - m_0H_0(T) \quad (2.28a)$$

where

$$H^{(0)}(T) = m_1 \sum_{i=1}^{n} H_i(T) f_i(T) \qquad (2.28b)$$

and

$$C^{(0)}(T) = \frac{d}{dT} H^{(0)}(T) \qquad (2.29)$$

Regarding $C^{(0)}(T)$ as the heat capacity function of a given system, we may continue the deconvolution. It should be noted that $C^{(0)}(T)/m_1$ is the heat capacity function of an isomeric reaction described by the unit per mole of the system. The scanning calorimetry data of such an isomeric system can be deconvoluted as discussed in the previous chapter.

2.4 Double deconvolution

When we assume more general model including one intermediate state-1 such as

$$m_0A_0 \rightleftarrows m_1A_1 \rightleftarrows m_2A_2 \qquad (2.30)$$

we must know $\Delta H_0(T)$ and $\Delta H_2(T)$ for the deconvolution using the following equations [see Eqs.(2.6) and (2.14)]:

$$\frac{d}{dT}\left(-m_0 \log f_0 + m_0 f_0 + m_1 f_1 + m_2 f_2 \right) = \Delta H_0/RT^2 \qquad (2.31a)$$

$$\frac{d}{dT}\left(-m_2 \log f_2 + m_0 f_0 + m_1 f_1 + m_2 f_2 \right) = \Delta H_2/RT^2 \qquad (2.31b)$$

$$f_0 + f_1 + f_2 = 1 \qquad (2.31c)$$

When we eliminate $f_1(T)$ in Eqs.(2.31a) and (2.31b) by Eq.(2.31c) and integrate Eqs.(2.31a) and (2.31b) from T_0 to T and from T_2 to T, respectively, we obtain

$$m_0 \log(f_0/f_0^*) - (m_0-m_1)(f_0-f_0^*) - (m_2-m_1)(f_2-f_2^{**}) + F_0 = 0 \qquad (2.32a)$$

$$m_2 \log(f_2/f_2^*) - (m_0-m_1)(f_0-f_0^{**}) - (m_2-m_1)(f_2-f_2^*) + F_2 = 0 \qquad (2.32b)$$

where the four constants f_0^*, f_0^{**}, f_2^* and f_2^{**} are assumed to be $f_0(T_0)$, $f_0(T_2)$, $f_2(T_2)$ and $f_2(T_0)$, respectively. $F_0(T)$ is the

same function as defined in Eq.(2.23), and $F_2(T)$ is defined similarly by

$$F_2(T) = \int_{T_2}^{T} \Delta H_2(T)/RT^2 \, dT$$

When we analyze the experimental data, usually we should choose the temperature T_0 and T_2 where f_0^* and f_2^* can be regarded as 1, and f_0^{**} and f_2^{**} as 0. From Eqs.(2.32a) and (2.32b), we obtain

$$\log \left(\frac{f_0^{m_0}(T)}{f_0^{*m_0}} \Big/ \frac{f_2^{m_2}(T)}{f_2^{*m_2}} \right) = \Delta F_{02}(T) \qquad (2.33)$$

where

$$\Delta F_{02}(T) = F_2(T) + (m_2-m_1)(f_2^*-f_2^{**}) - [\, F_0(T) + (m_0-m_1)(f_0^*-f_0^{**}) \,] \qquad (2.34)$$

By Eq.(2.33), we can eliminate $f_0(T)$ or $f_2(T)$, and Eqs.(2.32a) and (2.32b) become

$$m_0 \log(f_0/f_0^*) - (m_0-m_1)(f_0-f_0^*) - (m_2-m_1)[f_2^*(f_0/f_0^*)^{m_0/m_2} \exp(-\Delta F_{02}/m_2) - f_2^{**}] + F_0 = 0 \qquad (2.35a)$$

$$m_2 \log(f_2/f_2^*) - (m_2-m_1)(f_2-f_2^*) - (m_0-m_1)[f_0^*(f_2/f_2^*)^{m_2/m_0} \exp(\Delta F_{02}/m_0) - f_0^{**}] + F_2 = 0 \qquad (2.35b)$$

The numerical solutions of the above two equations at each temperature give $f_0(T)$ and $f_2(T)$, respectively.

If $F_0(T)$ and $F_2(T)$ are positive and m_1 is greater than both m_0 and m_2, it is easy to show that both equations have the only one solution as similarly as shown in the single deconvolution. Actually we solve the equations by Newton's method.

As we assume that our system is described by Eq.(2.30), $\Delta H_0(T)$ can be assumed as

$$\Delta H_0(T) = \Delta H_{01}(T) f_1(T) + \Delta H_{02}(T) f_2(T) \qquad (2.36)$$

Then we can calculate $\Delta H_{01}(T)$ as

$$\Delta H_{01}(T) = \frac{\Delta H_0(T) - \Delta H_{02}(T) f_2(T)}{1 - f_0(T) - f_2(T)} \qquad (2.37)$$

where $\Delta H_{02}(T)$ is calculated as

$$\Delta H_{02}(T) = \Delta H_0(T) - \Delta H_2(T) \qquad (2.38)$$

We call this kind of the deconvolution as a double deconvolution.

Similarly to single deconvolution, when the intermediate state-1 consists of many thermodynamic states that have the same stoichiometric coefficients, the double deconvolution is exact. In this case, we must denote the calculated function $\Delta H_{01}(T)$ as $\Delta H_0^{(0,2)}(T)$. This function is defined as a hypothetical

function which would be observed if the system included neither state-0 nor state-2.

As seen in Fig.2.3, the right-hand side of Eq.(2.37) diverges at the high and low extreme temperatures even when the true model is used. The divergence occurs because we assumed the constants for the molar fraction functions, f_0^* and f_2^* as 1; f_0^{**} and f_2^{**} as 0 in Eq.(2.32a) and (2.32b), and for the difference enthalpy functions, ΔH_0^* and ΔH_2^* as 0. This is the similar situation of the deconvolution for the isomeric system (see Section 1.4). In the case of line-2 (true model) in Fig.2.3, the divergences do not appear, and the calculated function agrees with the true function even at the extreme temperatures if we use true values for the six constants.

2.5 Two-state analysis

When we calculate $\Delta C_0(T)$, $\Delta C_2(T)$ and $\Delta H_0(T)$, $\Delta H_2(T)$, and assume the stoichiometric coefficients for state-0, state-2 and the intermediate state, we can deconvolute the scanning calorimetry data as shown in the previous section and calculate the molar fraction function of the intermediate state $f_1(T)$ as

$$f_1(T) = 1 - f_0(T) - f_2(T) \tag{2.39}$$

If the function can be regarded as zero within the experimental error, the system can be described by the two-state model including only state-0 and state-2. In this section, I present more convenient method to check whether the system can be regarded as a two-state system or not.

If we can calculate $\Delta H_i(T)$ and $\Delta H_j(T)$, we obtain a calorimetric enthalpy function as similarly as the isomeric reaction by

$$\Delta H^{cal}(T) = \Delta H_i(T) - \Delta H_j(T) \tag{2.40}$$

It is the same function as $\Delta H_{ij}(T)$ which is an enthalpy difference between state-i and state-j as seen in Eqs.(2.11) and (2.15).

When we assume that the system consists of only these two states such as

$$m_i A_i \rightleftarrows m_j A_j \tag{2.41}$$

we can assume

$$\Delta H_i(T) = \Delta H_{ij}(T) f_j(T) \tag{2.42a}$$

$$\Delta H_j(T) = - \Delta H_{ij}(T) f_i(T) \tag{2.42b}$$

The equilibrium constant between state-i and state-j, $K_{ij}(T)$, is defined as

$$K_{ij}(T) = \frac{(A_j)^{m_j}}{(A_i)^{m_i}} = \frac{(m_j f_j)^{m_j}}{(m_i f_i)^{m_i}} M^{m_j - m_i} \tag{2.43}$$

Using Eqs.(2.42a) and (2.42b), $K_{ij}(T)$ can be described without f_i and f_j as

$$K_{ij}(T) = \frac{(m_j \Delta H_i)^{m_j}}{(-m_i \Delta H_j)^{m_i}} (\Delta H_{ij}/M)^{m_i - m_j} \tag{2.44}$$

A van't Hoff enthalpy function is defined as

$$\Delta H^{vH}(T) = RT^2 \frac{d}{dT} \log K_{ij}(T)$$

and from Eq.(2.44) it is easily calculated as

$$\Delta H^{vH}(T) = RT^2 [m_j \frac{\Delta C_i(T)}{\Delta H_i(T)} - m_i \frac{\Delta C_j(T)}{\Delta H_j(T)} + (m_i - m_j) \frac{\Delta C_{ij}(T)}{\Delta H_{ij}(T)}] \tag{2.45}$$

If the system really consists of the two states, the van't Hoff enthalpy function must be equal to the calorimetric enthalpy function.

Reversely, if the van't Hoff enthalpy function agrees with the calorimetric enthalpy function, namely

$$\Delta H^{cal}(T) = \Delta H^{vH}(T)$$

the following equation holds:

$$\Delta H_{ij}(T) = RT^2[m_j\frac{\Delta C_i(T)}{\Delta H_i(T)} - m_i\frac{\Delta C_j(T)}{\Delta H_j(T)} + (m_i - m_j)\frac{\Delta C_{ij}(T)}{\Delta H_{ij}(T)}] \tag{2.46}$$

When I define $f_i(T)$ and $f_j(T)$ as

$$f_i(T) = -\Delta H_j(T)/\Delta H_{ij}(T) \tag{2.47a}$$

$$f_j(T) = \Delta H_i(T)/\Delta H_{ij}(T) \tag{2.47b}$$

it is easy to shown that $f_i(T)$ and $f_j(T)$ satisfy the following equations using Eq.(2.46):

$$\frac{d}{dT}\left(-m_i \log f_i + m_i f_i + m_j f_j \right) = \frac{\Delta H_i(T)}{RT^2} \tag{2.48a}$$

$$\frac{d}{dT}\left(-m_j \log f_j + m_i f_i + m_j f_j \right) = \frac{\Delta H_j(T)}{RT^2} \qquad (2.48b)$$

$$f_i(T) + f_j(T) = 1 \qquad (2.48c)$$

This fact proves that the system can be described by the following two-state model,

$$m_i A_i \rightleftarrows m_j A_j \qquad (2.49)$$

The divergences of the right-hand side of Eq.(2.45) appear at the extreme temperatures as seen in Fig.2.2. Even if the real reaction mechanism is two-state, and the exact model and the exact heat capacity functions of the two states are used for the calculation of the van't Hoff enthalpy function, the divergences will occur unless the true constants are used for calculating the difference enthalpy functions in Eq.(2.18). Thus the van't Hoff enthalpy function must be compared with the calorimetric enthalpy function avoiding the region of the divergences.

2.6 Concentration dependence analysis of calorimetry data

What we have discussed above is about how to determine the thermodynamic functions from scanning calorimetry data at one fixed concentration of a sample. We can check whether the assumed model for the deconvolution is appropriate or not by comparing the heat capacity data at various concentrations.

One of the simplest checking points is whether the enthalpy difference between any two thermodynamic states, $\Delta H_{ij}(T)$, does not depend on the reduced molar concentration, M. From Eq.(2.10c), $\Delta H_{ij}(T)$ must be same among all the concentration data if the assumption for calculation of the thermodynamic function is proper. The condition that $\Delta H_{ij}(T)$ between any two states does not depend on the concentration is, however, a necessary factor but not a sufficient factor that all the data of various concentrations can be explained by the assumed model.

We need to check the concentration dependence of other kinds of thermodynamic functions such as Gibbs free energy. The Gibbs free energy function can be calculated from the molar fraction functions of state-i and state-j as follows [see Eq.(2.43)].

$$\Delta G_{ij}(T) = -RT \log K_{ij}(T)$$

$$= -RT \log \frac{(m_j f_j)^{m_j}}{(m_i f_i)^{m_i}} - RT(m_j - m_i)\log M \qquad (2.50)$$

Using Eqs.(2.33) and (2.34), we can calculate the function directly from $\Delta H_i(T)$ and $\Delta H_j(T)$ as

$$\Delta G_{ij}(T) = RT \left[\int_{T_j}^{T} \Delta H_j(T)/RT^2 dT + m_j - m_j \log m_j \right.$$

$$\left. - \int_{T_i}^{T} \Delta H_i(T)/RT^2 dT - m_i + m_i \log m_i \right] - RT(m_j - m_i)\log M \qquad (2.51)$$

where we assume that f_0^* and f_2^* are 1, and f_0^{**} and f_2^{**} are 0. Eq.(2.51) indicates that $\Delta G_{ij}(T)$ can be calculated without the assumption of the stoichiometric coefficient of intermediate state. In other words, the calculation of $\Delta G_{ij}(T)$ does not depend on the assumption.

If the system has been confirmed to consists of two states by the two-state analysis, the Gibbs free energy difference is calculated more easily using Eq.(2.44) as

$$\Delta G_{ij}(T) = -RT \log \left[\frac{(m_j \Delta H_i)^{m_j}}{(-m_i \Delta H_j)^{m_i}} (\Delta H_{ij})^{m_i - m_j} \right]$$

$$- RT(m_j - m_i)\log M \qquad (2.52)$$

If the functions of Eqs.(2.50), (2.51) or (2.52) calculated from all the data at various concentrations agree with each other within the experimental error, it indicates that the assumed model is appropriate.

It is also clear that the apparent Gibbs free energy function, $\Delta G_{ij}^a(T)$, is calculated from the first term of Eqs.(2.50), (2.51) and (2.52) because the function is related to $\Delta G_{ij}(T)$ as Eq.(2.10a).

As seen in Fig.2.5, the curve of the Gibbs free energy difference, $\Delta G_{01}(T)$, bends upward at the extreme temperatures because the molar fraction of the intermediate state is calculated slightly smaller owing to the wrong assumptions of the constants in the double deconvolution as similarly as the divergences of the double deconvolution. Therefore, the functions must be compared with each other avoiding the bending region at the extreme temperatures.

2.7 Non-linear least-squares fitting of scanning calorimetry data

As discussed below, the double deconvolution method and the least-squares method are complementary with each other. In the double deconvolution method, there were some serious problems pointed out in the previous chapter. The problem about the ambiguities of the assumptions of the heat capacity functions and the integral constants of each state, is solved by the least-squares method by adjusting the parameters for the heat capacity functions and the constants to fit the experimental data. One more problem of the double deconvolution method is about the evaluation of the errors of the estimated thermodynamic parameters. It is difficult to know them only from the double deconvolution method especially when the recursive procedures are necessary. However, they can be calculated by the error analysis of the least-squares method using the variance-covariance matrix (e.g. see Brandt 1975). The model function of the least-squares method becomes non-linear, and it requires a good initial parameter set. Moreover, we must assume the numbers of the states of the fitting model and the stoichiometries. The double deconvolution method with the concentration dependence analysis gives the good initial parameter set and also the appropriate stoichiometry of the system.

When we assume the mechanism of Eq.(2.1), the Gibbs free energy differences of any two states, $\Delta G_{ij}(T)$, and the reduced molar concentration M, we can calculate the heat capacity function of the model system. From Eqs.(2.6) and (2.7), we

obtain

$$\sum_j \frac{(m_i f_i)^{m_i/m_j}}{m_j} \exp[-\Delta G^a_{ij}(T)/m_j RT] = 1 \qquad (2.53)$$

When we differentiate the both sides of Eq.(2.12b),

$$C(T) = \frac{d}{dT} H(T)$$

$$= \sum_i m_i C_i(T) f_i(T) + \sum_i m_i H_i(T) \frac{d}{dT} f_i(T)$$

From Eq.(2.13), we get

$$\frac{f_i}{m_i} \frac{d}{dT} f_j - \frac{f_j}{m_j} \frac{d}{dT} f_i = \frac{\Delta H_{ij}}{RT^2} \frac{f_i f_j}{m_i m_j}$$

Summing up the both sides of the above equation about suffix j, we obtain

$$\sum_j \frac{f_j}{m_j} \frac{d}{dT} f_i = - \sum_j \frac{\Delta H_{ij}}{RT^2} \frac{f_i f_j}{m_i m_j}$$

$$\therefore \sum_i m_i H_i \frac{d}{dT} f_i = - \frac{\sum_{i,j} m_i H_i \Delta H_{ij} \frac{f_i f_j}{m_i m_j}}{RT^2 \sum_j \frac{f_j}{m_j}}$$

Then we obtain the following equation finally:

$$C(T) = \sum_i m_i C_i(T) f_i(T) + \frac{\sum_{i<j} \Delta H_{ij}^2 \frac{f_i f_j}{m_i m_j}}{RT^2 \sum_i \frac{f_i}{m_i}} \qquad (2.54)$$

When we assume the Gibbs free energy differences between any two thermodynamic states, $\Delta G_{ij}(T)$, and all the stoichiometric coefficients, m_i, the molar fraction functions can be determined by solving Eq.(2.53) at each temperature. This equation can be solved by Gauss-Newton method. Then we can calculate the heat capacity function of the system by Eq.(2.54) assuming the thermodynamic functions, $m_i C_i(T)$ and $\Delta H_{ij}(T)$.

The thermodynamic functions are related with each other. When we assume the heat capacity function $m_i C_i(T)$s of all the thermodynamic states, the heat capacity differences of any two states, $\Delta C_{ij}(T)$, are determined as

$$\Delta C_{ij}(T) = m_j C_j(T) - m_i C_i(T) \qquad (2.55)$$

and the enthalpy differences, $\Delta H_{ij}(T)$, are also determined by

$$\frac{d}{dT} \Delta H_{ij}(T) = \Delta C_{ij}(T) \qquad (2.56)$$

where one integral constant must be introduced. The Gibbs free

energy differences $\Delta G_{ij}(T)$ are also determined by

$$\frac{d}{dT}\left(-\frac{\Delta G_{ij}(T)}{T}\right) = \frac{\Delta H_{ij}(T)}{T^2} \qquad (2.57)$$

where one more integral constant must be introduced.

For example, if we assume all the heat capacity functions are linear functions of temperature, they can be described as

$$m_i C_i(T) = 2a_i T + b_i \qquad (i=0,1,2,\ldots,n) \qquad (2.58)$$

where a_i and b_i are constants.

The enthalpy differences are described as

$$\Delta H_{ij}(T) = \Delta a_{ij} T^2 + \Delta b_{ij} T + \Delta c_{ij} \qquad (i,j=0,1,2,\ldots,n) \qquad (2.59)$$

where

$$\Delta a_{ij} = a_j - a_i$$

$$\Delta b_{ij} = b_j - b_i$$

and Δc_{ij} is integral constant. The Gibbs free energy difference is described as

$$\Delta G^a_{ij}(T) = -\Delta a_{ij} T^2 - \Delta b_{ij} T \log T + \Delta c_{ij} + \Delta d_{ij} T \qquad (2.60)$$

where one more integral constant Δd_{ij} must be introduced. Then if we consider the k-state model, the number of parameters for describing thermodynamic functions is 4k-2. When we adopt more restricted model, for example, in which the values of a_i of all states are the same, the number is reduced to 3k-1.

We may determine these parameters so that the model function is best fitted to the experimental data by least-squares method. It is obvious from Eq.(2.54) that this problem becomes non-linear as similarly as discussed in the previous chapter about the isomeric reaction. Therefore the iteration procedure such as Gauss-Newton method for searching the minimum point of the residual sum of squares is necessary. We must start with good initial parameter set, or the calculation will stop at a local minimum far from the true parameter values, or it will require a very long time to reach the final values.

The results of the two-state analysis, single deconvolution, double deconvolution and concentration dependence analysis will give the good initial parameter set, and they also give a good fitting model and the stoichiometric coefficients as shown in Figs.2.6 and 2.7.

For an example of the application of the method presented in this paper to the actual system, I present the analysis of the scanning calorimetry data of Vibrio parahaemolyticus hemolysin (molecular weight = 18650) briefly. These experimental data were reported previously by H. Uedaira et al.(1983). The peak temperature and the shape of the heat capacity functions of this protein depend on the protein concentration. By the monomeric

two-state analysis, the van't Hoff enthalpy function becomes larger than the calorimetric enthalpy function and at least the dimeric cooperative unit must be considered in order to explain the data.

In Table 2.2, the fittings with different models are compared. This table indicates that the most appropriate model for the experimental data is $N_2 \rightleftarrows 2I \rightleftarrows 2D$. The noise level, 0.5 μW/ml, agrees with the value reported previously (Privalov 1980). In this analysis, Δa_{ij} is fixed to zero for the three-state fitting. Even when Δb_{01} is fixed to zero, the root mean squares deviation increased only slightly in the $N_2 \rightleftarrows 2I \rightleftarrows 2D$ model. If Δb_{01} is free, the value is found to tend to become negative. The negative value means that heat capacity of the intermediate state is smaller than that of native state, and it seems to be unrealistic. I think that this is due to the overfitting of the parameters, and I adopt the three-state model with $\Delta b_{01}=0$. The fitted functions of the model and the observed heat capacity functions are plotted in Fig.2.7(a). In Table 2.3, I present the thermodynamic parameters determined by the fitting of the model. The molar fraction functions of the three states calculated by the parameters are shown in Fig.2.7(b). The results agree with the chromatographic observation that the protein molecules are dimeric in the native state (Takeda et al. 1978).

2.8 Discussion

There are two kinds of possible situations that we should check the possibility of the dissociation/association of the given system.

The first case is that the van't Hoff enthalpy function, which is calculated according to the isomeric reaction, is greater than the calorimetric enthalpy function, which is calculated per mole of the molecule. It indicates that the interaction between molecules exists in the reaction. If we apply the double deconvolution method for the isomeric reaction (see Chapter 1) the sum of the molar fraction function of the two states becomes greater than 1, and thus the deconvolution fails. If we calculate the calorimetric enthalpy function per mole of oligomers such as dimer or trimer etc., the function becomes greater than, or agree with, the van't Hoff enthalpy function of the isomeric model. However, the double deconvolution for the isomeric mechanism leads to the false results unless the oligomers do not associate or dissociate during the reaction, because the true relations between the molar fraction functions and the enthalpy function for the system including self-dissociation/association process is not Eq.(2.16) but Eq.(2.14). If the reaction of the oligomers includes neither dissociation nor association, the reaction is isomeric, and the deconvolution for the isomeric system is exact.

The second case is that the heat capacity function of the system depends on the concentration of the molecules. If the reaction is isomeric, the function must not depend on the

concentration of the molecules. If the system includes dissociation/association process, increasing the concentration leads to the shift of the equilibrium to the association at each temperature, and decreasing the concentration works contrary. Traditionally the concentration dependence are analyzed with only the temperature at which the heat capacity of the system is maximum (Takahashi & Sturtevant 1981). The method can not be applied to the multi-state system, and it needs approximations even for the two-state system. On the other hand, the method presented in this chapter can be applied to the multi-state system, and the relations are strictly exact mathematically.

When we deconvolute the data by the double deconvolution using the concentration dependence, first we must determine the stoichiometric coefficients of the initial and final state, m_0 and m_2 in Eq.(2.30). In this stage, the concentration dependence analysis may be useful. Without assuming the stoichiometric coefficient of the intermediate state, we can check whether the applied model is appropriate or not, because Eq.(2.50) does not depend on the assumption. On the other hand, the concentration dependence analysis of the intermediate state is affected by the assumed stoichiometric coefficients of the two states, m_0 and m_2.

When the appropriate stoichiometric coefficients of the two states are determined, next we must determine the stoichiometric coefficient of the intermediate state. When the molar fraction of the intermediate state is small, the determination of its stoichiometric coefficient from calorimetry data only at one concentration becomes difficult, because even the model with the slightly different stoichiometric coefficient for the

intermediate state can well fit the calorimetry data in the case of small intermediate population as seen in Fig.2.6. However, the concentration dependence analysis helps us to find out the correct model as shown in Fig.2.5.

As discussed previously, in the double deconvolution, we must assume the three-state mechanism as Eq.(2.30). If the system includes two intermediate states whose stoichiometric coefficients are different with each other, the deconvolution will give wrong results. It can be easily shown that the molar fraction function of the four states whose stoichiometric coefficients are different with each other cannot determined only from the two difference enthalpy functions, $\Delta H_0(T)$ and $\Delta H_2(T)$. This kind of limitation of the double deconvolution must be noted. Exceptionally the double deconvolution becomes exact if the stoichiometric coefficients of the intermediate states are the same as discussed previously.

Similarly if the system is multi-state, the single deconvolution, which is based on the assumptions of the two-state mechanism, can not be applied, strictly speaking. However, if the molar fractions of the other states than the two states are small within the transition region, it may give good approximated values of the thermodynamic functions of the system as shown in the case of $f_2(T)$ in Fig.2.8.

Even in the case that the double or single deconvolution can not be applied strictly as discussed above, they may be useful if they give the well approximated values for the thermodynamic functions. Using the values as the initial values of the fitting

parameters, we can improve the values by the least-squares method presented in this chapter.

When we determine the parameters with fitting to the calorimetry data at various concentrations, the parameters, Δa_{ij}, Δb_{ij} and Δc_{ij} of Eq.(2.59) must be common within the expected errors, and the parameter, Δd_{ij}, in Eq.(2.60) must show the concentration dependence as

$$\Delta d_{ij}(M) = \Delta d^{*}_{ij} + (m_j - m_i)RlogM \qquad (2.61)$$

where Δd^{*}_{ij} is a constant. If all the parameters satisfied with these relations, it shows that the assumed mechanism explain all the experimental data. The most reliable way to determine the common parameters, Δa_{ij}, Δb_{ij}, Δc_{ij}, and Δd^{*}_{ij}, may be to search the minimum point of total sum of all the residual sum of squares at various concentrations at once as shown in the analysis of hemolysin data.

The deconvolution method presented in this paper may be easily changed in order to deal with a different mechanism from Eq.(2.1). For example, I present a method for the multi-state thermal denaturation of DNA involving strand separation.

If the two strands of DNA double helix are the same (in the case of self-complementary DNA), the system will be described as

$$A_0 \rightleftarrows A_1 \rightleftarrows A_2 \rightleftarrows \cdots \rightleftarrows A_{n-1} \rightleftarrows 2A_n \qquad (2.62)$$

This equation is included in Eq.(2.1), and no modification for the analysis of this chapter is necessary to deal with the

system. If the two strands are different, the system will be

$$A_0 \rightleftarrows A_1 \rightleftarrows A_2 \rightleftarrows \cdots \rightleftarrows A_{n-1} \rightleftarrows B + C \qquad (2.63)$$

where B and C correspond to the separated state of the two different single stranded DNAs, respectively.

An attempt to deconvolute the scanning calorimetry data of these mechanism was made using the deconvolution method for an isomeric mechanism (Freire & Biltonen 1978b). However, the basic relations between the molar fraction functions and the scanning calorimetry data for isomeric system are different from those for the system including self-dissociation and association as shown in this chapter. Therefore, the method of Freire and Biltonen leads to the wrong results.

In the system of Eq.(2.63), the thermodynamic equations on which our theory is based are

$$\frac{(A_j)}{(A_i)} = \exp[\ -\Delta G_{ij}(T)/RT\ ] \qquad (i,j=0,1,\ldots,n-1) \quad (2.64)$$

$$\frac{(B)(C)}{(A_i)} = \exp[\ -\Delta G_{in}(T)/RT\ ] \qquad (i=0,1,\ldots,n-1) \quad (2.65)$$

and

$$\sum_{i}^{n-1} (A_i) + (B) = M \qquad (2.66)$$

where (A_i) indicates the molar concentration of the i-th thermodynamic state, M is the reduced concentration, and $\Delta G_{in}(T)$ is defined as

$$\Delta G_{in}(T) = 2G_n(T) - G_i(T) \tag{2.67}$$

$$G_n(T) = [G_B(T) + G_C(T)] / 2 \tag{2.68}$$

and we assume that (B)=(C) holds during the reaction. The molar fraction functions are defined as

$$f_i = (A_i) / M \qquad (i=0,1,2,\ldots,n-1) \tag{2.69a}$$

$$f_n = (B) / M \tag{2.69b}$$

Thus Eqs.(2.64), (2.65), and (2.66) are described respectively as

$$\frac{f_j}{f_i} = \exp[\ -\Delta G_{ij}(T)/RT\ ] \tag{2.70}$$

$$\frac{f_n^2}{f_i} = \exp[\ -\Delta G^a_{in}(T)/RT\ ] \tag{2.71}$$

and

$$\sum_{i=1}^{n} f_i = 1 \tag{2.72}$$

where the apparent Gibbs free energy, $\Delta G^{a}_{in}(T)$, is defined as

$$\Delta G^{a}_{in}(T) = \Delta G_{in} + RT\log M \tag{2.73}$$

The molar enthalpy function of the system is defined as

$$H(T) = \sum_{i=1}^{n-1} \frac{(A_i)}{M} H_i(T) + \frac{(B)}{M} H_B(T) + \frac{(C)}{M} H_C(T) \tag{2.74}$$

Using Eqs.(2.69a) and (2.69b), we obtain

$$H(T) = \sum_{i=1}^{n-1} f_i(T) H_i(T) + 2f_n(T) H_n(T) \tag{2.75}$$

where $H_n(T)$ are defined from Eq.(2.68) as

$$H_n(T) = [H_B(T) + H_C(T)] \; / \; 2 \tag{2.76}$$

When the both sides of Eq.(2.71) are multiplied by 4, we obtain

$$\frac{(2f_n)^2}{f_i} = \exp\left[-\Delta G^{a'}_{in}(T)/RT \right] \tag{2.77}$$

where

$$\Delta G^{a'}_{in}(T) = \Delta G^{a}_{in}(T) - RT\log 4 \qquad (2.78)$$

Equations (2.70), (2.77), (2.72), and (2.75) become the same forms as the correspondent equations for the system of Eq.(2.62). This result indicates that the data of the system of Eq.(2.63) can be deconvoluted by the same method as that of Eq.(2.62). The enthalpy function of state-n means the mean of the enthalpy function of state-B and C, and the apparent Gibbs free energy function given by the deconvolution, $\Delta G^{a'}_{in}(T)$ must be corrected as $\Delta G^{a}_{in}(T)$ by Eq.(2.78). The correction value RTlog4 corresponds to the mixing entropy of the different two strands.

Table 2.1

Parameters for three-state test data

$$N_2 \rightleftarrows \frac{1}{2}I_4 \rightleftarrows 2D$$

state-i	state-0 (N_2)	state-1 (I_4)	state-2 (D)
m_i	1	1/2	2
$m_i \frac{d}{dT} C_i$ ($JK^{-2}mol^{-1}$)	130	130	130
$m_i C_i(320)$ ($kJK^{-1}mol^{-1}$)	22	25	28
$\Delta H_{0i}(320)$ (kJ/mol)	0	200	400
Tm_{0i} [a] (K)	–	320	320

The heat capacity functions $m_i C_i(T)$ and the difference enthalpy functions, $\Delta H_{0i}(T)$, are determined as same as those of the test data of isomeric system in the previous chapter referring to the thermodynamic functions of lysozyme. The heat capacity functions and the difference enthalpy functions are the linear functions of temperature. Temperature range of the data is from 280 K to 360 K. The number of data points is 401, and the temperature interval of the data point is 0.2 K.

a) Tm_{0i} indicates the temperature at which the difference Gibbs free energy function, $\Delta G_{0i}(T)$, becomes zero. The apparent Gibbs free energy function, $\Delta G^a_{0i}(T)$, is described as

$$\Delta G^a_{0i}(T) = \Delta G_{0i}(T) + (m_i - m_0)RT\log M$$

where M is the reduced concentration of the system which is defined in Section 2.2. Therefore it must be noticed that $\Delta G^{a}_{01}(T)$ is not zero at $T = Tm_{0i}$ generally. In these models, M is varied from 0.1 to 10. With the variation, the maximum molar fraction of the intermediate state changes from 0.01 (at M = 0.1) to 0.81 (at M = 10).

Table 2.2

Root mean square (RMS) deviations of the non-linear least-squares fitting to the data of hemolysin with several different models.

Model Scheme	Number of parameters	RMS deviation (μW/ml)
$N \rightleftarrows D$	6	1.09
$N_2 \rightleftarrows D_2$	6	1.13
$N_2 \rightleftarrows 2D$	6	0.91
$N_2 \rightleftarrows 2I \rightleftarrows 2D$ [a)]	8	0.53
$N_2 \rightleftarrows 2I \rightleftarrows 2D$ [a,b)]	7	0.57
$N_2 \rightleftarrows I_2 \rightleftarrows 2D$ [a)]	8	0.75
$N_2 \rightleftarrows (2/3)I_3 \rightleftarrows 2D$ [a)]	8	0.82

Non-linear least-squares fitting was done as described in text and Fig.2.6. Numbers of the data points are 150 for each concentrations.

a)The temperature dependence of all ΔC_{ij} is restrained to be the same.

b)ΔC_{01} is restrained to be fixed to zero.

Table 2.3

The best fitted thermodynamic parameters and the error estimations of the model $N_2 \rightleftarrows 2I \rightleftarrows 2D$[a)]

Parameters	Estimated values
$\Delta H_{01}(320)$	231±26 kJ/mol
$\Delta S^a_{01}(320)$[b)]	704±78 J/(K.mol)
ΔC_{01}	0[a)]
$\Delta H_{02}(320)$	938±10 kJ/mol
$\Delta S^a_{02}(320)$[b)]	2870±32 J/(K.mol)
ΔC_{02}	8.4±1.2 kJ/(K.mol)

All the values are represented per mole of dimer.

a) ΔC_{01} is restrained to be fixed to zero.

b) ΔS^a is represented at the concentration, 0.57 mg/ml.

Figure captions

Fig.2.1 Test data of three-state model, C(T), which is calculated by Eqs.(2.53) and (2.54) using parameters listed in Table 2.1. The reduced concentrations of the data, M, are indicated in the figure. The higher the concentration increases, the larger the population of the intermediate state becomes in this model. In the two-state analysis, the single and double deconvolution, I use the true heat capacity functions of state-0 and state-2 which are shown in the figure by broken lines, $m_0C_0(T)$ and $m_2C_2(T)$. I assume

$$\Delta H_0^* = \Delta H_2^* = 0$$

$$f_0^* = f_2^* = 1$$

$$f_0^{**} = f_2^{**} = 0$$

in the following calculation. The generation of the test data and the calculation of deconvolutions were done on the micro computer NEC PC9801. The numerical integrations were done by Simpson's rule.

Fig.2.2 The van't Hoff enthalpy function, $\Delta H^{vH}(T)$, and the calorimetric enthalpy function, $\Delta H^{cal}(T)$ of the two-state analysis of various concentration data. I assume the following mechanism to calculate the van't Hoff enthalpy function:

$$N_2 \rightleftarrows 2D$$

the calorimetric enthalpy functions of these data are all the same. The van't Hoff enthalpy function agrees well with the calorimetric enthalpy function at M = 0.1 except the region of the divergence of the van't Hoff enthalpy function at the extreme temperatures. It indicates that the calorimetry data at the concentration can be well approximated by the two-state mechanism. Actually the molar fraction of the intermediate state is 1 % at the maximum. On the other hand, the large differences between the van't Hoff enthalpy function and the calorimetric enthalpy function at the higher reduced concentrations indicate that the system can not be described by the two-state model. The van't Hoff enthalpy function becomes larger than the calorimetric enthalpy function in some temperature region. It indicates that higher associated state such as trimer, tetramer or pentamer state etc. must be considered.

Fig.2.3 Results of the double deconvolution of the test data at the reduced concentration M = 10 with assuming the following three mechanisms respectively:

line 1: $N_2 \rightleftarrows \frac{2}{3}I_3 \rightleftarrows 2D$ (trimer model)

line 2: $N_2 \rightleftarrows \frac{1}{2}I_4 \rightleftarrows 2D$ (tetramer model)

line 3: $N_2 \rightleftarrows \frac{2}{5}I_5 \rightleftarrows 2D$ (pentamer model)

$\Delta H_{01}(T)$s calculated with the various mechanisms are shown in the figure together with the true function, $\Delta H_{01}(T)^{true}$ (broken line) and $\Delta H_0(T)$.

Fig.2.4 Concentration dependence analysis of the test data. The apparent Gibbs free energy change, $\Delta G^a_{02}(T)$, and Gibbs free energy change, $\Delta G_{02}(T)$, are calculated from the molar fraction functions obtained by the double deconvolution as

$$\Delta G^a_{02}(T) = -RT\log\frac{(2f_2)^2}{f_0}$$

$$\Delta G_{02}(T) = \Delta G^a_{02}(T) - 2RT\log M$$

$\Delta G^a_{02}(T)$ at M = 0.1 (line 1), M = 0.3162276 (line 2), M = 1 (line 3), M = 3.162276 (line 4), M = 10 (line 5) are plotted, and $\Delta G_{02}(T)$s calculated from all the data at various concentrations agree with line 3. These results do not depend on the assumptions of the stoichiometric coefficient of the intermediate state in the double deconvolution. Namely all the mechanisms in Fig.2.3 give the same results.

Fig.2.5 Concentration dependence analysis of test data. The Gibbs free energy change $\Delta G_{01}(T)$ are calculated from the molar

fraction functions obtained by the double deconvolution using Eq.(2.50) based on the three kinds of models in Fig.2.3. The models are (a) trimer model, (b) tetramer model, and (c) pentamer model analyzing the test data at various concentrations (line numbers are the same as in Fig.2.4). The agreement of all the concentration data except the region of the extreme temperature in (b) proves that the appropriate model for the data is tetramer model.

Fig.2.6 Non-linear least-squares fitting of the test data at M = 10. The assumed three kinds of models are trimer model (line 1), tetramer model (thick line), and pentamer model (line 3). The test data can not be distinguished from the thick line. The non-linear least-squares fitting was done with the program SALS (Nakagawa & Oyanagi 1980) on a computer HITAC M-680H of Computer Centre of the University of Tokyo. The modified Marquardt method is used. The initial parameter values are determined by the double deconvolution.

As shown in this figure, the double deconvolution method gives a good initial parameter set for the fitting. This figure also shows that the fairly good signal to noise ratio for the data should be required if we determine the stoichiometry of the reaction from one fixed concentration data (i.e. without the concentration dependence analysis).

Fig.2.7 Non-linear least-squares method for the data of Vibrio parahaemolyticus hemolysin at pH 7.0. (a) Circles indicate a

part of the heat capacity function at the three different concentrations indicated by the numbers; 1; 0.21 mg/ml, 2; 0.38 mg/ml, 3; 0.57 mg/ml. The measurement was done by DASM-1M microcalorimeter (Privalov 1980) at the heating rate of 1 K/min. Phosphate buffers are used (Uedaira et al. 1982). The solid lines indicate the calculated functions with the best fitted parameters (Table 2.3) of the model $N_2 \rightleftarrows 2I \rightleftarrows 2D$ with $\Delta C_{01} = 0$. (b) The calculated molar fraction functions of the three states using the best fitted parameters. The numbers indicate the concentrations as above.

Fig.2.8 Results of single deconvolution of test data at M = 10. First the molar fraction function of state-2, $f_2(T)$, is calculated from $\Delta H_2(T)$ by single deconvolution assuming the following model

$$\frac{1}{2}I_4 \rightleftarrows 2D$$

and the hypothetical heat capacity function, $C^{(2)}(T)$, which would be obtained if the system did not include the state-2, is calculated. Then $C^{(2)}(T)$ is deconvoluted again by single deconvolution with $\Delta H_0^{(2)}(T)$ assuming the following model, and we obtain $f_0(T)$:

$$N_2 \rightleftarrows \frac{1}{2}I_4$$

$f_1(T)$ is calculated as

$$f_1(T) = 1 - f_0(T) - f_2(T)$$

$f_i(T)^{true}$ (i=0,1,2) indicates the true molar fraction function. When the order of the two single deconvolutions are changed (data not shown), the molar fraction function of state-2 can be well obtained while that of state-0 does not agree with either the true function or the function calculated by the repeated single deconvolutions in this figure. All the molar fraction functions obtained by the double deconvolution method assuming the tetramer model of Fig.2.3 agree completely with the corresponding true functions in the figure.

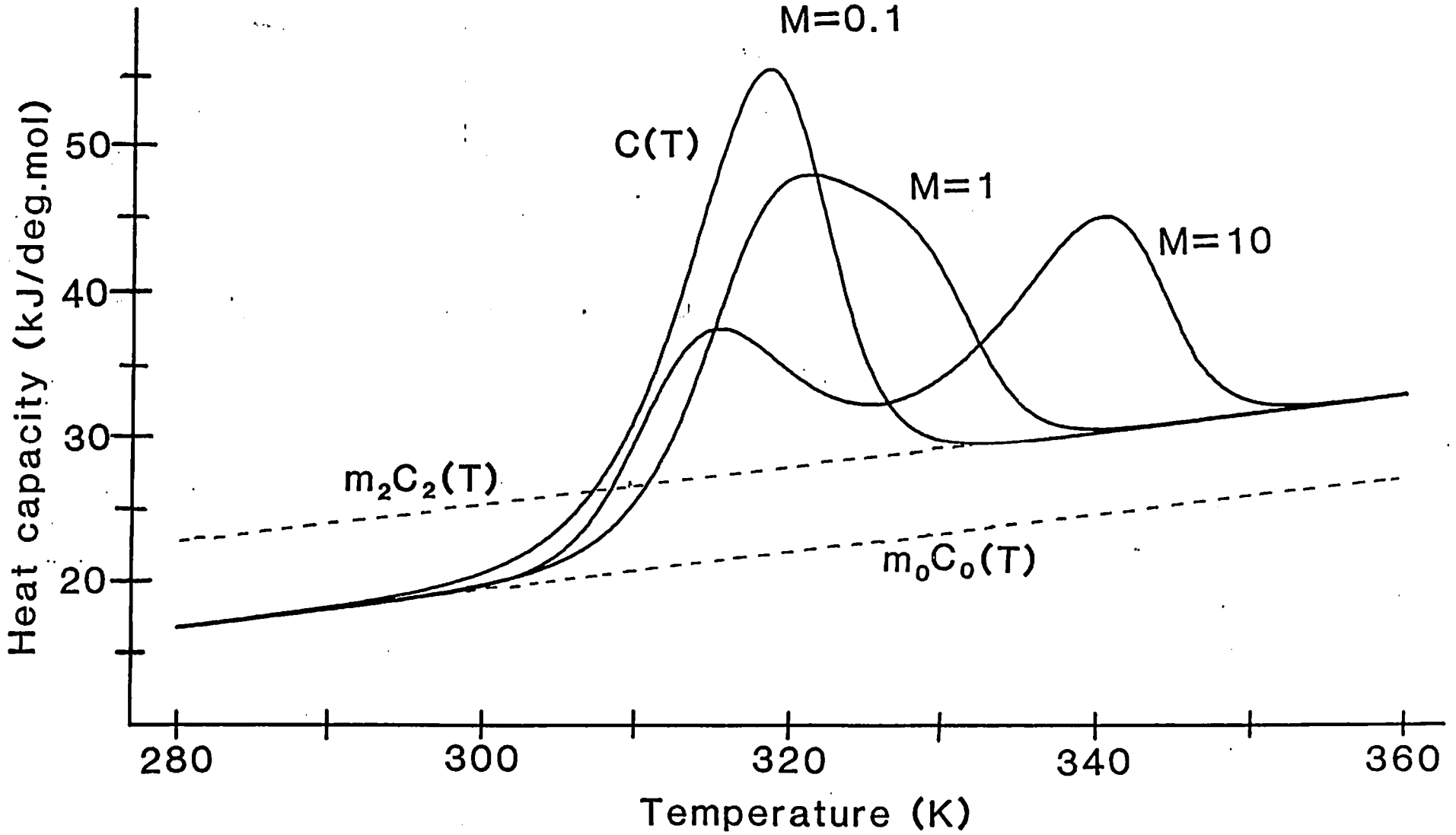
M=0.1
C(T)
M=1
M=10
$m_2C_2(T)$
$m_0C_0(T)$
Heat capacity (kJ/deg.mol)
50
40
30
20
280
300
320
340
360
Temperature (K)

Fig.2.1

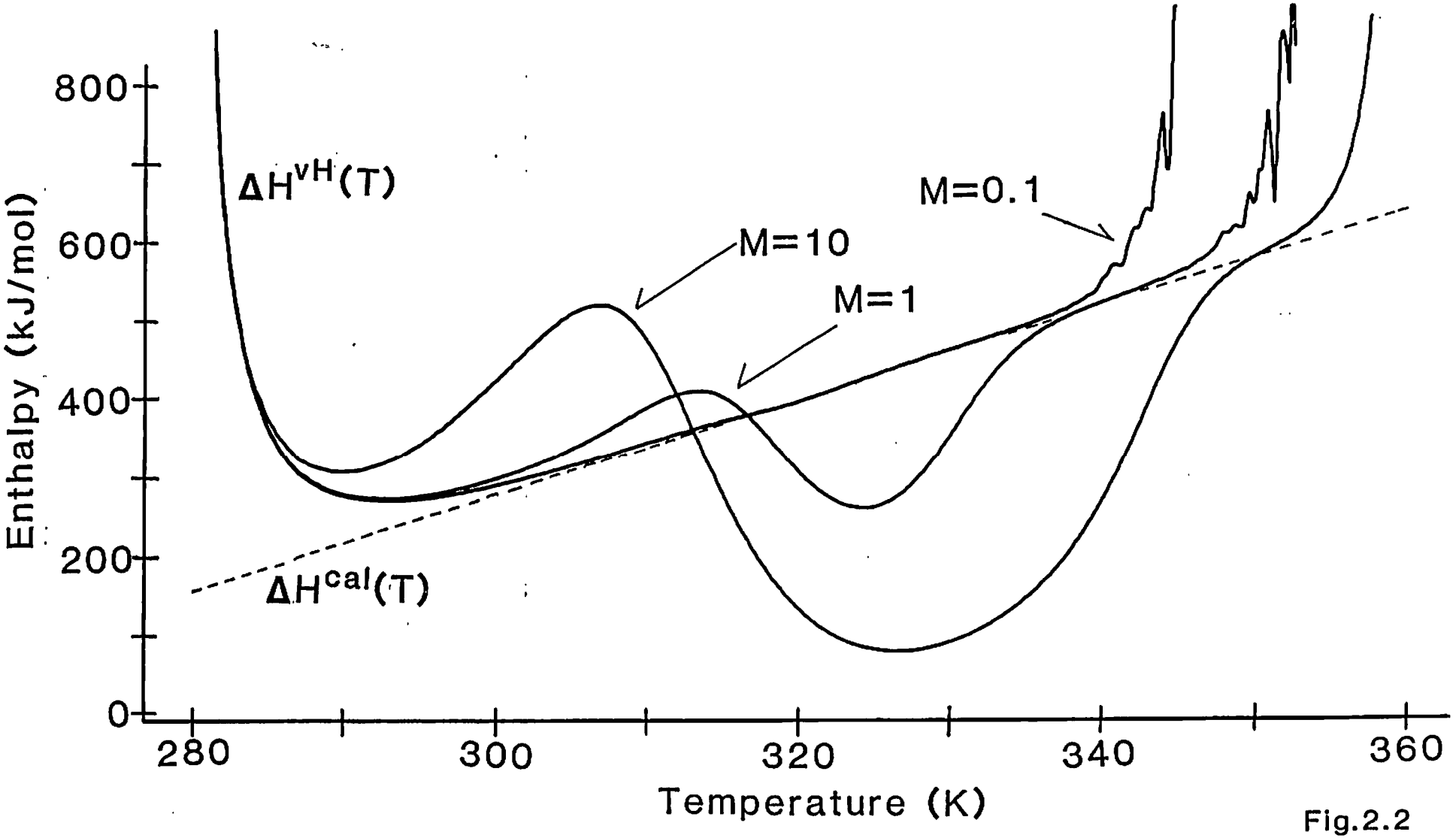
800
600
400
200
0
Enthalpy (kJ/mol)
ΔH^vH(T)
M=0.1
M=10
M=1
ΔH^cal(T)
280
300
320
340
360
Temperature (K)

Fig.2.2

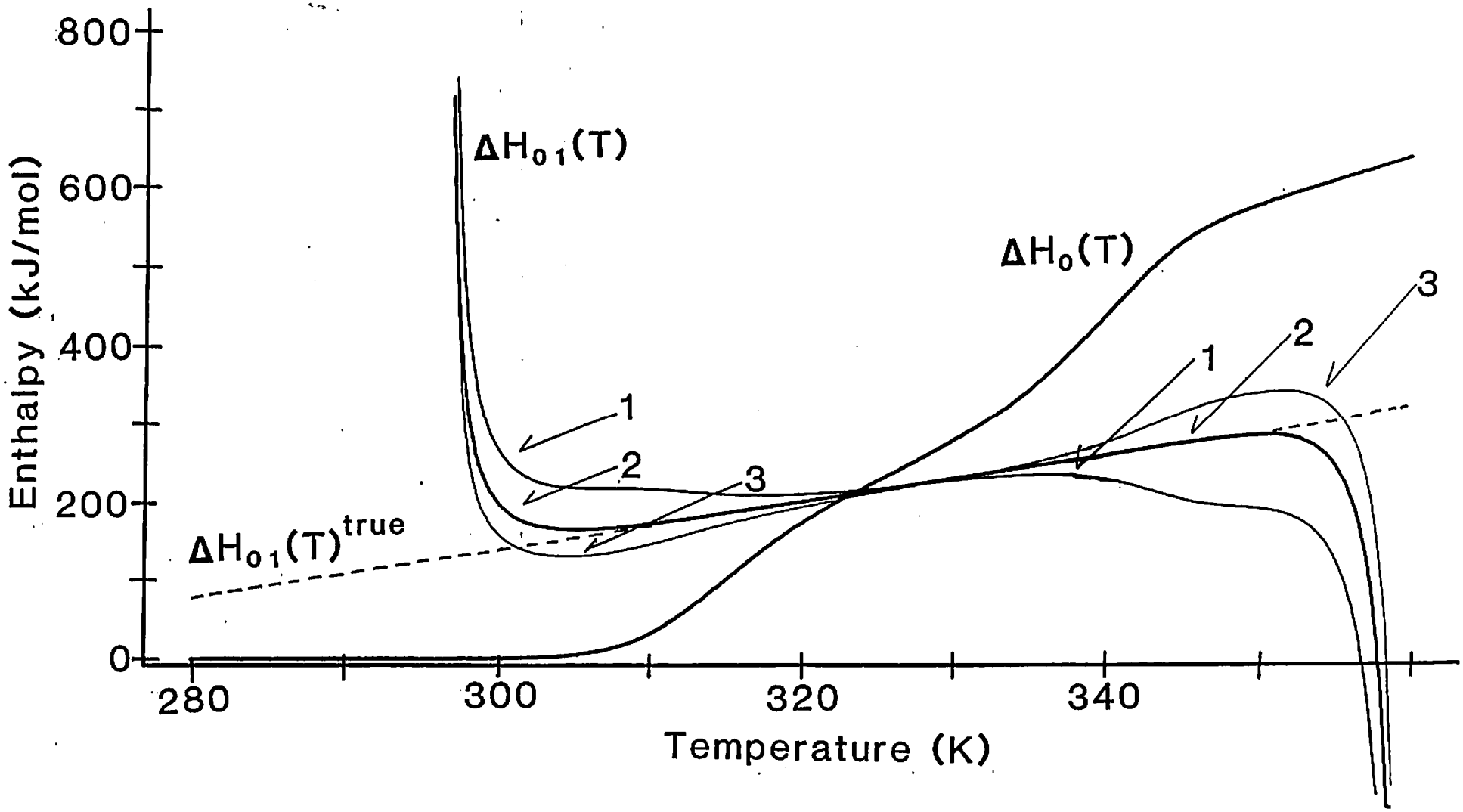
800
600
400
200
0
Enthalpy (kJ/mol)
280
300
320
340
Temperature (K)
$\Delta H_{01}(T)$
$\Delta H_{0}(T)$
$\Delta H_{01}(T)^{true}$
1
2
3
1
2
3

Fig.2.3

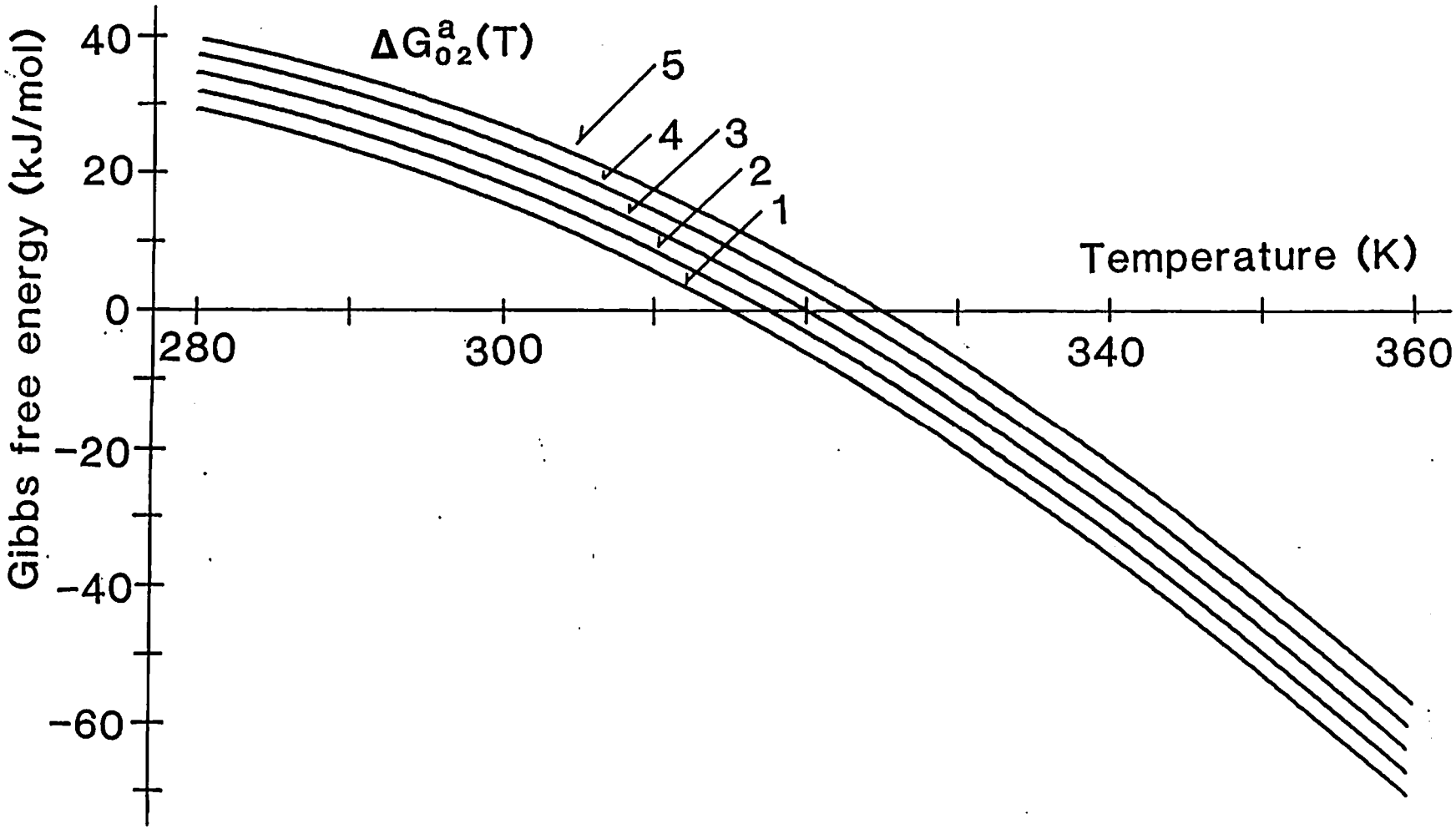
$\Delta G^{a}_{02}(T)$
5
4
3
2
1
40
20
0
-20
-40
-60
280
300
340
360
Temperature (K)
Gibbs free energy (kJ/mol)

Fig.2.4

Fig.2.5

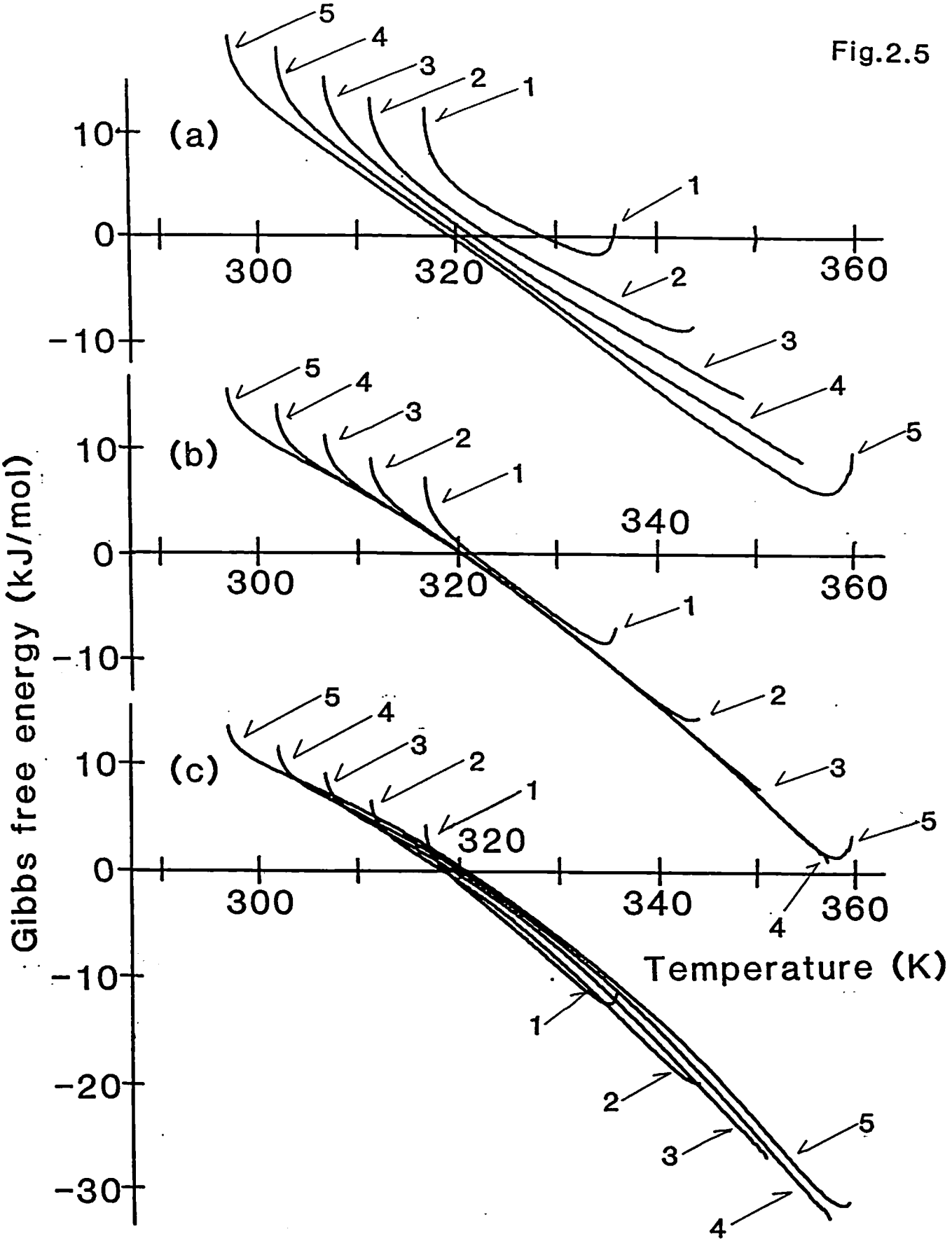
(a)
(b)
(c)
10
0
-10
-20
-30
300
320
340
360
1
2
3
4
5
Gibbs free energy (kJ/mol)
Temperature (K)

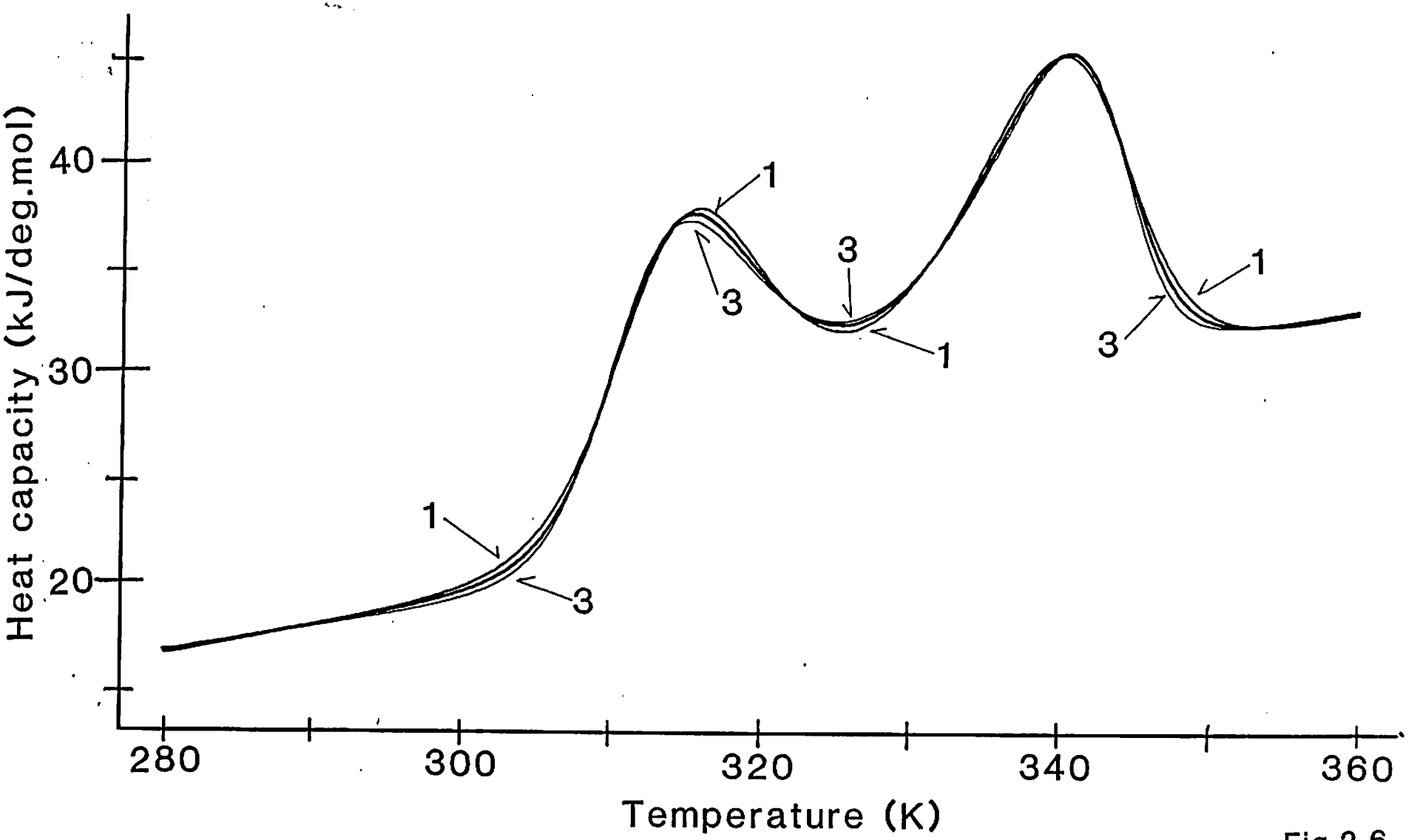
Heat capacity (kJ/deg.mol)
40
30
20
280
300
320
340
360
Temperature (K)
1
3
1
3
3
1
1
3

Fig.2.6

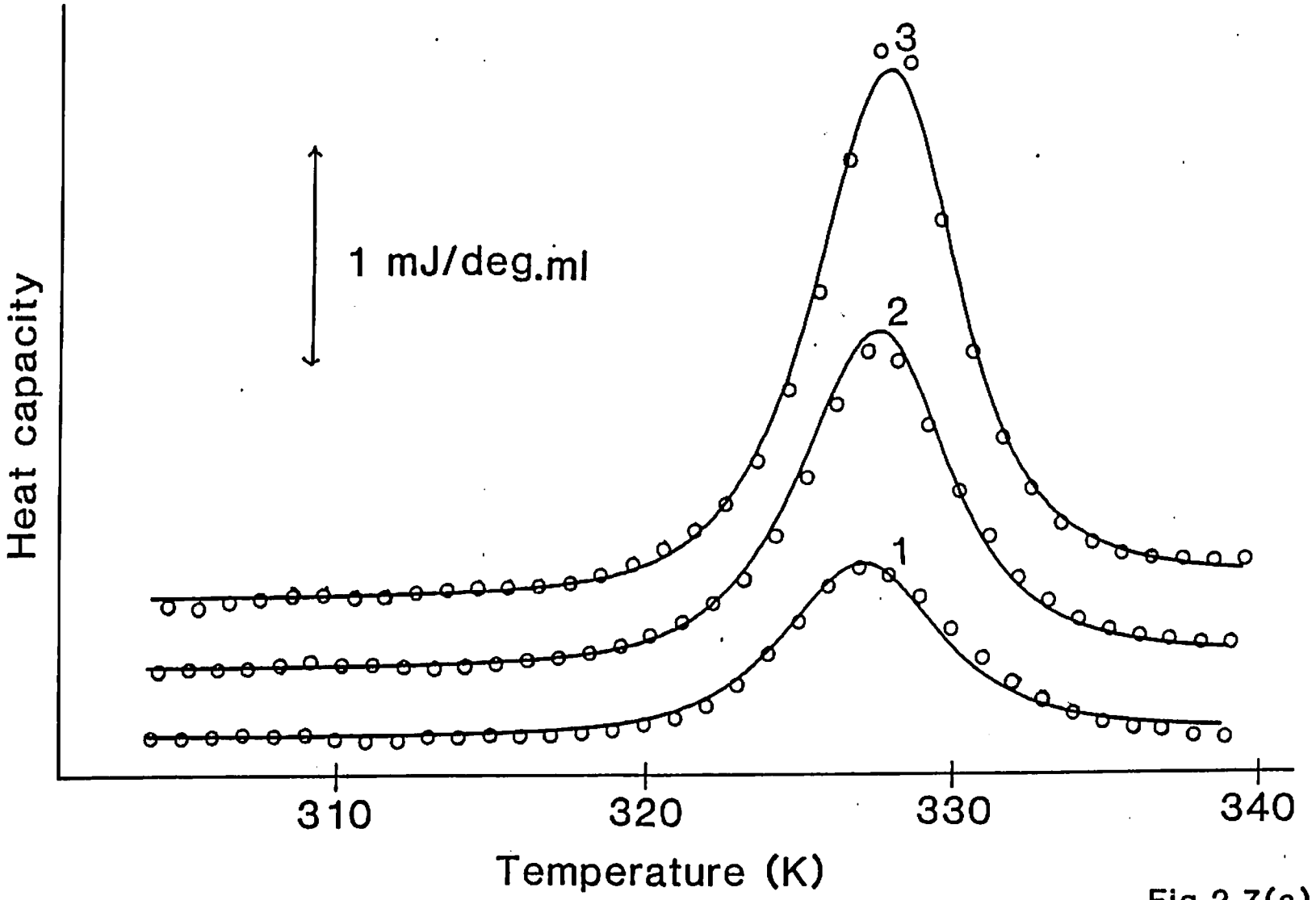

Fig.2.7(a)

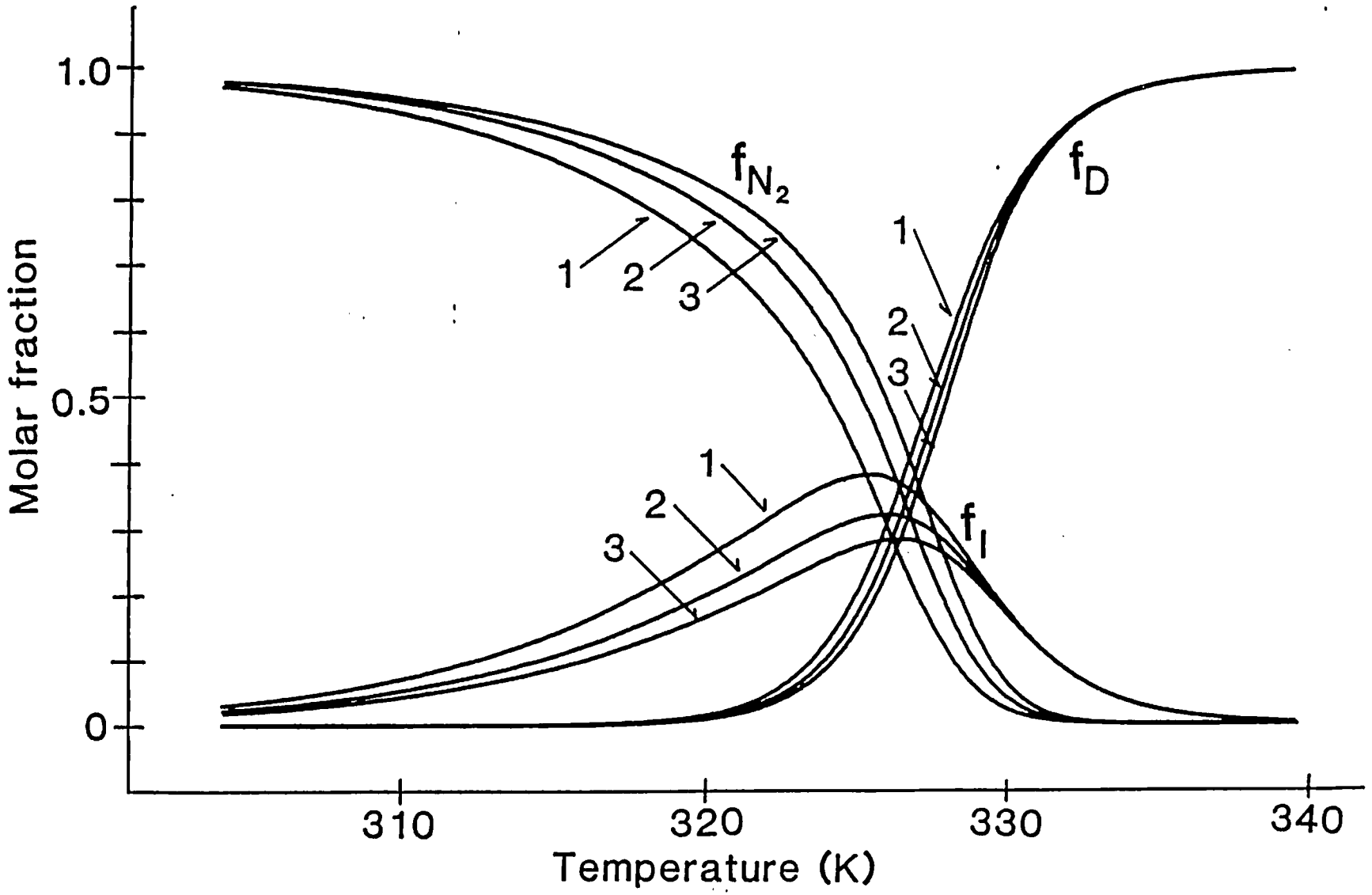
1.0
0.5
0
Molar fraction
f_{N_2}
f_D
f_I
1
2
3
310
320
330
340
Temperature (K)

Fig.2.7(b)

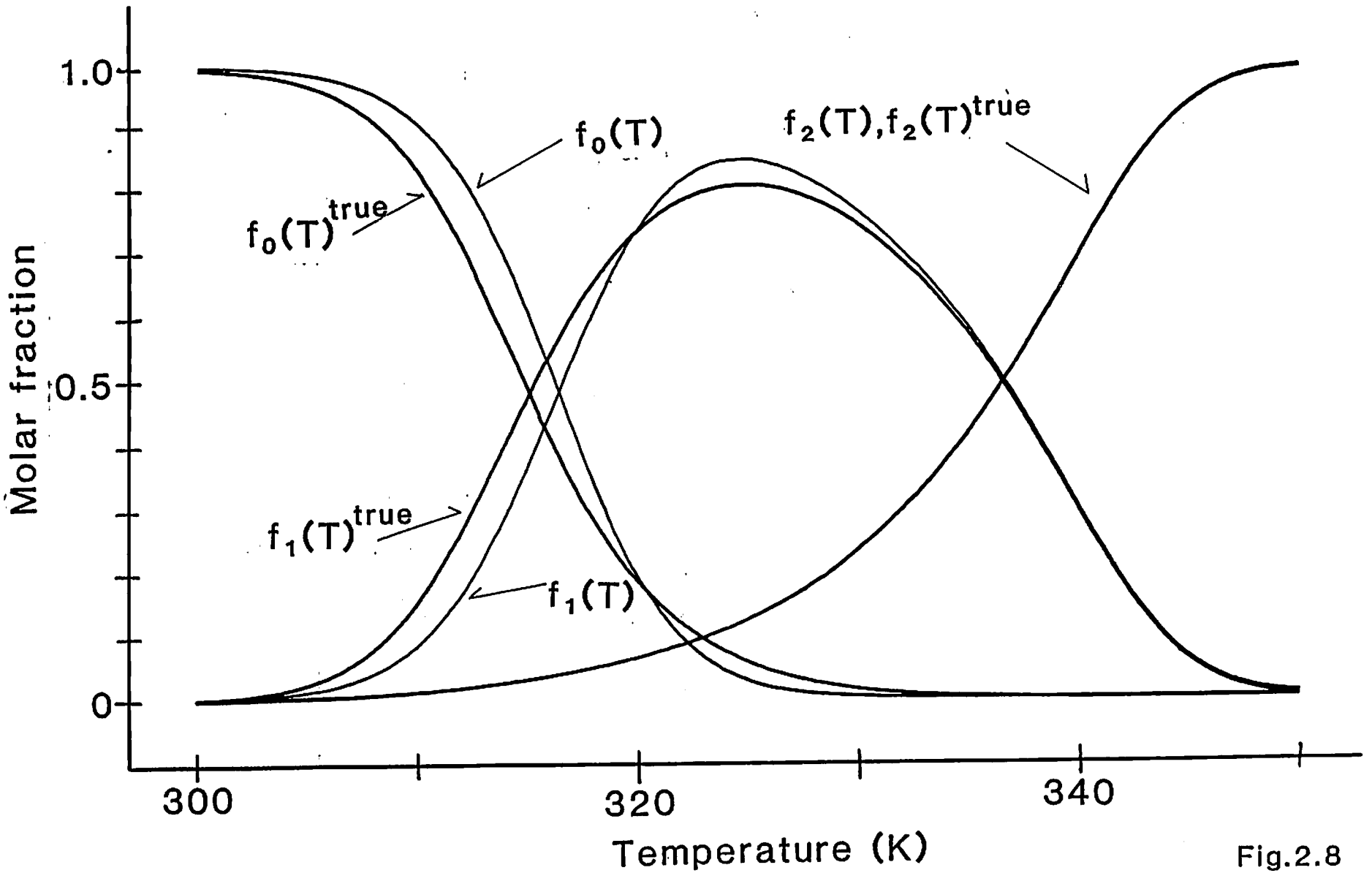
1.0
0.5
0
Molar fraction
$f_0(T)$
$f_0(T)^{true}$
$f_2(T), f_2(T)^{true}$
$f_1(T)^{true}$
$f_1(T)$
300
320
340
Temperature (K)

Fig.2.8

Chapter 3. Four-state thermal denaturation of pepsinogen

Abstract

The thermal transitions of porcine pesinogen in the range from pH 6.8 to 9.0 are studied in detail thermodynamically by scanning calorimetry and recently developed analysis methods, which are described in Chapters 1 and 2 in this paper. A new statistical mechanical treatment of pH dependence of thermodynamic functions is presented and applied to the analysis of the transitions. With these methods, a four-state model is proved to explain all the experimental data consistently rather than a three-state model previously proposed (P. L. Privalov et al. (1981) J.Mol.Biol., 152, 445-464). The pH dependence of thermodynamic functions of these four states is discussed.

3.1 Introduction

Calorimetry is widely realized now as one of the most powerful methods for elucidating the molecular origin of the stability of biological macromolecules such as proteins, DNAs, tRNAs and membranes. The special feature of calorimetry is its faculty of direct observation of thermodynamic functions of the molecules. Taking advantage of this aspect, I have presented a theoretical basis and new methods of the determination of thermodynamic functions of multistate system in Chapter 1 and 2.

Thermodynamic properties of small globular proteins which show two-state thermal transitions have been extensively studied. Some general features of the thermal transition of these systems have been revealed (Privalov 1979, for a review) as discussed later in this chapter.

Therefore, it is valuable to clarify whether or not the thermodynamic properties found in the small globular proteins can be generalized to those in the multi-state system. As one example, thermal transition of pepsinogen, which is known to exhibit multistate transition, is examined in detail in this chapter.

It was initially found by calorimetry that the thermal transition of this protein is not a two-state transition (Mateo & Privalov 1981); this was later confirmed by multidimensional spectroscopy (Wada et al. 1983). This transition was recognized as a three-state transition in the range from pH 6.0 to 8.0 (Privalov et al. 1981).

In the course of the present study, I found a new transition

at above pH 7.0, and not a three-state but a four-state model is proved to explain all the calorimetry data consistently. In order to analyze the pH dependence of the thermodynamic functions of the four states, I develop a new statistical mechanical treatment of calorimetry data for the system that includes ligand bindings which enables us to analyze the pH effect on the thermodynamic functions, and I clarify the relationship between this method and the basis of deconvolution method of Chapter 1.

The results of the analysis of calorimetry data at the various pH solutions clearly indicate that the difference enthalpy functions between any two thermodynamic states are dependent on pH. This observation does not agree with one of the well-known aspects of small globular proteins as discussed later. According to my theory on the pH dependence of thermodynamic functions, however, the results of pH-stat method that the difference of proton-binding-number function accompanied with the thermal transition is dependent on temperature (Pfeil & Privalov 1976) are found to be consistent with the present results.

3.2 Materials and Methods

3.2.1 Materials

Porcine pepsinogen (Grade I, P0258), lyophilized powder prepared chromatographically was purchased from Sigma Chemical Co. which was checked to make a single band with SDS polyacrylamide gel electrophoresis. All other chemicals were of reagent grade.

Protein solutions were prepared by dissolving the lyophilized powder in buffer solutions (about 5 ml) and they were dialyzed against a large volume (about 500 ml) of buffer solutions for 36 hours at 4 ℃ with two changes of the dialysis fluid. The buffers were 50 mM sodium phosphate buffer (50 mM NaH_2PO_4/NaOH) except for pH 9.0 solution, in which 50 mM sodium borate buffer (12.5 mM $Na_2B_4O_7$/HCl) was used. The pH values were measured by a glass electrode at 22 ℃. The temperature dependence of pH of the buffers in this work are 0.002 and 0.008 pH/K, for phosphate and borate buffer, respectively, which can be evaluated from their deprotonation enthalpy values (see Section 3.4.2), 3.8 kJ/mol and 13.8 kJ/mol at 25 ℃ (Christensen & Izatt 1962, Jordan 1958). Because of these small values, the temperature dependence of pH was neglected throughout this study. This approximation was found to be satisfactory in this study as discussed in Section 3.4.2.

The ionic strength of the buffers was calculated to be about 100 mM [from 90 mM (pH 6.8) to 140 mM (pH 8.0)] for the phosphate buffers, and 30 mM (pH 9.0) for the borate buffer. No salts for the adjustment of the ionic strength were added because the

reversibility of the thermal transition of globular proteins is lowered if the concentration of the solution is increased. The ionic strength dependence of the thermodynamic functions in the above range are neglected throughout the present study. Their solution-condition dependence can be explained with the pH dependence only as shown later.

Concentrations of the protein solutions were determined spectrophotometrically at 278 nm at 22 ℃ using the molar absorption coefficient of 5.17×10^4 $cm^{-1}(mol/l)^{-1}$ (Arnon & Perlmann 1963). The protein concentrations of all the measurements were about 1 mg/ml. The molecular weight used was 3.97×10^4 which was calculated by Privalov et al. (1981) from the amino acid sequences of the protein.

3.2.2 Calorimetric measurements

Calorimetric measurements were carried out in a differential adiabatic scanning microcalorimeter DASM-1M (Privalov 1980). Temperature scanning rate of all the measurements was 1 K/min. The detail on this apparatus was described by Privalov (1980). The calorimeter has two gold cells. One of them is used for a sample solution and the other is for a reference solution. Joule heat was added to the both cells for the temperature scanning. The temperature difference between the two cells due to their heat capacity difference is detected by thermocoupler, and simultaneously appropriate feedback compensation of Joule heat was operated as to make the temperature difference kept to be zero. The necessary feed back heat is plotted on a X-Y recorder

as shown in Fig.3.1. These curves are processed by a digitizer (KD4030 (Graphtec, Tokyo) equipped with a microcomputer PC9801 (NEC Co., Tokyo) and stored in flexible disks. With the experimental values of protein concentration and the height of a calibration heater of 50 μW (see Fig.3.1), the heat capacity functions are calculated from the stored data of both the first run and the corresponding base line, following the procedure outlined by Privalov and Khechinashvili (1974).

Reversibilities of the thermal transitions were checked by reheating the protein solution immediately after the cooling from the first run (see Fig.3.1). As seen in this figure, the transition is highly reversible as previously mentioned by Privalov et al. (1981). From the reversibility, I assume in the following that thermodynamic analysis can be adaptable to the calorimetric data of the transition.

3.2.3 Data analysis

3.2.3.1 Analysis of calorimetry data at each pH value

Two-state analysis, double deconvolution method and non-linear least squares fitting method were used. They were described in detail in the previous two chapters. Two-state analysis and double deconvolution method were done on the microcomputer PC9801 using my BASIC programs. A HITAC M680H of Computer Centre of the University of Tokyo was used for the calculation of non-linear least-squares fitting with my FORTRAN programs using program SALS (Nakagawa & Oyanagi 1980).

3.2.3.2 Statistical thermodynamic analysis of pH dependence of thermodynamic functions

By examining the thermal transitions in some different pH values, the pH dependence of the thermodynamic functions are obtained by the above methods. I shall show the statistical thermodynamic basis of the pH dependence analysis.

Generally, a protein molecule has several proton-binding-sites such as an amino group at N-terminus, a carboxylic acid group of C-terminus, and many ionizable groups of side chains. The protons are regarded as ligands. The statistical mechanical treatments which were discussed in Chapter 1 can be extended for the system that includes ligand bindings, as shown in the following.

When η-th microstate of the system has the energy ϵ_η, and it binds j_η ligands whose chemical potential in the solution is

μ, the grand partition function $Z(T,\mu)$ is described as

$$Z(T,\mu) = \sum_{\eta} \omega_{\eta} \exp[-(\varepsilon_{\eta} - j_{\eta}\mu)/RT] \qquad (3.1)$$

where ω_{η} is the degeneracy of the η-th microstate. The chemical potential of the ligand, μ, is the function of both temperature, T, and the activity of the ligand, a, as shown in the following equation:

$$\mu(T,a) = \mu_0(T) + RT \log a \qquad (3.2)$$

where μ_0 is the standard chemical potential at a = 1. In this study, the activity of the ligand is assumed to be independent of temperature. We use below the parameter set (T,a) instead of (T,μ) to clarify the independence of the two variables. The grand partition function, $Z(T,\mu)$, is designated as Z(T,a), for example.

The Gibbs free energy function of i-th thermodynamic state, $G_i(T,a)$, and the enthalpy function of the state, $H_i(T,a)$, are defined by Eqs.(3.3a) and (3.3b), respectively, where the molar fraction of the η-th microstate in the i-th thermodynamic state, $f_{\eta}^{i}(T,a)$ is defined by Eq.(3.4):

$$\exp[-G_i(T,a)/RT] = \sum_{\eta \in i} \omega_{\eta} \exp[-(\varepsilon_{\eta} - j_{\eta}\mu)/RT] \qquad (3.3a)$$

$$H_i(T,a) = \sum_{\eta \in i} (\varepsilon_{\eta} - j_{\eta}h)\ f_{\eta}^{i}(T,a) \qquad (3.3b)$$

$$f^{i}_{\eta}(T,a) = \omega_{\eta} \exp[-(\epsilon_{\eta}-j_{\eta}\mu)/RT] \Big/ \sum_{\theta \epsilon i} \omega_{\theta} \exp[-(\epsilon_{\theta}-j_{\theta}\mu)/RT] \qquad (3.4)$$

where h is the enthalpy of the free ligand which is defined as

$$h = -T^2 \frac{\partial}{\partial T}\left(\frac{\mu}{T}\right)_a = -T^2 \frac{d}{dT}\left[\frac{\mu_0(T)}{T}\right] \qquad (3.5)$$

It is easy to confirm that $G_i(T,a)$ and $H_i(T,a)$ satisfy the thermodynamic relation:

$$\frac{\partial}{\partial T}\left[G_i(T,a)/T \right]_a = -H_i(T,a)/T^2 \qquad (3.6)$$

When all the microstates are classified into n thermodynamic states, the grand partition function described as similarly as in Eq.(1.4) using n thermodynamic states as

$$Z(T,a) = \sum_{i}^{n} \exp[-G_i(T,a)/RT] \qquad (3.7)$$

With these preparations, the same equations as Chapter 1 can be

obtained when temperature differentiations of the equations in Chapter 1 are changed to partial differentiations under the condition that the ligand activity is kept constant. For example, Eq.(1.3) would be changed to Eq.(3.6) if the ligand binding is considered explicitly.

The mean number of the ligands which are bound to the system, $\langle j \rangle(T,a)$ is defined as

$$\langle j \rangle(T,a) = \sum_{\eta} j_{\eta} f_{\eta}(T,a) \qquad (3.8)$$

where the molar fraction of η-th microstate is described as

$$f_{\eta}(T,a) = \omega_{\eta} \exp[-(\varepsilon_{\eta} - j_{\eta}\mu)/RT] \Big/ \sum_{\theta} \omega_{\theta} \exp[-(\varepsilon_{\theta} - j_{\theta}\mu)/RT] \qquad (3.9)$$

From the above equations, it is easy to derive the following:

$$\langle j \rangle(T,a) = \left(\frac{\partial \log Z}{\partial \log a}\right)_T \qquad (3.10)$$

Similarly, the mean binding number of the i-th thermodynamic state is described as

$$\langle j \rangle_i(T,a) = \sum_{\eta \in i} j_{\eta} f_{\eta}^{i}(T,a) \qquad (3.11)$$

where f_{η}^{i} is defined by Eq.(3.4). From these equations, we easily obtain:

$$\langle j \rangle_i(T,a) = -\frac{1}{RT}\left[\frac{\partial G_i(T,a)}{\partial \log a}\right]_T \qquad (3.12)$$

This equation was obtained first by thermodynamic consideration of the liganded system (Wyman 1964), and I have clarified here its statistical mechanical basis.

In this paper, pH dependence of thermodynamic functions is analyzed using Eq.(3.12). Experimentally it is convenient that the activity of the proton is represented by pH, and ν_i is used instead of $\langle j \rangle_i$ as traditionally used. Then Eq.(3.12) is described as

$$\frac{1}{RT}\left[\frac{\partial G_i(T,pH)}{\partial pH}\right]_T = (\log 10)\,\nu_i(T,pH) \qquad (3.13)$$

By partially differentiating both sides of this equation with T, we obtain the following using Eq.(3.6):

$$-\frac{1}{RT^2}\left[\frac{\partial H_i(T,pH)}{\partial pH}\right]_T = (\log 10)\left[\frac{\partial \nu_i(T,pH)}{\partial T}\right]_{pH} \qquad (3.14)$$

The above two equations mean that pH dependence of thermodynamic functions is caused by the proton-binding-number function,

$\nu_i(T,pH)$. When this function is given over the entire temperature-pH plane, pH dependence of all the thermodynamic functions can be predicted. On the contrary, we can know $\nu_i(T,pH)$ under certain conditions by analyzing the pH dependence of thermodynamic functions as shown in this chapter. As our interest is in the differences of the thermodynamic function, between thermodynamic states, their pH dependence should be derived from Eqs.(3.13) and (3.14) as shown in the followings:

$$\left[\frac{\partial \Delta G_{ij}(T,pH)}{\partial pH}\right]_T = (\log 10)RT\Delta\nu_{ij}(T,pH) \qquad (3.15a)$$

$$\left[\frac{\partial^2 \Delta G_{ij}(T,pH)}{\partial pH^2}\right]_T = (\log 10)RT\left[\frac{\partial \Delta\nu_{ij}(T,pH)}{\partial pH}\right]_T \qquad (3.15b)$$

$$\left[\frac{\partial \Delta H_{ij}(T,pH)}{\partial pH}\right]_T = -(\log 10)RT^2\left[\frac{\partial \Delta\nu_{ij}(T,pH)}{\partial T}\right]_{pH} \qquad (3.15c)$$

where the differences of the thermodynamic functions between i-th state and j-th state such as $\Delta G_{ij}(T,pH)$ are defined as

$$\Delta G_{ij}(T,pH) = G_j(T,pH) - G_i(T,pH)$$

It is worthwhile to point out that there is a conflict in that $\Delta\nu_{ij}(T,pH)$ of thermal denaturation of lysozyme is reported to be dependent on temperature (Pfeil & Privalov 1976), although the enthalpy of these small globular proteins is independent of pH (Privalov & Khechinashvili 1974). This conflict will be

discussed later in Section 3.4.2.

Because the differences of heat capacity functions between the native and heat denatured states of several small proteins are known to be experimentally independent of pH, it is of interest to examine what thermodynamic property of the proton-binding-number function produces this independence. From Eq.(3.15c), the temperature dependence of the difference of the proton-binding-number function is derived because the partial differentiation of the left hand side of the equation with temperature should be zero:

$$\Delta\nu_{ij}(T,pH) = A(pH)/T + B(pH) \qquad (3.16)$$

where A(pH) and B(pH) are functions of pH and are independent of temperature.

Comparing Eq.(3.16) with Eqs.(3.15a) and (3.15c), we obtain

$$A(pH) = \frac{1}{(\log 10)R}\left(\frac{\partial \Delta H_{ij}}{\partial pH}\right)_T \qquad (3.17a)$$

$$B(pH) = -\frac{1}{(\log 10)R}\left(\frac{\partial \Delta S_{ij}}{\partial pH}\right)_T \qquad (3.17b)$$

where ΔS_{ij} is the difference entropy function between i-th and j-th states. Equations (3.17a) and (3.17b) insist that not only the partial differentiation of enthalpy with pH but also that of entropy is independent of temperature.

It should be concluded (1) that when the difference of heat capacity function is independent of pH, the difference of the proton-binding-number function should be linearly dependent on reciprocal of temperature under the condition that pH is constant, and (2) that even in this case, the pH dependence of the difference of the proton-binding-number function is not restrained.

3.3 Results

3.3.1 Two-state analysis

Heat capacity function of pepsinogen at pH 7.6 is shown in Fig.3.2. A broad shoulder can be seen in the high-temperature side of a rather sharp peak. When we assume the heat capacity functions, $C_N(T)$ and $C_D(T)$ for native state and heat denatured states, respectively, we can calculate the van't Hoff enthalpy $\Delta H^{vH}(T)$ and $\Delta H^{cal}(T)$ as shown in Fig.3.3. When the heat capacity functions are determined, I assume two properties, i.e. (1) that the heat capacity functions of native and heat denatured states are linearly dependent on temperature, i.e.,

$$\left(\frac{\partial^2 C_i(T,pH)}{\partial T^2}\right)_{pH} = 0 \qquad (i = N,D) \tag{3.18}$$

and (2) that the difference of the heat capacity function between the two thermodynamic states are independent of temperature, i.e.,

$$\left(\frac{\partial \Delta C_{ND}(T,pH)}{\partial T}\right)_{pH} = 0 \tag{3.19}$$

These two properties are well established experimentally in the case of small globular proteins that exhibit two-state thermal denaturations (Privalov 1979, for a review).

As seen in Fig. 3.3, $\Delta H^{vH}(T)$ is lower than $\Delta H^{cal}(T)$ except in the low and high temperature region where the divergences of

$\Delta H^{vH}(T)$ occur as discussed in Section 1.5. This proves that the thermal transition is a multi-state one. Under the solution condition of other examined pH, $\Delta H^{vH}(T)$ is found to be lower than $\Delta H^{cal}(T)$. In Table 3.1, I show the midpoint temperature of the transition, Tm, van't Hoff and calorimetric enthalpy values at the temperature, $\Delta H^{vH}(Tm)$, $\Delta H^{cal}(Tm)$, and the ratio of the two enthalpy values. It is concluded that the thermal transitions of pepsinogen under the solution condition of the pH values between 6.8 and 9.0 are not two-state ones as Mateo and Privalov originally reported (1981).

3.3.2 Double deconvolution and non-linear least-squares fitting

As discussed in Chapter 1, we can proceed to the double deconvolution of the heat capacity function upon the same assumptions on the heat capacity function of the thermodynamic states as the two-state analysis [Eqs.(3.18) and (3.19)].

Figure 3.4 shows the molar fraction functions of the native and the heat denatured states obtained by the double deconvolution method. It indicates clearly that at least one intermediate state exists and that the sum of molar fraction functions of the intermediate state exceeds 0.5 near 323 K. Figure 3.5 shows the hypothetical enthalpy function $H^{(N,D)}(T)$ of a hypothetical system that contains the microstates of neither the native nor the heat denatured state. The hypothetical function is seen to be sigmoidal. This indicates that at least two intermediate states exist whose enthalpy functions are $H_{I1}(T)$

and $H_{I2}(T)$ as shown in this figure. The two-state analysis or the double deconvolution method can be used by assuming these enthalpy functions of the intermediate states, and it is found that $H^{(N,D)}(T)$ is well explained by a two-state transition between I_1 and I_2. Namely, the thermal transition of pepsinogen at pH 7.6 is a four-state one as

$$N \rightleftarrows I_1 \rightleftarrows I_2 \rightleftarrows D \qquad (3.20)$$

In this stage, I have assumed that Eqs.(3.18) and (3.19) should also hold in the case of the intermediate states. Namely I assumed (1) that the heat capacity functions of the four thermodynamic states including intermediate states are linearly dependent on temperature, and (2) that the differences of the heat capacity functions between any two states are independent of temperature. Using these assumptions, the thermodynamic functions of the four states are obtained by double deconvolution method.

The results of the double deconvolution can be refined by non-linear least-squares method as discussed in Sections 1.6 and 2.7. The best fitted heat capacity function which is determined under the above two restrictions with a four-state model is presented in Fig.3.6. This model explains the experimental data well. In Fig.3.7, I show the molar fraction functions of the four states at pH 7.6 which are calculated with the best fitted thermodynamic parameters.

In pH 6.8, the heat capacity function has only one peak, and

the broad shoulder in the high-temperature side of a sharp peak which exists in pH 7.6 is not observed as shown later in Fig.3.9. The hypothetical enthalpy function $H^{(N,D)}$ of pH 6.8 is not sigmoidal, and the three-state model can well explain this experimental data. In pH 9.0, although the heat capacity function has two broad peaks, this experimental data can be well explained by a three-state model similarly as in pH 6.8. In other pH values from pH 7.0 to pH 8.0, the four-state model rather than the three-state model can well fit the experimental data.

In Fig.3.8, I illustrate the thermodynamic parameters determined by the double deconvolution method and the least-squares fitting method at several pH values examined. From this figure, it can be easily observed (1) that the difference enthalpy values between the native and the heat denatured states at the midpoint temperature of their transitions depend almost linearly on temperature; (2) that the difference enthalpy values between the native and I_2 states (one of the two intermediates that has larger enthalpy value) at pH 7.0, 7.6 and 8.0, and the difference enthalpy value between the native and the intermediate states of pH 9.0 are found to depend linearly on temperature; (3) that the difference enthalpy values between the native and I_1 states (one of the two intermediates that has smaller enthalpy value) at pH 7.0, 7.6 and 8.0, and the difference enthalpy value between the native and the intermediate states at pH 6.8 are observed to depend linearly on temperature. Midpoint temperature between i-th and j-th states is defined as the temperature which satisfies the equation:

$\Delta G_{ij}(T)=0.$

3.3.3 pH dependence analysis

In the case of thermal transition of small globular proteins, the following two pieces of experimental evidence were reported about the pH dependence of heat capacity function and enthalpy function: (1) that the difference of heat capacity function between native and heat denatured states is well approximated to be independent of pH, i.e.,

$$\left(\frac{\partial \Delta C_{ND}(T,pH)}{\partial pH}\right)_T = 0 \qquad (3.21)$$

and (2) that the difference of enthalpy function between the native and the heat denatured states at the fixed temperature is well approximated to be independent of pH, i.e.,

$$\left(\frac{\partial \Delta H_{ND}(T,pH)}{\partial pH}\right)_T = 0 \qquad (3.22)$$

The two aspects above are not independent but clearly the condition of Eq.(3.22) is included by the condition of Eq.(3.21).

As seen in Fig.3.8, ΔC_{ND}s of several pH values which are the slopes of the bars of each data point take similar values (from 14.9 $kJK^{-1}mol^{-1}$ at pH 9.0 to 22 $kJK^{-1}mol^{-1}$ at pH 7.6).

However, all the values are lower than the slope of the broken line (33.8 $kJK^{-1}mol^{-1}$). In the cases of the intermediate states I_1 and I_2, the difference enthalpy functions have similar slopes except that of pH 7.0. The negative slopes of the difference enthalpy functions of I_1 and I_2 states are strange because the change of the heat capacity accompanied with the denaturation is never negative among cases of not only proteins but also DNAs and tRNAs. This may be due to the overfitting which can be caused by too much freedom of the model function as the fraction of I_2 state of pH 7.0 is the smallest among all the four-state cases. In any event, the slopes of the enthalpy functions are less than the corresponding broken line.

I examined the possibility that Eq.(3.21) holds between any two states. The nonlinear least-squares fitting under the restriction of Eq.(3.21) was done, and the best fitted parameters were obtained. The residual sum of squares is 0.573 $\mu W/ml$, which almost agrees with the noise level of the calorimeter (Privalov 1980).

However one of the best fitted parameter ΔC_{01} was found to be negative, i.e. $-5.3\ kJK^{-1}mol^{-1}$. This value may not be adopted for the reason mentioned before. Therefore, nonlinear least squares method has been used under the condition that ΔC_{01} is fixed to zero. The residual sum of squares of this fitting is 0.574 $\mu W/ml$. This value is slightly larger than the previous model. Considering (1) that the freedom of this model is less than the old model by one, (2) that the residual sum is almost equivalent, and (3) that the negative difference heat capacity is never reported, I concluded that the model in which ΔC_{01} is

fixed to zero is most probable for the present data. In Fig.3.9, the best fitted function of this model is shown to be well fitted to the correspond experimental data.

The best fitted parameters of this model are presented in Table 3.2. As shown in Fig.3.10, all the difference enthalpy functions presented in this table decrease with increasing pH. This aspect can be expected from the results of the double deconvolution as mentioned above (see Fig.3.8). If a more restricted model is used in which the difference enthalpy function is approximated to be independent of pH, this model can not be fitted to the experimental data. It is concluded that the difference enthalpy function is depend on pH in the case of the thermal transition of pepsinogen in the range from pH 6.8 to pH 9.0. The difference enthalpy values at the fixed temperature of 320 K can be well approximated to depend linearly on pH.

In Fig.3.11, I show the pH dependence of difference Gibbs free energies at a fixed temperature of 320 K. The difference Gibbs free energies decrease when pH increases. The dependence is approximated by the 2nd order polynomials which are shown by the broken lines.

In Table 3.3, the partial differentiation coefficients of the thermodynamic functions are presented. The proton-binding-number and its partial differentiation coefficients are estimated from these values by Eqs.(3.15a), (3.15b) and (3.15c).

3.4 Discussion

3.4.1 Necessity of four thermodynamic states

Privalov et al. showed that the thermal transitions of pepsinogen in the pH from 6.0 to 8.0 are explained by three-state transitions although the heat capacity function has one sharp peak (Privalov et al. 1981). In this work, I observe that the thermal transition at pH 6.8 is well approximated by three states, which agrees with their observation. Above pH 7.0, however, a broad shoulder in the high-temperature side of the sharp peak is observed, and the broad shoulder becomes one broad peak at pH 9.0. In order to explain my observations, it is necessary to consider four thermodynamic states including two intermediate states as shown in Section 3.3.2. This necessity is supported by the pH dependence of the thermodynamic functions obtained by this model as shown in Section 3.3.3.

In the analysis in Section 3.3.2, I assumed (1) that the heat capacity function of any thermodynamic states is approximated to be dependent on temperature linearly, i.e.,

$$\left[\frac{\partial^2 C_i(T,pH)}{\partial T^2}\right]_{pH} = 0 \qquad (3.23)$$

and (2) that the difference of the heat capacity function between any two thermodynamic states, i-th state and j-th state, is approximated to be independent of temperature, i.e.,

$$\left[\frac{\partial \Delta C_{ij}(T,pH)}{\partial T}\right]_{pH} = 0 \qquad (3.24)$$

A more general model without these restrictions can well explain the data, of course. However, we must adapt a model with the minimal freedom in order to increase the reliability of the model by avoiding the overfittings.

3.4.2 pH dependence of thermodynamic functions

In Section 3.3.3, it was shown that even the restricted model whose difference heat capacity functions between any two thermodynamic states are independent of pH can well explain the experimental data of all the pH solutions from pH 6.8 to pH 9.0. Namely, the following equation holds:

$$\left[\frac{\partial \Delta C_{ij}(T,pH)}{\partial pH}\right]_{T} = 0 \qquad (3.25)$$

where the suffixes, i and j, indicate the native, the heat-denatured, and the two intermediate states. Equations (3.24) and (3.25) mean that ΔC_{ij} is constant on temperature and pH, and it agrees with the well-known observation of small globular proteins which show two-state thermal denaturation (Privalov 1979, for a review).

However this is the first time to show clearly by high precision scanning calorimetry that the difference enthalpy functions, ΔH_{ij}, at a fixed temperature depend on pH values.

From Eq.(3.15c), the existence of the pH dependence is supported by the fact that the difference of the proton-binding-number of lysozyme is observed to depend on temperature (Pfeil & Privalov 1976). From the temperature dependence of $\Delta\nu_{ND}$ of lysozyme, about $-0.03\ K^{-1}$ at least, between 25 ℃ and 60 ℃ at pH 2.5 (from Fig.11 of Pfeil & Privalov 1976), the pH dependence of ΔH_{ND} should be observed as about 60 kJ/mol per pH-unit at pH 2.5, 50 ℃, at least. As the pH dependence of the transition temperature is about 15 K per pH-unit between pH 2 and 3 (from Fig.4 of Privalov & Khechinashvili 1974), and the difference heat capacity between the native and the heat denatured state is 6.7 $kJK^{-1}mol^{-1}$ (Khechinashvili et al. 1973), the contribution of the change of transition temperature to the difference enthalpy function will be 100 kJ/mol per pH-unit. Thus the pH dependences of ΔH_{ND}, 60 kJ/mol per pH-unit cannot be negligible.

From Table 3.3, the difference enthalpy value per one protonation under the condition of constant temperature of 320 K at pH 7.6 can be evaluated as about −80 kJ/mol by the following equation:

$$\left(\frac{\partial \Delta H_{ij}}{\partial \Delta \nu_{ij}}\right)_T = \left(\frac{\partial \Delta H_{ij}}{\partial pH}\right)_T \Big/ \left(\frac{\partial \Delta \nu_{ij}}{\partial pH}\right)_T \qquad (3.26)$$

This value is larger than the protonation enthalpy of the amino acid monomer. For example, that of a histidine monomer (pK = 6.0, at 25 ℃) is reported as −30 kJ/mol (Christensen et al. 1969). This discrepancy may indicate that some of the interactions in the tertiary structure of the protein are affected by the

protonation.

On the contrary, if we assume that the difference enthalpy at a fixed temperature is independent of pH:

$$\left[\frac{\partial \Delta H_{ij}(T,pH)}{\partial pH}\right]_T = 0 \qquad (3.27)$$

the following equation holds from Eq.(3.26)

$$\left(\frac{\partial \Delta H_{ij}(T,pH)}{\partial \nu_{ij}}\right)_T = 0 \qquad (3.28)$$

where $\Delta \nu_{ij}$ is thought to have to depend on pH generally, otherwise it is strange that both acid and base denaturation occur. Equation (3.28) seems strange because it indicates that the protonation number does not affect the difference enthalpy function. The validity of Eq.(3.27) in the small globular proteins must be re-examined by the method developed in this study.

It is worthwhile to consider the effect of protonation enthalpy of buffers, which are neglected in this study. As the thermal transition occurs in buffer solution, the protons which are released from (or required by) a protein molecule during the reaction, are "absorbed" (or "supplied") by buffer molecules, so that the pH of the buffer solution is kept constant. Thus, generally the observed enthalpy is the sum of both the enthalpy of the system which is discussed in Section 3.2.3.1 and a

protonation enthalpy of the buffers. Namely, we get

$$\Delta H_{ij}^{Obs} = \Delta H_{ij} + \Delta \nu_{ij} \Delta H^{b} \qquad (3.28)$$

where ΔH^{b} is the deprotonation enthalpy of the buffer. Using the reported value for phosphate buffer, 3.8 kJ/mol at 25 ℃ (Christensen & Izatt 1962), the observed enthalpy function of the system may be corrected by about -20 kJ/mol in the maximum case of pH 7.6 ($\Delta \nu \fallingdotseq -5$). As the absolute value of $\Delta \nu$ increases in more acidic solution, the correction may become larger. The correction is, however, the same order of magnitude as that of pH 7.6, and it can be neglected in the discussion of the present study. In the case of borate buffer, the deprotonation enthalpy is 13.8 kJ/mol at 25 ℃ (Jordan 1958), which is larger than that of phosphate buffer. As the absolute value of the difference of proton-binding-number function becomes small in this pH region, however, the correction is also negligible.

From Eq.(3.29), we obtain

$$\Delta C_{ij}^{Obs} = \Delta C_{ij} + \left(\frac{\partial \Delta \nu_{ij}}{\partial T}\right) \Delta H^{b} + \Delta \nu_{ij} \left(\frac{\partial \Delta H^{b}}{\partial T}\right) \qquad (3.30)$$

The second term of the right-hand side is evaluated as about 0.6 $kJK^{-1}mol^{-1}$ and the last term is about 0.5 $kJK^{-1}mol^{-1}$ in the maximum case where the temperature dependence of the deprotonation enthalpy of phosphate buffer, about -0.1 $kJK^{-1}mol^{-1}$ (Bates & Acree 1943) is used. Therefore, in the case of heat capacity evaluation, it is found to be a good approximation to

neglect the protonation enthalpy of the buffer in the present case.

On the contrary, if the protonation enthalpy of the buffer is not negligible, we will be faced with two serious and complicated problems.

First, no evaluation of the heat capacity function of the system can be made without the information about the proton-binding-number function, as easily realized from Eq.(3.30). This information may be obtained using the pH-stat method (Pfeil & Privalov 1976). From the scanning calorimetry alone, however, it will be complicated to evaluate the $\Delta\nu_{ij}$ when the protonation enthalpy of the buffer molecule is not negligible.

Second, the pH value of the buffer solution cannot be assumed as constant during the transition when the protonation enthalpy of the buffer is large. The temperature dependence of pH value of the buffer solution is mainly determined by the temperature dependence of pK of the buffering compound, and it is related to the deprotonation enthalpy as

$$\frac{d}{dT}pK = -\frac{1}{(\log 10)}\left(\frac{\Delta H^b}{RT^2}\right) \qquad (3.31)$$

Thus the large protonation enthalpy is responsible for the large temperature dependence of pH of the solution. If the dependence cannot be neglected, strictly speaking, we cannot use the present analysis methods such as two-state analysis, double deconvolution, etc., which are valid under the condition that the

ligand activity is constant during the reaction, as seen in Section 3.2.3.2.

In the case of phosphate and borate buffers of the present study, the temperature dependence of pKs is 0.002 and 0.008 pH/K, using the deprotonation enthalpies, 3.8 J/mol and 13.8 J/mol, respectively. The effect of the temperature dependence of pH on the temperature dependence of proton binding number may be estimated as

$$(\frac{\partial \Delta \nu_{ij}}{\partial pH}) \times (\frac{d}{dT} pK)$$

In the case of pH 7.6, it is about 0.005 K^{-1} which is within the estimated error of the partial differentiation of $\Delta \nu_{ij}$ with temperature, and can be neglected. Also, the effects on the enthalpy function and Gibbs free energy function can be evaluated similarly, which must be compared with the differences of entropy function and heat capacity functions, respectively; they are found to be within the corresponding estimation error.

3.4.3 Estimation of the structural properties of the intermediate state

Using the relationship between thermodynamic and structural properties of globular proteins, indirect information on the structural aspects could be obtained from calorimetry data. It must be noted, however, that we can know only thermodynamic properties of the observed system by calorimetry, and cannot

obtain any structural information directly from the data, strictly speaking.

One of the relationships which have been well examined is the relation between the heat capacity change accompanied by the thermal denaturation and its tertiary structure, such as the contact number of the nonpolar side chains. This relation was originally pointed out by Privalov & Khechinashvili (1974). As the heat capacity of aqueous solution will be generally increased when a hydrophobic solute is dissolved in the solution (Gill et al. 1985), it seems reasonable that the heat capacity increases when the nonpolar side chains which were buried in the tertiary structure of native state are exposed to the solvent during denaturation.

Recently, a quantitative approach has been proposed to evaluate the change of thermodynamic properties accompanied with the thermal denaturation. The change can be calculated using both the change of the accessible surface area of the atomic groups which are calculated with the atomic coordinates of the protein and an empirical linear relation between the accessible surface area of the group and its heat capacity obtained experimentally (Ooi & Oobatake 1988). These calculated values for several small globular proteins agree with the corresponding experimental ones well. This indicates that the main contribution on the heat capacity change comes from the change of the accessible surface area of the atoms of the protein.

Upon this relationship, we can evaluate the change of accessible surface area from the native state to the two intermediate states in the case of pepsinogen. From Table 3.2,

the heat capacity of the intermediate state, I_1, is estimated to be almost the same as that of the native state, and that of the intermediate state, I_2, is evaluated to be almost the middle value between those of the native and the denatured states. These indicate that the accessible surface area of the atoms in the I_1 state is almost the same as that in the native state, and that almost the half portion of the inner atoms is estimated to be exposed to the solvent in the I_2 state.

3.5 Concluding Remarks

I show in this chapter that the rigorous analysis of the precise scanning calorimetry data can reveal the schemes and the thermodynamic function of a complex thermal transition of a globular protein. The structural properties of the intermediate states which are predicted by the calorimetry will be revealed directly by a structural method such as a spectroscopic measurement. Even in the case of small globular proteins, which are regarded as two-state transition, the precise analysis may be necessary for the re-examination of the pH dependence of thermodynamic functions. The pH dependence is closely related to the proton-binding-number functions. Also a more accurate study such as a pH-stat method on the functions will be required in order to compare the results of the calorimetry.

Table 3.1

Tm, calorimetric enthalpy at T_m, $\Delta H^{cal}(Tm)$, van't Hoff enthalpy at T_m, $\Delta H^{vH}(Tm)$ of pepsinogen which are calculated by two-state analysis.

pH	Tm (K)	ΔH^{cal} (kJ/mol)	ΔH^{vH} (kJ/mol)	$\Delta H^{vH}/\Delta H^{cal}$
6.8	332.8	1196	500	0.42
7.0	329.0	1129	571	0.51
7.6	323.1	936	476	0.51
8.0	321.4	864	397	0.46
9.0	310.0	530	119	0.22

Table 3.2

Thermodynamic parameters for four-state thermal transitions of pepsinogen at several pHs which are determined by non-linear least-squares fitting.

pH	6.8	7.0	7.6	8.0	9.0
				($kJK^{-1}mol^{-1}$)	
ΔC_{01} [a]	0	0	0	0	–
ΔC_{02} [b]	–	10.2±1.2	10.2±1.2	10.2±1.2	10.2±1.2
ΔC_{03} [b]	19.7±0.5	19.7±0.5	19.7±0.5	19.7±0.5	19.7±0.5
				($kJmol^{-1}$)	
$\Delta H_{01}(320)$	571±23	472±7	363±12	257±8	–
$\Delta H_{02}(320)$	–	942±15	765±10	721±6	410±15
$\Delta H_{03}(320)$	982±7	1008±13	885±10	885±9	613±19
				($kJmol^{-1}$)	
$\Delta G_{01}(320)$	19.4±0.1	11.5±0.2	3.2±0.2	−1.3±0.2	–
$\Delta G_{02}(320)$	–	26.7±0.4	7.0±0.2	−1.5±0.2	−15.4±0.5
$\Delta G_{03}(320)$	43.0±0.2	32.6±0.6	12.3±0.4	3.2±0.3	−14.4±0.3

The suffixes, 0, 1, 2, 3, indicate the thermodynamic states, i.e., the native state, the intermediate state, I_1, the intermediate state, I_2, and the heat denatured state, respectively.

a) ΔC_{01} is fixed to zero.

b) ΔC_{02} and ΔC_{03} are restricted to have the common value at all the pH values

Table 3.3

(a) pH partial differentiation coefficients of thermodynamic functions at pH 7.6, 320 K, which are calculated from the least-squares fitting curves in Figs.3.10 and 3.11, and (b) the proton-binding-number functions and their partial differentiation coefficients, at pH 7.6, 320 K, which are evaluated from (a) by Eqs.(3.15).

(a)

i	$\frac{\partial \Delta G_{Ni}}{\partial pH}$ (kJ/mol)	$\frac{\partial^2 \Delta G_{Ni}}{\partial pH^2}$ (kJ/mol)	$\frac{\partial \Delta H_{Ni}}{\partial pH}$ (kJ/mol)
I_1	−11.9±26.0	20.5±16.1	−243±27
I_2	−27.0±3.0	15.2±1.6	−262±22
D	−30.1±4.3	15.3±2.4	−171±29

(b)

i	$\Delta \nu_{Ni}$	$\frac{\partial \Delta \nu_{Ni}}{\partial pH}$	$\frac{\partial \Delta \nu_{Ni}}{\partial T}$ (K^{-1})
I_1	−2.0±4.2	3.3±2.6	0.124±0.014
I_2	−4.4±0.5	2.5±0.3	0.133±0.011
D	−4.9±0.7	2.5±0.4	0.087±0.015

Figure captions

Fig.3.1 Tracing of DSC recordings of pepsinogen in pH 8.3, 50 mM borate buffer at a scanning rate of 1 K/min. Curve 1 (thick line), first heating; curve 2 (thin line), re-heating of the protein solution in the calorimeter cell immediately after the cooling (for 1.5 h) from the first run. Concentration of pepsinogen is 1.34 mg/ml. Base line indicates the recording when both cells are filled with the same buffer solution, with 50 μW calibration mark from 61 ℃ to 67 ℃.

Fig.3.2 Heat capacity function of porcine pepsinogen at pH 7.6 measured by DASM-1M differential adiabatic scanning microcalorimeter at a scanning rate of 1 K/min. Heat capacity is plotted as the excess value from the assumed heat capacity function of the native state, $C_N(T)$. The heat capacity function of the heat denatured state, $C_D(T)$, is assumed as it has the same temperature coefficient as $C_N(T)$.

Fig.3.3 Calorimetric enthalpy function, $\Delta H^{cal}(T)$, and van't Hoff enthalpy function, $\Delta H^{vH}(T)$, of pepsinogen at pH 7.6. These are calculated by Eqs.(1.31) and (1.37), respectively, using the heat capacity functions in Fig.3.2.

Fig.3.4 Molar fraction functions of the native and the heat denatured states of pepsinogen at pH 7.6 (thin lines) and their sum (thick line). They are calculated by double deconvolution method using the heat capacity functions in Fig.3.2.

Fig.3.5 Enthalpy function of pepsinogen at pH 7.6, H(T), and the

hypothetical enthalpy function, $H^{(N,D)}(T)$, obtained by the double deconvolution method. Enthalpies are plotted as the excess values from the assumed enthalpy function of the native state, $H_N(T)$. The enthalpy functions of two intermediate states, $H_{I1}(T)$ and $H_{I2}(T)$, are assumed.

Fig.3.6 The best fitted heat capacity function (solid line) to the observed values of pepsinogen at pH 7.6 (circles). The parameters of the model are restricted as all the Δa_{ij}s are fixed to zero in Eq.(2.60). Heat capacity functions are plotted as the excess value from the heat capacity function of the native state.

Fig.3.7 Molar fraction functions of the four states, i.e., the native state (N), the heat denatured state (D), and the two intermediate states, (I_1), (I_2), of pepsinogen at pH 7.6. They are calculated from the best fitted thermodynamic parameters determined by non-linear least-squares fitting of Fig.3.6.

Fig.3.8 Difference enthalpy functions between the three thermodynamic states, (I_1), (I_2), (D), and the native state (N) at each midpoint temperature, Tm_{ij}, are plotted. Tm_{ij} is defined as the temperature at which $\Delta G_{ij}(T) = 0$. Filled circles indicate ΔH_{01}: filled triangles, ΔH_{02}: filled squares, ΔH_{03}. The suffixes, 0, 1, 2, 3, indicate N, I_1, I_2, D state, respectively. The numbers designate pH values and the bars represent the temperature dependence of the enthalpy functions. They are calculated with the thermodynamic parameters determined by non-linear least-squares fitting at each pH data. Broken lines are

determined by linear least-squares fitting with the linear functions of temperature using the plotted points.

Fig.3.9 Heat capacity functions of pepsinogen at the indicated pH (circles) measured by DASM-1M calorimeter at a heating rate of 1 K/min. Protein concentrations are about 1 mg/ml. Solid lines are their best fitted functions determined by non-linear least-squares fitting method with four-state model under the restrictions that all the Δa_{ij}s in Eq.(2.60) are fixed to zero and each Δb_{ij} in this equation is common to all the data of these pH values, and especially Δb_{01}, i.e., the difference heat capacity between native and I_1 state is fixed to zero (see text in detail).

Fig.3.10 pH dependence of difference enthalpy functions at a fixed temperature of 320 K from Table 3.2. The suffixes and symbols are the same as in Fig.3.8. Broken lines are determined by least-squares fitting with linear functions of pH using the data of the same symbol.

Fig.3.11 pH dependence of difference Gibbs free energy function at a fixed temperature of 320 K from Table 3.2. The suffixes and symbols are the same as in Fig.3.8. Broken lines are determined using the data of the same symbol by linear least-squares fitting with quadratic functions of pH.

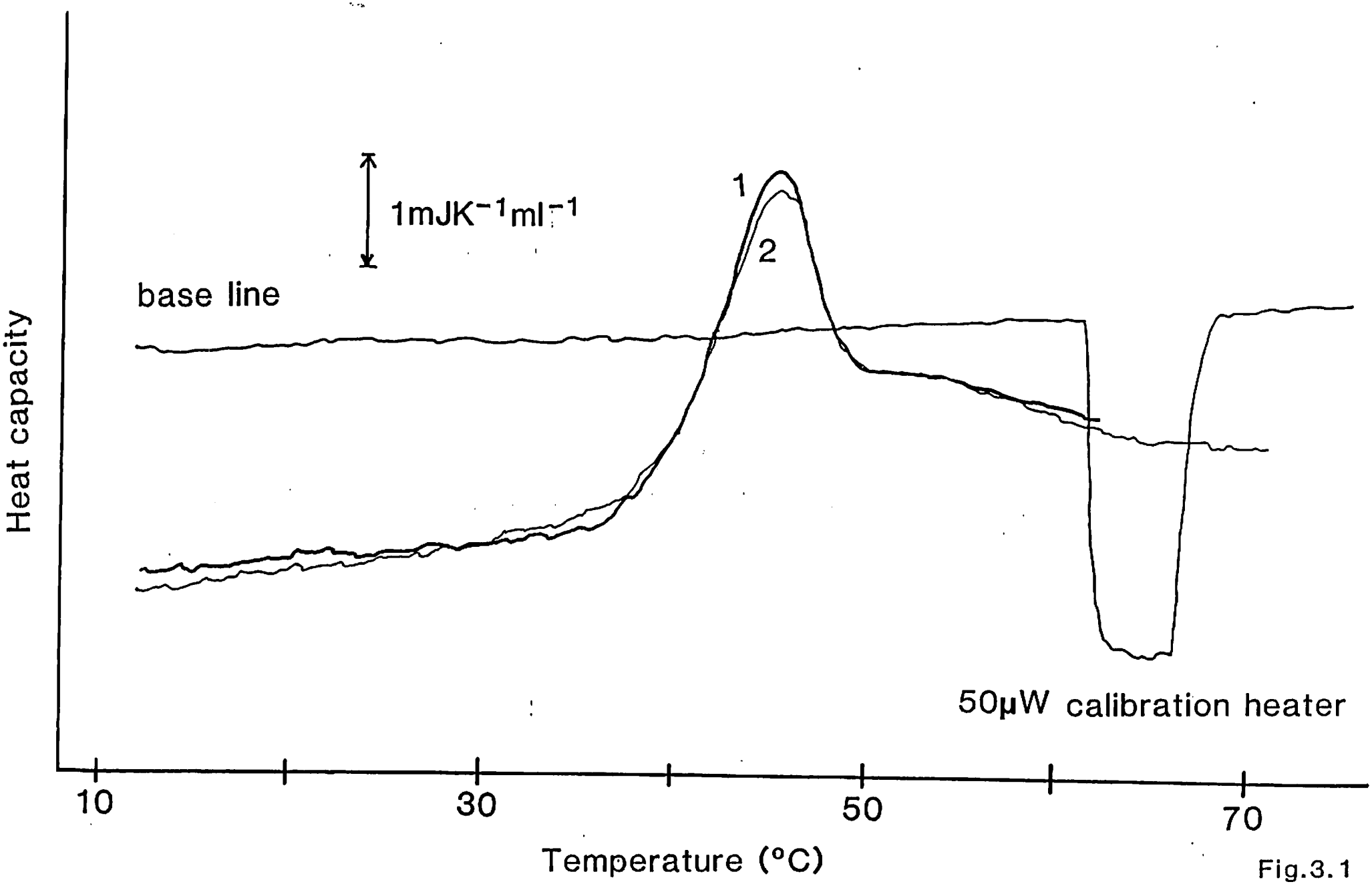
1mJK⁻¹ml⁻¹
1
2
base line
Heat capacity
50μW calibration heater
10
30
50
70
Temperature (°C)

Fig.3.1

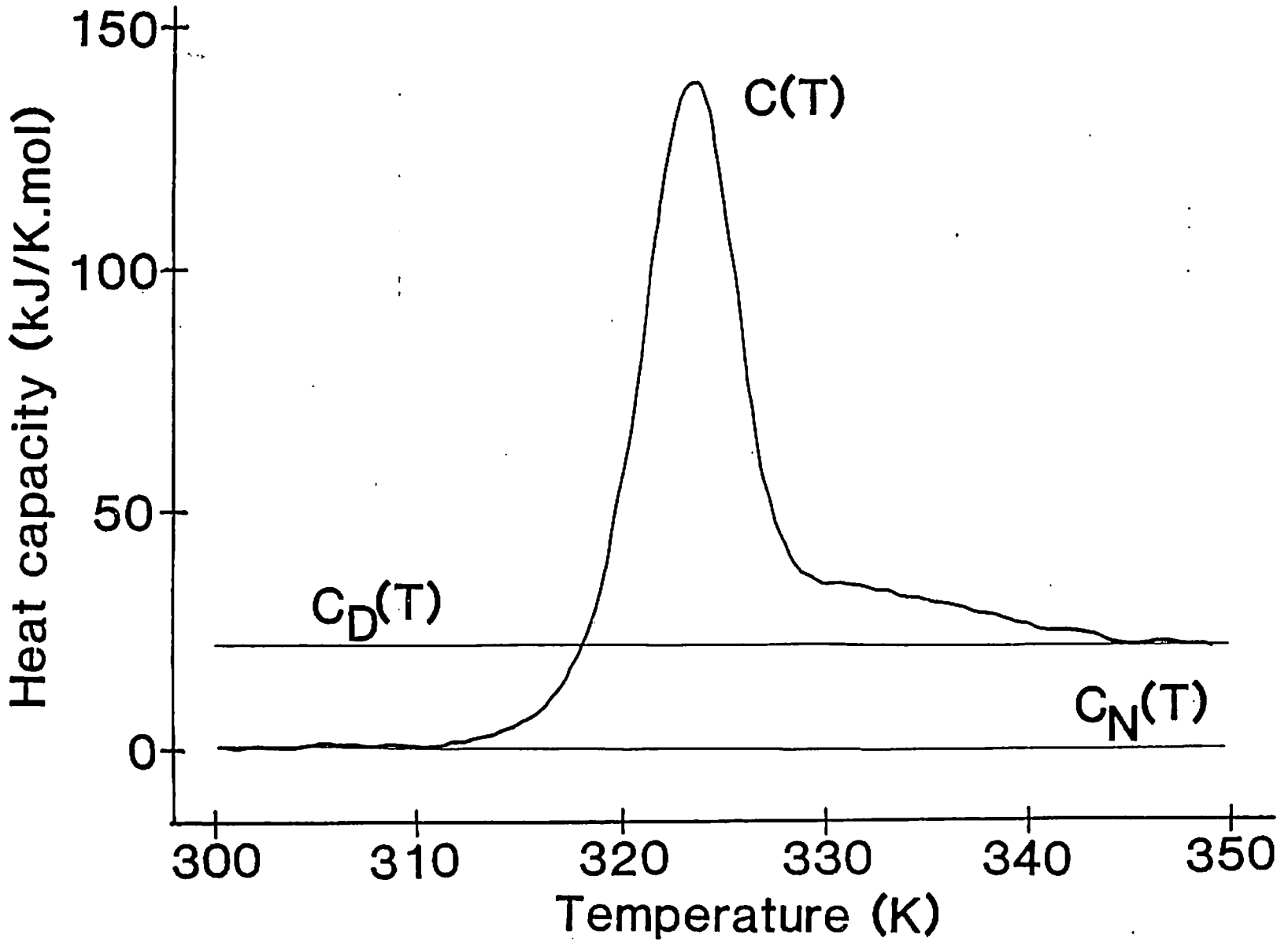
150
100
50
0
Heat capacity (kJ/K.mol)
C(T)
$C_D(T)$
$C_N(T)$
300
310
320
330
340
350
Temperature (K)

Fig.3.2

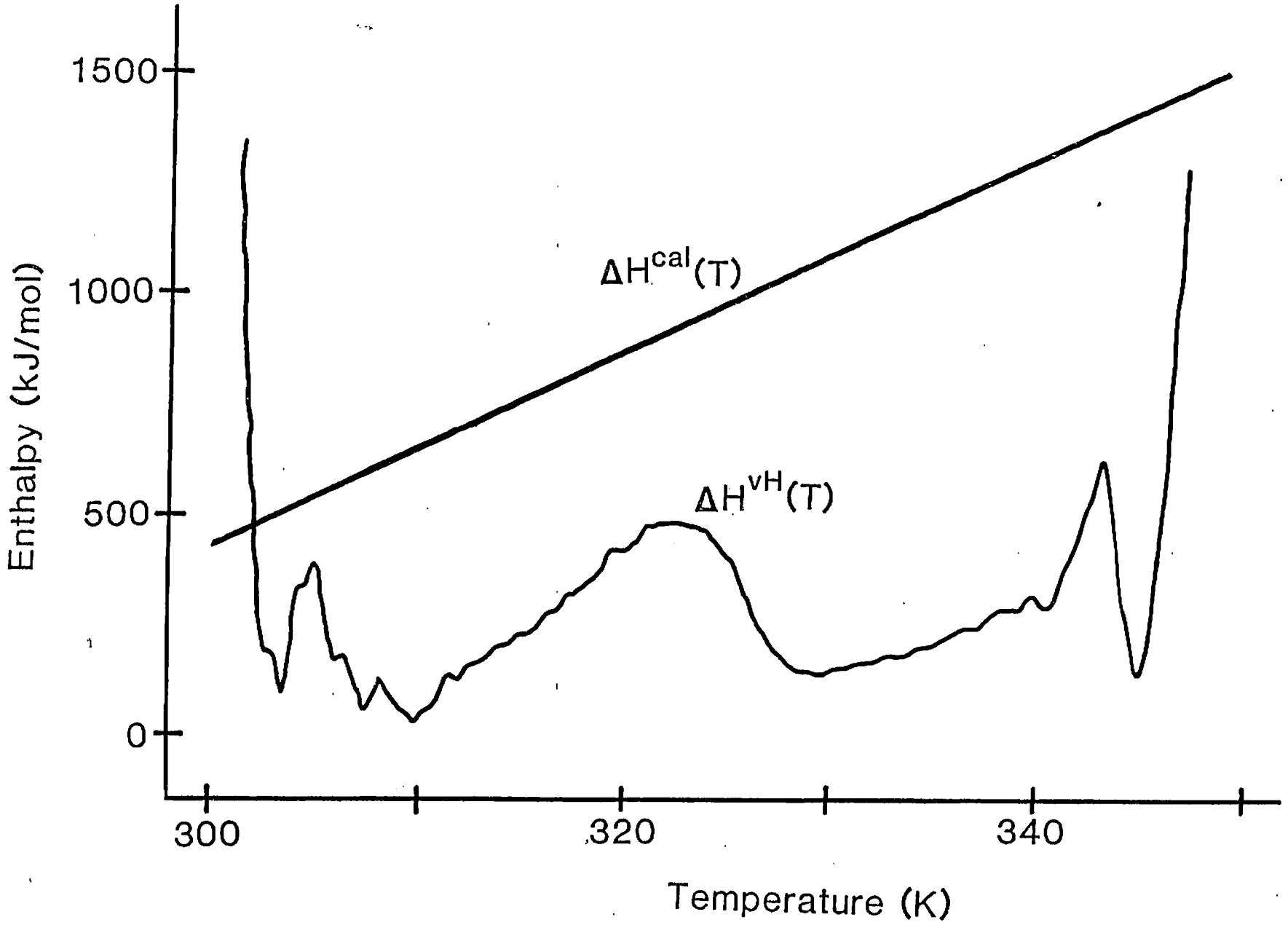
1500
1000
500
0
Enthalpy (kJ/mol)
$\Delta H^{cal}(T)$
$\Delta H^{vH}(T)$
300
320
340
Temperature (K)

Fig.3.3

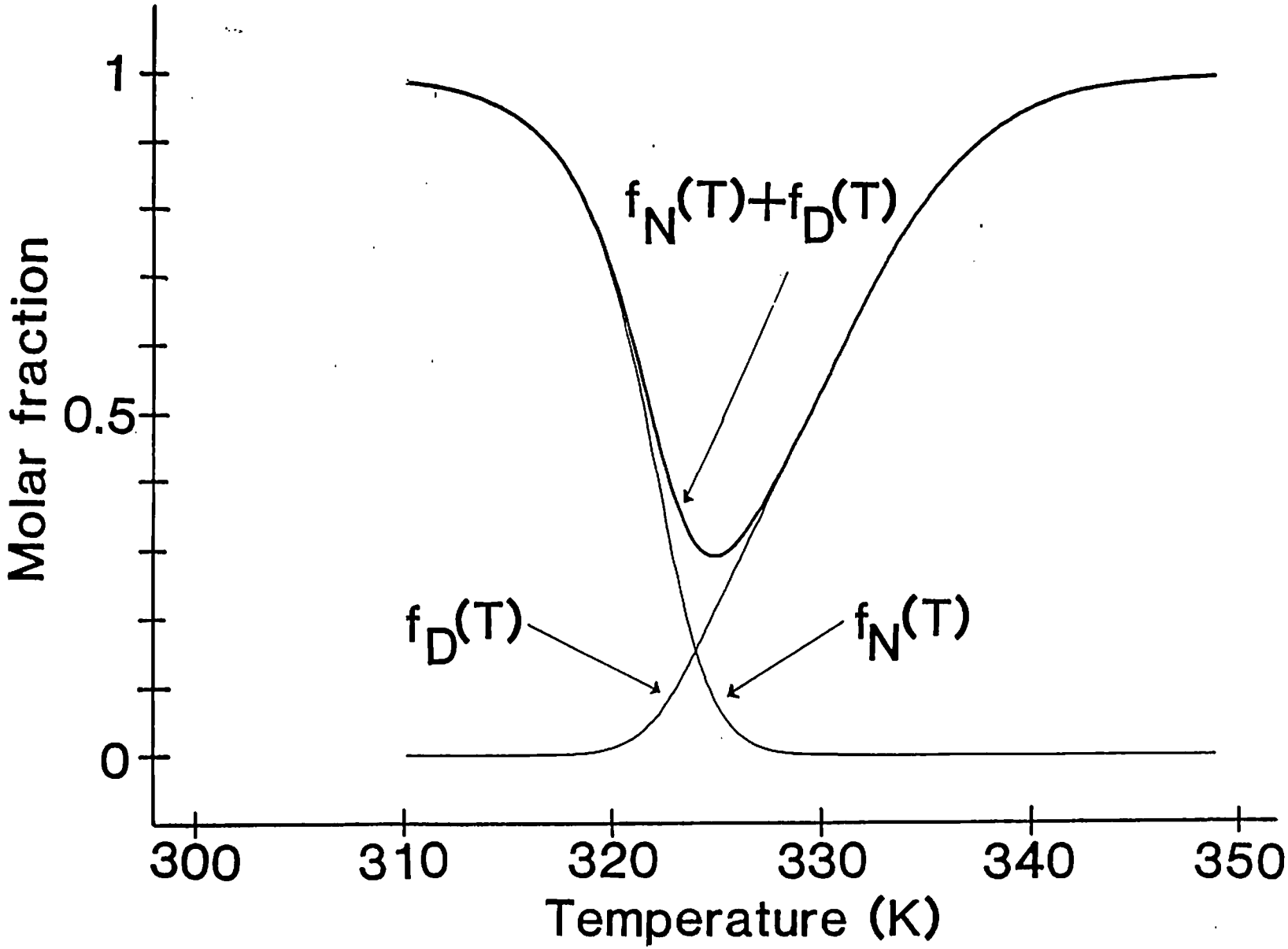
1
0.5
0
Molar fraction
$f_N(T)+f_D(T)$
$f_D(T)$
$f_N(T)$
300
310
320
330
340
350
Temperature (K)

Fig.3.4

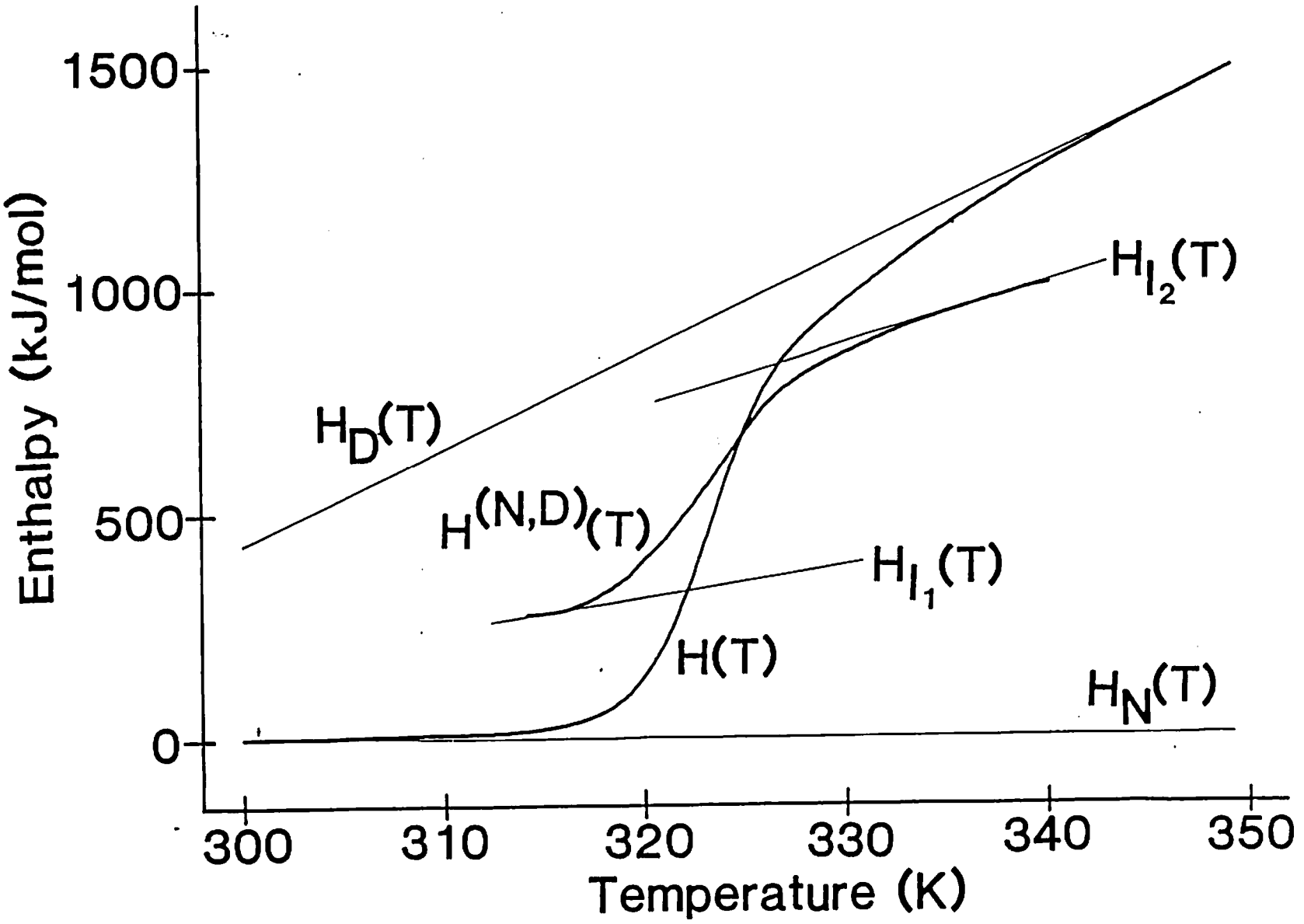
1500
1000
500
0
Enthalpy (kJ/mol)
$H_D(T)$
$H^{(N,D)}(T)$
$H_{I_2}(T)$
$H_{I_1}(T)$
H(T)
$H_N(T)$
300
310
320
330
340
350
Temperature (K)

Fig.3.5

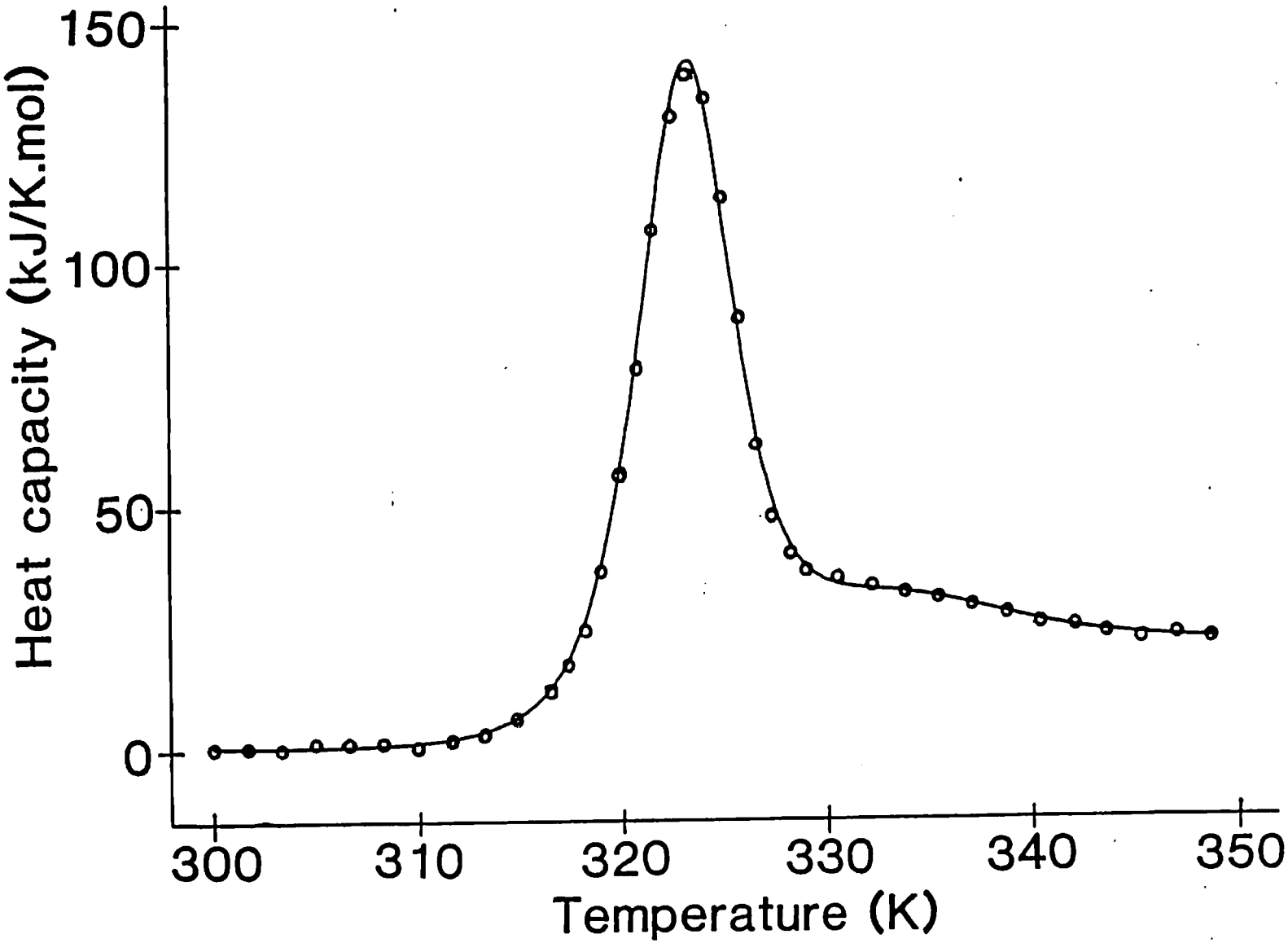
150
100
50
0
Heat capacity (kJ/K.mol)
300
310
320
330
340
350
Temperature (K)

Fig.3.6

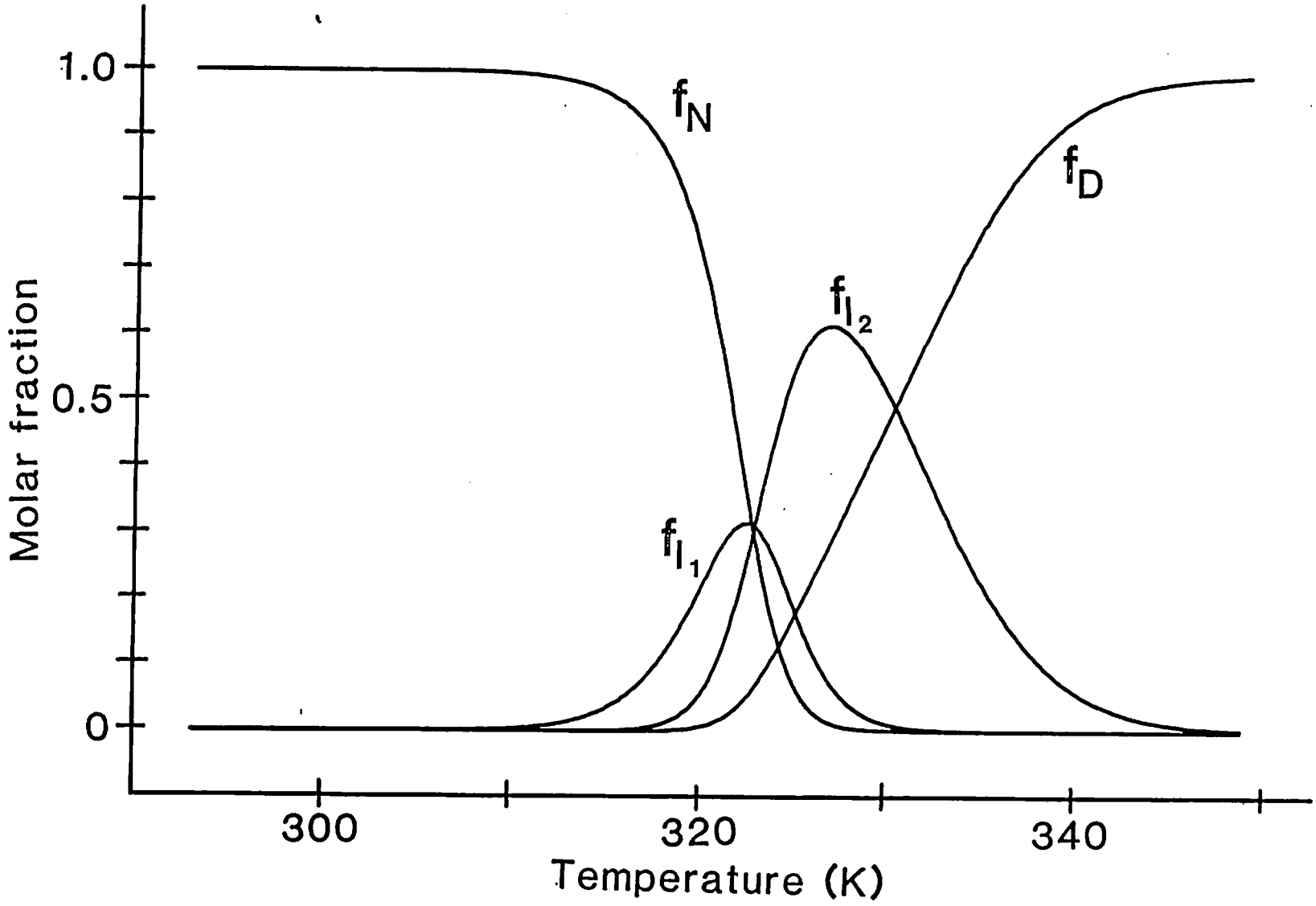

Fig.3.7

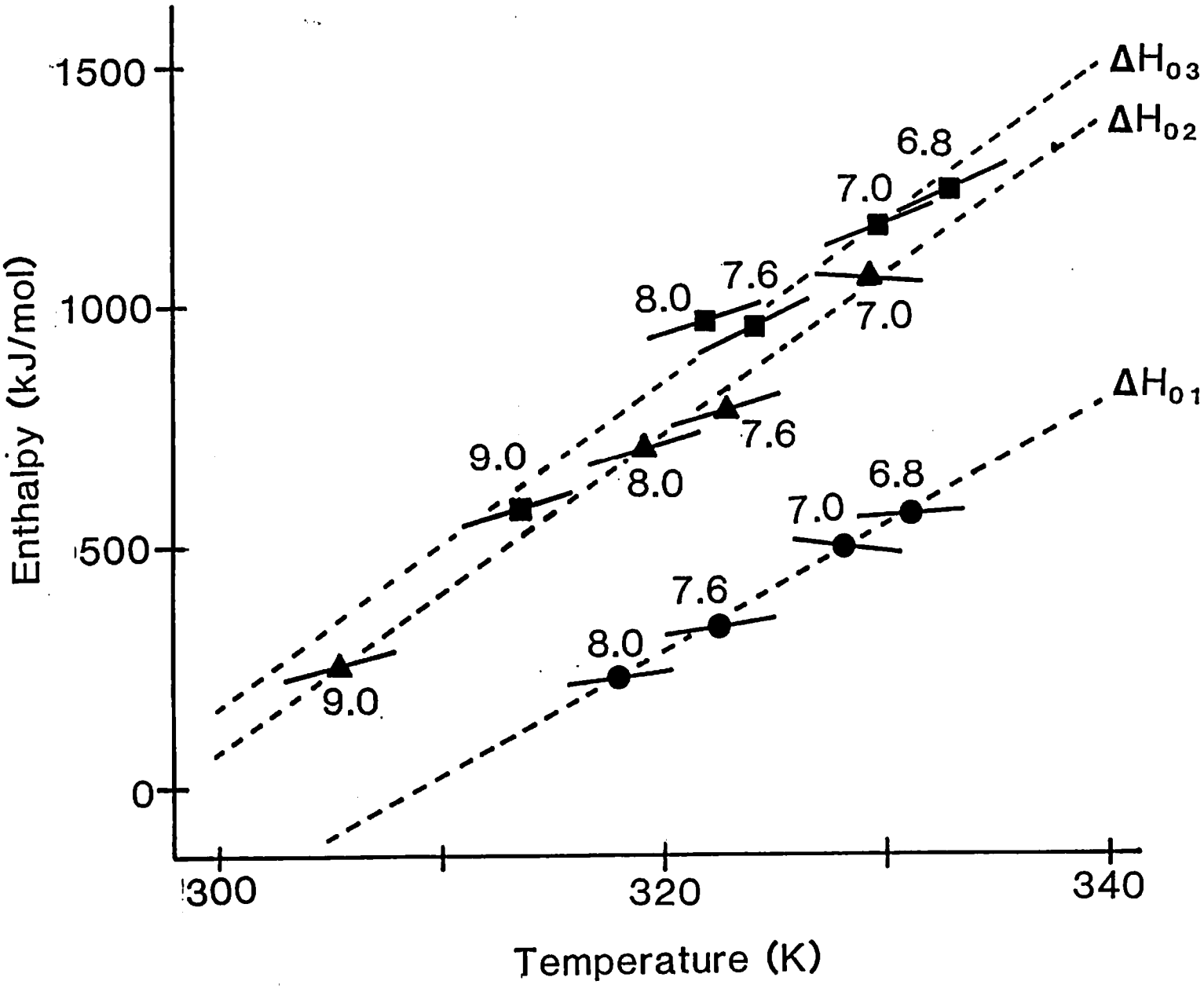
1500
1000
500
0
Enthalpy (kJ/mol)
300
320
340
Temperature (K)
ΔH_{03}
ΔH_{02}
ΔH_{01}
6.8
7.0
8.0
7.6
7.0
9.0
7.6
8.0
6.8
7.0
7.6
8.0
9.0

Fig.3.8

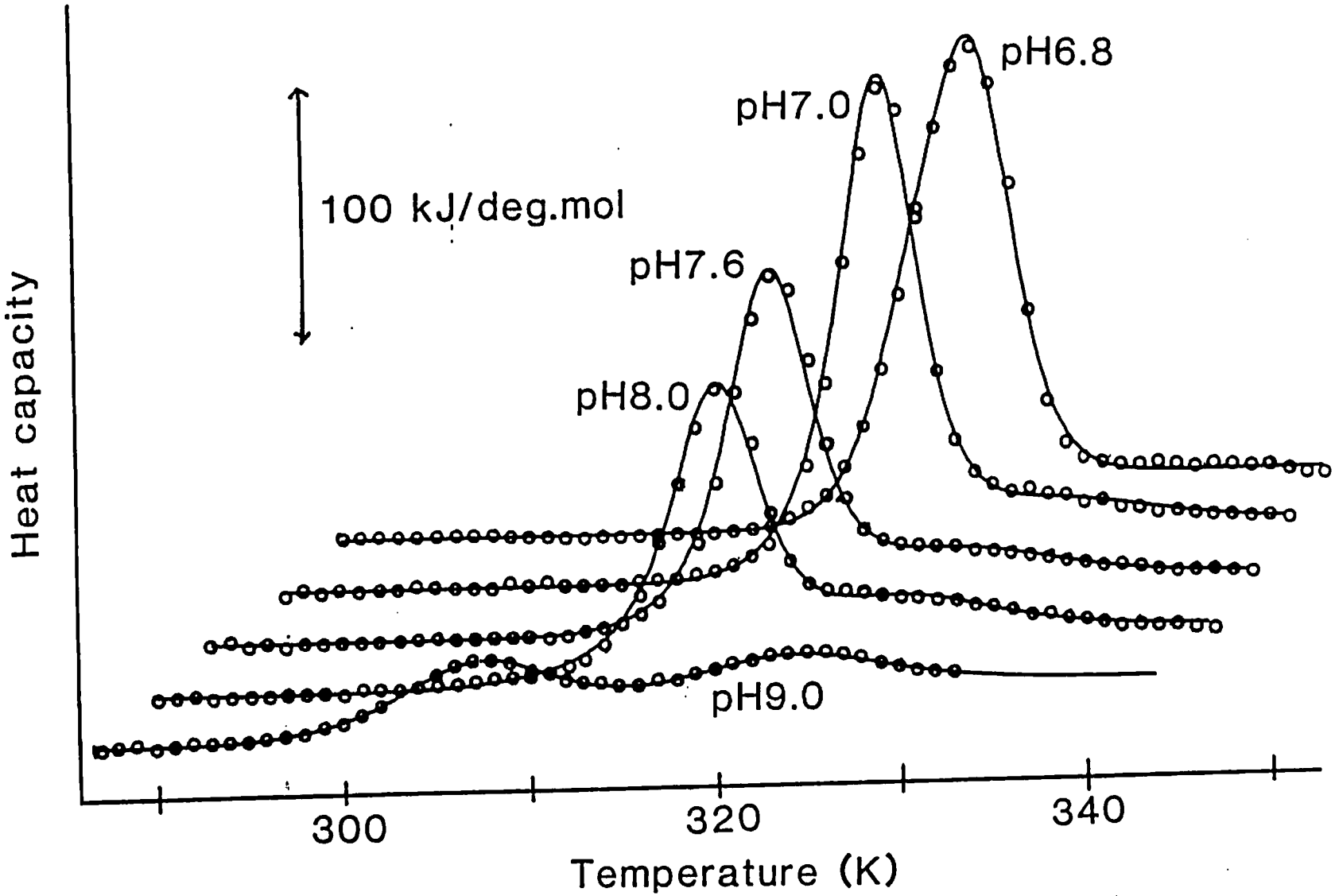
pH6.8
pH7.0
100 kJ/deg.mol
pH7.6
pH8.0
pH9.0
Heat capacity
300
320
340
Temperature (K)

Fig.3.9

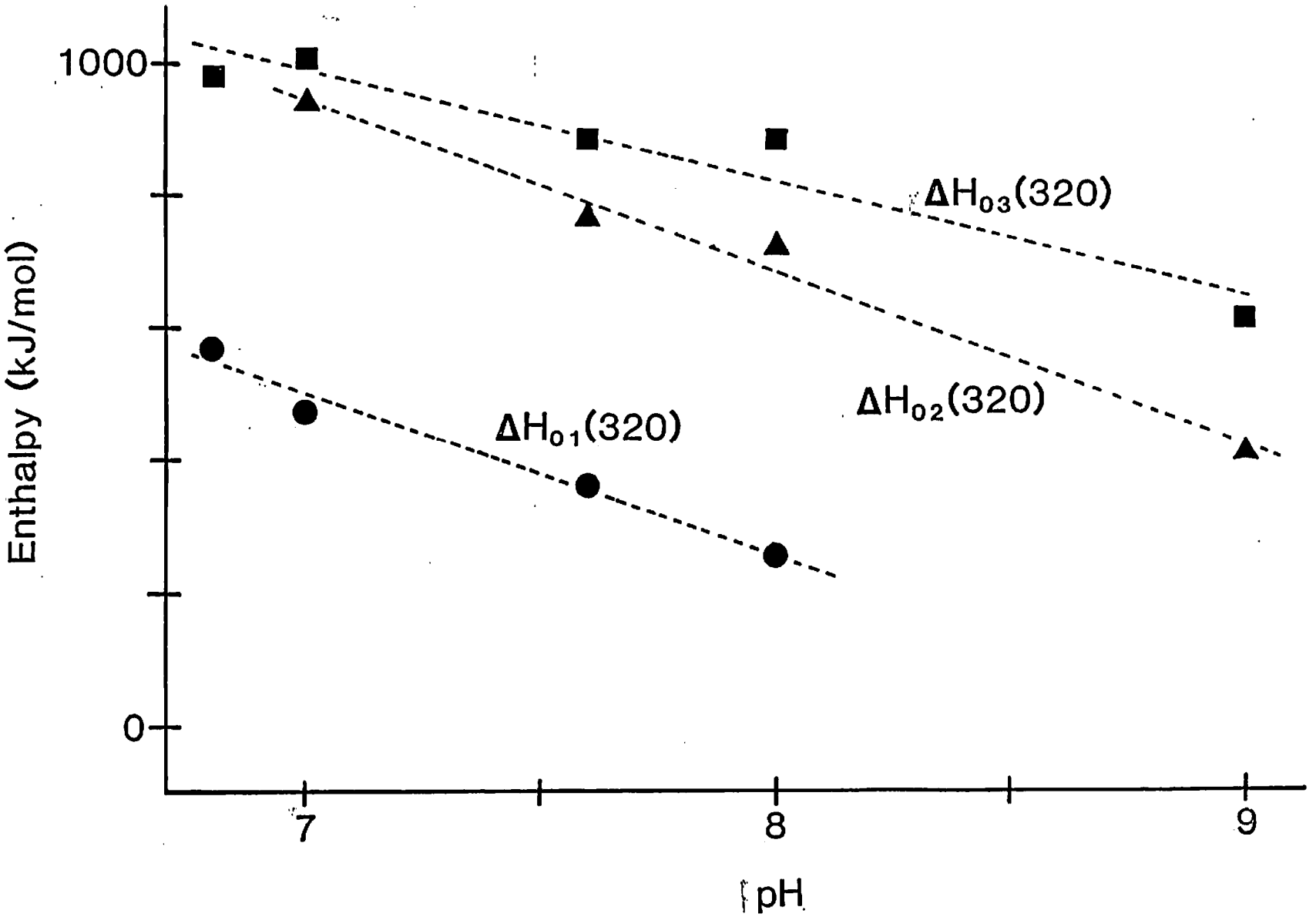
1000
0
Enthalpy (kJ/mol)
$\Delta H_{03}(320)$
$\Delta H_{02}(320)$
$\Delta H_{01}(320)$
7
8
9
pH

Fig.3.10

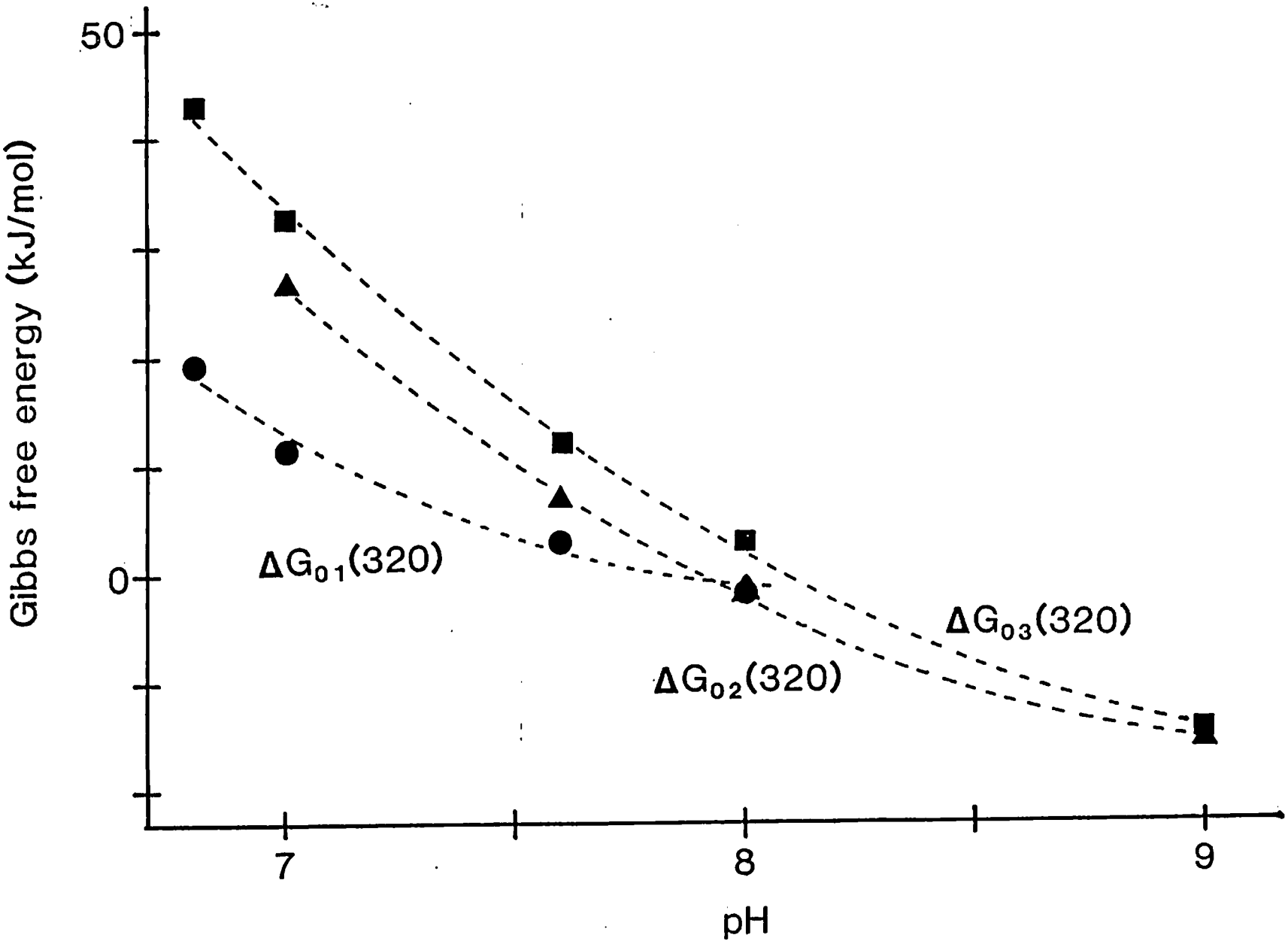

Fig.3.11

Acknowledgments

I wish to express my sincere gratitude to Professor Akiyoshi Wada, Department of Physics, Faculty of Science, the University of Tokyo, for his advice and encouragement during the present work.

I wish to thank Dr. Hatsuho Uedaira, Chief of Energy Transformation Laboratory, Research Institute for Polymers and Textiles, for her advice and kind help to perform the measurement of differential scanning calorimetry.

I wish to thank all the members of the Laboratory of Biophysics for their stimulus discussions and encouragement.

Finally, I express my grateful thanks to my family for their continuous support and encouragement.

Appendix Statistical mechanical treatment of the system that includes self-dissociation/association process

A thermodynamic state is defined as an ensemble of some of the quantum mechanical microstates (see Chapter 1). When the energy and degeneracy of the μ-th microstate are denoted as ε_μ and ω_μ, respectively, the partition function of the state, $Z^i(T)$, is defined as

$$Z^i(T) = \sum_{\mu \in i} \omega_\mu \exp(-\varepsilon_\mu / RT) \qquad (A.1)$$

The partition function of the whole system which consist of n thermodynamic states are described as

$$Z(N_0, N_1, \ldots, N_n, T) = \prod_{i=0}^{n} Z^i(T)^{N_i} / N_i! \qquad (A.2)$$

where N_i is defined as the particle number of the i-th state. From the mass conservation low, the next equation holds where m_i is the stoichiometry of the i-th state, and N_r is defined as the reduced particle number which must be constant.

$$\sum_{i=0}^{n} N_i / m_i = N_r \qquad (A.3)$$

In equilibrium, the set of N_i which makes the partition function of the whole system maximum is realized. The set can be obtained

to maximize the following function I, which is defined as Eq.(A.4), using a Lagrange's undetermined coefficient, λ, as

$$I = \log Z + \lambda \sum_{i=0}^{n} N_i/m_i \qquad (A.4)$$

$$N_i = Z^i(T) \exp(\lambda/m_i) \qquad (A.5)$$

I define the molar fraction function of i-th state, $f_i(T)$, as

$$f_i(T) = \frac{N_i/m_i}{N_r} \qquad (A.6)$$

From Eqs.(A.3) and (A.6), the following equation holds:

$$\sum_{i=0}^{n} f_i(T) = 1 \qquad (A.7)$$

Equation (A.8) can be derived from Eqs.(A.2), (A.5) and (A.6):

$$\log Z = N_r \left[\sum_{k=0}^{n} m_k f_k - m_i \log(f_i m_i N_r) + m_i \log Z^i \right] \qquad (A.8)$$

Using the relation between the enthalpy function and the partition function (see Chapter 1), we obtain

$$H(T) = RT^2 \frac{d}{dT} \left[-m_i \log f_i + \sum_{k=0}^{n} m_k f_k \right] + m_i RT^2 \frac{d}{dT} \log Z^i \qquad (A.9)$$

As the last term of the right-hand side of Eq.(A.9) is equal to $m_i H_i(T)$ from the definition, the next equation is derived finally,

$$\frac{d}{dT}\left[-m_i \log f_i + \sum_{k=0}^{n} m_k f_k \right] = \Delta H_i(T)/RT^2 \qquad (A.10)$$

References

Arnon, R. & Perlmann, G.E. (1963) The amino acid composition of chromatographically purified pepsinogen. J. Biol. Chem. 238, 653–656.

Brandt, S. (1975) Statistical and computational methods in data analysis, 2nd ed., North-Holland Publishing Co.

Bates, R.G. & Acree, S.F. (1943) pH values of certain phosphate–chloride mixtures, and the second dissociation constant of phosphoric acid from 0°C to 60°C. J. Res. Natl. Bur. Standards 30, 129–155.

Calderon, R.O., Stolowich, N.J., Gerlt, J.A. & Sturtevant, J.M. (1985) Thermal denaturation of Staphylococcal nuclease. Biochemistry 24, 6044–6049.

Christensen, J.J. & Izatt, R.M. (1962) Thermodynamics of proton dissociation in dilute aqueous solutions. II. Heats of proton dissociation from ribonucleotides and related compounds determined by a thermometric titration procedure. J. Phys. Chem. 66, 1030–1034.

Christensen, J.J., Izatt, R.M., Wrathall, D.P. & Hansen, L.D. (1969) Thermodynamics of proton ionization in dilute aqueous solution. part XI. pK, ΔH^0, and ΔS^0 values for proton ionization from protonated amines at 25°C. J. Chem. Soc. A. 1969, 1212–1223.

Cooper, A. (1984) Protein fluctuations and the thermodynamic uncertainty principle. Prog. Biophys. Molec. Biol. 44, 181–214.

Filimonov, V.V., Potekhin, S.A., Matveev, S.V. & Privalov, P.L. (1982) Thermodynamic analysis of scanning microcalorimetric data I. Algorithms for deconvolution of complex heat absorption curves. Mol. Biol. 16, 551–562.

Freire, E. & Biltonen, R.L. (1978a) Statistical mechanical deconvolution of thermal transitions in macromolecules. I. Theory and application to homogeneous systems. Biopolymers 17, 463–479.

Freire, E. & Biltonen, R.L. (1978b) Statistical mechanical deconvolution of thermal transitions in macromolecules. II. General treatment of cooperative phenomena. Biopolymers 17, 497–510.

Fukada, H., Sturtevant, J.M. & Quiocho, F.A. (1983) Thermodynamics of the binding of l-arabinose and of d-galactose to the l-arabinose-binding protein of Escherichia coli. J. Biol. Chem. 258, 13193–13198.

Gill, S.J., Richey, B., Bishop, G. & Wyman, J. (1985) Generalized binding phenomena in an allosteric macromolecule. Biophys. Chem. 21, 1–14.

Gill, S.J., Dec, S.F., Olofsson, G. & Wadsoe, I. (1985) Anomalous heat capacity of hydrophobic solvation. J. Phys. Chem. 89, 3758–3761.

Jordan, J. (1958) Thermochemical titrations. Rec. Chem. Prog. 19, 193–213.

Khechinashvili, N.N., Privalov, P.L. & Tiktopulo, E.L. (1973) Calorimetric investigation of lysozyme thermal denaturation. FEBS Lett. 30, 57–60.

Kidokoro, S. & Wada, A. (1987) Determination of thermodynamic functions from scanning calorimetry data. Biopolymers 26, 213–229.

Kidokoro, S., Uedaira, H. & Wada, A. (1988) Determination of thermodynamic functions from scanning calorimetry data. II. For the system that includes self-dissociation/association process. Biopolymers 27, 271–297.

Kim, P.S. & Baldwin, R.L. (1983) Specific intermediates in the folding reactions of small proteins and the mechanism of protein folding. Ann. Rev. Biochem. 51, 459–489.

Mateo, P.L. & Privalov, P.L. (1981) Pepsinogen denaturation is not a two-state transition. FEBS Lett. 123, 189–192.

Nakagawa, T. & Oyanagi, Y. (1980) Program system 'SALS' for nonlinear least-squares fitting in experimental sciences. in Recent developments in statistical inference and data analysis, Matusita, K., ed., North-Holland Publishing Co., 221–225.

Ooi, T. & Oobatake, M. (1988) Effects of Hydrated water on protein unfolding. J. Biochem. 103, 114–120.

Pfeil, W. & Privalov, P.L. (1976) Thermodynamic investigations of proteins I. Standard functions for proteins with lysozyme as an example. Biophys. Chem. 4, 23–32.

Privalov, P.L. & Khechinashvili, N.N. (1974) A thermodynamic approach to the problem of stabilization of globular protein structure: A calorimetric study. J. Mol. Biol. 86, 665–684.

Privalov, P.L. (1979) Stability of proteins. Small globular proteins. Adv. Protein Chem. 33, 167–241.

Privalov, P.L. (1980) Scanning microcalorimeters for studying macromolecules. Pure Appl. Chem. 52, 479–497.

Privalov, P.L., Mateo, P.L., Khechinashvili, N.N., Stepanov, V.M. & Revina, L.P. (1981) Comparative thermodynamic study of pepsinogen and pepsin structure. J. Mol. Biol. 152, 445–464.

Privalov, P.L. (1982) Stability of proteins. Proteins which do not present a single cooperative system. Adv. Protein Chem. 35, 1–104.

Privalov, P.L., Griko, Yu.V., Venyaminov, S.Yu. (1986) Cold denaturation of myoglobin. J. Mol. Biol. 190, 487–498.

Saito, Y. & Wada, A. (1983a) Comparative study of GuHCl denaturation of globular proteins. Ⅰ. Spectroscopic and chromatographic analysis of the denaturation curves of ribonuclease A, cytochrome c, and pepsinogen. Biopolymers 22, 2105–2122.

Saito, Y. & Wada, A. (1983b) Comparative study of GuHCl denaturaion of globular proteins. Ⅱ. A phenomenological classification of denaturation profiles of proteins. Biopolymers 22, 2123–2132.

Takahashi, K. & Sturtevant, J.M. (1981) Thermal denaturation of Streptomyces subtilisin inhibitor, subtilisin BPN', and the inhibitor–subtilisin complex. Biochemistry 20, 6185–6190.

Takeda, Y., Taga, S. & Miwatani, T. (1978) Evidence that thermostable direct hemolysin of Vibrio parahemolyticus is composed of two subunits. FEMS Microbiol. Lett. 4, 271–274.

Uedaira, H., Honda,T., Takeda, Y., Miwatani, T., Uedaira, H. & Ohsaka, A. (1983) Thermal denaturation of the thermostable direct hemolysin of Vibrio parahaemolyticus. the 19th

Japanese conference on calorimetry and thermal analysis, Tokyo, Oct. 5–7.

Wada, A., Saito, Y., & Ohgushi, M. (1983) Multiphasic conformation transition of globular proteins under denaturating perturbation. Biopolymers 22, 93–99.

Wyman, J. (1964) Linked functions and reciprocal effects in hemoglobin. A second look. Adv. Prot. Chem. 19, 223–286.